Examining the Relationship Between Whole Body Resting Metabolic Rate and the Efficiency of SR Ca^{2+} Handling in Human Skeletal Muscle

by

Karlee Jenna Hall

A thesis
presented to the University of Waterloo
in fulfilment of the
thesis requirement for the degree of
Master of Science
in
Kinesiology

Waterloo, Ontario, Canada, 2011

AUTHOR'S DECLARATION:

I hereby declare that I am the sole author of this thesis. This is a true copy of the thesis, including any required final revisions, as accepted by my examiners.

I understand that my thesis may be made available electronically to the public.

Karlee Jenna Hall

ABSTRACT

The purpose of this study was to investigate whether skeletal muscle sarcoplasmic reticulum (SR) Ca^{2+} transport efficiency and expression levels of major SR Ca^{2+} regulatory proteins are associated with resting metabolic rate (RMR) in humans. Twenty five healthy and weight stable participants with mean age, height and weight of 22±3.6 years, 174.6±8.0 cm and 72.8±21 kg respectively, were recruited for the study. RMR was calculated using the Weir equation based upon measures of VO_2 and VCO_2, which were collected using the Vmax breath by breath indirect calorimetry system. Ca^{2+}-ATPase activity, Ca^{2+} uptake and Ca^{2+} leak analyses were performed *in vitro* on homogenates that were prepared from vastus lateralis muscle biopsies. Ionophore (IONO) ratio was assessed by measuring Ca^{2+}-ATPase activity in the presence and absence of Ca^{2+} Ionophore. The coupling ratio, a measure of SR Ca^{2+} transport efficiency, was calculated by taking the ratio of Ca^{2+} uptake to Ca^{2+}-ATPase activity. Expression levels of the major SR Ca^{2+} regulatory proteins, including SERCA1a, SERCA2a, phospholamban (PLN), and calsequestrin (CSQ) were assessed using Western blotting techniques. Pearson correlation coefficient analysis demonstrated a weak but significant negative correlation between coupling ratio and RMR (r^2= 0.2108, p =0.0240). Content of the SR Ca^{2+} regulatory proteins, IONO ratio and Ca^{2+} leak were not found to be significantly related to either RMR or coupling ratio, with the exception of the ratio of SERCA1a to SERCA2a, which showed a weak but significant positive relationship with RMR (r^2=0.1781, p=0.0400). Thus, the relationship between coupling ratio and RMR is not influenced by Ca^{2+} leak, SERCA pump efficiency or the SR Ca^{2+} regulatory proteins. Overall, these results suggest that the efficiency of SR Ca^{2+} transport is weakly related to whole body RMR. Further analysis is needed to assess this

relationship, and to determine which SR Ca^{2+} handling properties are influencing the relationship between coupling ratio and RMR.

ACKNOWLEDGEMENTS

I have spent 6 years of my life at the University of Waterloo, and have met and gotten to know so many great people who really made my experiences here great. I have been surrounded by amazing professors and friends who have made my years at U of W some of the best of my life.

Thank you very much to my supervisor, Dr. Russell Tupling. Dr. Tupling has been instrumental in my learning process and in my success here at U of W. He has spent many hours discussing the details of my research project with me, and has always been a great influence and mentor to me. I really appreciate all you have done for me over the years I have spent at U of W.

Thank you to my lab mates Chris Vigna, Dr. Eric Bombardier, Ryan Sayer, Dan Gamu, Ian Smith and Anton Trinh. I was always sure to have an exciting day working with this group of people. All of my lab mates have spent a great deal of time discussing my project with me and providing support where it was needed, and have been great friends as well. I especially need to thank Chris Vigna for all of the time he spent with me, teaching me essentially all the lab skills that I have gained and I would not have been able to complete this research project if not for him.

I also want to thank all of the professors and graduate students on the 2nd floor research labs of BMH. I have learned so much from all of these individuals and have been surrounded with a great atmosphere to work in thanks to them. Thank you to Dr. Mourtzakis, Dr. Quadrilatero, Dr. Rush, Dr. Stark and Dr. Hughson, and to all of my friends and colleagues in their laboratories.

Thank you to Marg Burnett, Dr. John Moule, Jing Ouyang, Ashley Patterson and Janice Skafel, who have helped me carry out my research in a number of different ways. You have been very supportive and helpful.

Finally, thank you very much to my family and loved ones for their continued support and encouragement. I was able to attend U of W because I have such a great and supportive family who have spent many hours throughout the past 6 years encouraging and cheering me on. I definitely cannot thank them enough. Thank you to all of my friends for the support as well, and for many fun times over the last 6 years.

DEDICATION

I dedicate this thesis to my family and loved ones, whose love and support has helped me a great deal throughout my academic career.

TABLE OF CONTENTS

LIST OF FIGURES

LIST OF ABBREVIATIONS

$[Ca^{2+}]_f$	Cytosolic free Calcium concentration
ATP	Adenosine triphosohate
ATP2A1-3	Genes which encode for SERCA pumps
BIA	Bioelectrical impedance analysis
BMR	Basal metabolic rate
BW	Body weight
Ca^{2+}	Calcium
CPA	Cyclopiazonic acid
CSQ	Calsequestrin
DXA	Dual energy x-ray absorptiometry
EC50	Ca^{2+} concentration needed for 50% of maximal SERCA activity
EDL	Extensor digitorum longus
EGTA	Ethylene glycol tetraacetic acid
FFA	Free fatty acids
FFM	Fat free mass
FM	Fat mass
GI	Gastrointestinal tract
HEPES	4-(2-hydroxyethyl)-1-piperazineethanesulfonic acid
HDL	High density lipoprotein
Ht^2	Height squared
IONO	Ca^{2+} ionophore
KCl	Potassium chloride
LDH	Lactate dehydrogenase
LDL	Low density lipoprotein
MET	Metabolic equivalent
$MgCl_2$	Magnesium chloride
NADH	Nicotinamide adenine dinucleotide
pCa	Negative logarithm of $[Ca^{2+}]_f$
PEP	Phosphoenol pyruvate
PLN	Phospholamban
PK	Pyruvate kinase
R_{50}	Resistance
RMR	Resting metabolic rate
RyR	Ryanodine receptor
SERCA	Sarco(endo)plasmic reticulum Ca^{2+}-ATPase
SDS-PAGE	Sodium dodecyl sulphate polyacrylamide gel electrophoresis
SLN	Sarcolipin
SMR	Sleeping metabolic rate
SR	Sarcoplasmic reticulum
T3	Triiodothyronine
T4	Thyroxine

T-tubule	Transverse tubule
VCO_2	Volume of carbon dioxide
VO_2	Volume of oxygen
Vmax	Maximal Ca^{2+}-ATPase activity
Wt	Weight
Xc	Reactance

CHAPTER ONE: INTRODUCTION

OVERVIEW

Studies examining resting metabolic rate (RMR) have shown significant variability between individuals (Boothby and Sandiford, 1922; Bogardus et al, 1986). It has been found that skeletal muscle metabolism contributes significantly to this variability (Zurlo et al, 1990). In skeletal muscle the sarcoplasmic reticulum (SR) Ca^{2+} pump (SERCA) plays a critical role in contraction and relaxation, but it also has an underappreciated role in energy metabolism and daily energy expenditure. The overall objective of this study was to investigate the relationship between the efficiency of SR Ca^{2+} transport and other SR properties, and resting metabolic rate in humans. Specifically, cross-sectional analyses were performed on muscle samples obtained from a group of healthy individuals, who were considered to be weight-stable and in energy balance, to determine whether RMR is associated with skeletal muscle SR Ca^{2+} transport efficiency (assessed by measuring the ratio of Ca^{2+} uptake:ATP hydrolysis, which is called the coupling ratio) and protein expression levels of major SR Ca^{2+} regulatory proteins that are thought to be involved in the regulation of the coupling ratio. It was hypothesized that RMR would be 1) negatively correlated with coupling ratio, 2) positively correlated with SR Ca^{2+} leak, and 3) negatively correlated with SERCA pump efficiency (assessed by the ratio of SR Ca^{2+}-ATPase activity measured with/without the Ca^{2+} ionophore, which is called the ionophore (IONO) ratio). Furthermore, it was hypothesized that any SR protein that is known to influence SR Ca^{2+} leak and/or SERCA pump efficiency would also be correlated with RMR. Finally, the assumptions regarding the role of different SR proteins in the regulation of the coupling ratio in skeletal muscle were assessed by correlational analyses.

The significance of this study is that it is the first study to examine the relationships between RMR and the various SR Ca^{2+} handling properties not only in humans, but in any species. The findings of the present study could lead to an improved understanding of the contribution of SR Ca^{2+} handling energetics to whole body RMR in humans, and could lead to the examination of SR Ca^{2+}handling energetics as a means of prevention and/or treatment for obesity.

BACKGROUND

Metabolism Foundations:

Both humans and other mammals alike use a substantial amount of energy in a basal state, that being when no net work is being done and all the free energy is dissipated (Rolfe and Brown, 1997). Studies examining the components of metabolism prove useful in understanding where energy is directed in the human body, what controls the usage of energy by different systems, what functions basal energy serves biologically and the possible reasons for differences in energy usage between individuals. Pinpointing these differences in energy storage, usage and the processes that function towards basal metabolism can provide much insight into the processes which contribute to the differences in metabolic rate seen between individuals.

Different states of metabolism can be measured in human beings, such as 'resting state' or during digestion. Basal metabolic rate (BMR), sleeping metabolic rate (SMR) and resting metabolic rate (RMR) are common terms used in the study of metabolism. RMR is the steady-state rate of production of heat by a human being under a set of standard conditions. These conditions include having the individual awake but resting, stress free, post-absorptive,

and having a temperature that does not bring about a thermoregulatory effect of heat production (Blaxter, 1989; Speakman, 2003). RMR can be accurately quantified by using indirect calorimetry to measure O_2 consumption rates which are then converted to energy expenditure using a standard equation (Schutz, 1995; Speakman, 2003). BMR is similar to RMR, however, it is the rate of energy metabolism of an individual which is needed to sustain the functioning of the vital organs and is measured when the participant has just awoken from a restful state (Henry, 2005). SMR is the energy expenditure of an individual while sleeping (Zurlo, 1990).

Total daily energy expenditure can be divided into three main components which include RMR, thermic effect of exercise, and thermic effect of food (Wu et al, 2011). The extent to which a process is coupled to oxygen consumption quantifies the energy flux through the process (Rolfe and Brown, 1997). The energy that is used in a basal state is sometimes identified as the fixed requirement for the basic functioning and maintenance of the individual (ie. functioning of the organs). Further energy usage is elicited from physical activity or muscle usage, feeding, growth, reproduction, and cold exposure (Rolfe and Brown, 1997). However, these factors are not always in addition to baseline RMR because the metabolic processes underlying RMR may increase or decrease in response to the additional energy demand which can be placed on the individual during one of these conditions (Wieser, 1989). For example, the metabolic rate of certain organs, such as the gut actually decreases due to the commencement of exercise and the metabolic rate of skeletal muscle increases. It can be taken from this that the processes which compose RMR can change under various conditions. Furthermore, metabolic rate has been shown to decrease by approximately 10

percent during sleep and decrease approximately 40 percent during long-term starvation, relative to RMR in humans (Blaxter, 1989).

Free energy is obtained from the oxidation of food molecules such as fats, protein and carbohydrates. This process is coupled to the reduction of NAD. The electron transport chain in the mitochondria is responsible for the oxidation of NADH, and this is coupled to the production of an electrochemical gradient across the inner membrane of the mitochondria (Lowell and Spiegelman, 2000). The synthesis of ATP is coupled to the channelling of protons through the ATP synthase with the concentration gradient. Protein synthesis, maintenance of the ion gradients and other processes such as muscle contraction are coupled to ATP hydrolysis (Lowell and Spiegelman, 2000; Rolfe and Brown, 1997). There is also a significant flux through the system which occurs through reactions that uncouple metabolism. Examples of uncoupling reactions include protein degradation, ion leaks, and muscle relaxation and these uncoupling processes also account for RMR (Rolfe and Brown, 1997). Furthermore, it is known that not all oxygen consumption is mitochondrial and thus coupled to oxidative phosphorylation, and that a significant proportion of mitochondrial respiration is not coupled to ATP synthesis (Lowell and Spiegelman, 2000; Zorratti et al, 1986; Brown and Brand, 1986)

The processes that contribute to RMR take place in different tissues throughout the body. The oxygen consumption rates and therefore the heat production by different organs within the human body during RMR have been measured in human beings using data taken from in vivo tissue respiration. There is not one specific organ that is responsible for the majority of an individual's metabolic rate, however, there are some organs which contribute a much larger fraction of the total RMR than their fractional mass or volume of the body. These

include the brain, kidney, heart and gastrointestinal (GI) tract (Altman and Dittmer, 1968; Aschoff, 1971; Field, 1939; Folke and Neil, 1971; Jansky, 1965; Lambertson, 1961; Schmidt-Nielsen and Scaling, 1984). However, some organs contribute much less to RMR. These include bone, white adipose tissue and skin. The relatively large contribution of skeletal muscle to RMR is based on the large amount of this tissue present in the body. The percentage of oxygen usage for different organs relative to whole body usage in humans can be found in table 1.

Table 1: Percent Tissue Oxygen Use in Humans:

Tissue	Percent Body Mass	Percent Oxygen Usage
Liver	2	17
GI Tract	2	10
Kidney	0.5	6
Lungs	0.9	4
Heart	0.4	11
Brain	2	20
Skeletal Muscle	42	20

This table is modified from Rolfe and Brown (1997) and the actual values are based on experimental data from references therein (Altman and Dittmer, 1968; Aschoff, 1971; Field, 1939; Folke and Neil, 1971; Jansky, 1965; Lambertson, 1961; Schmidt-Nielsen and Scaling, 1984). Abbreviation: GI, gastrointestinal.

The values give a total percentage body oxygen usage of 88%. It is evident that skeletal muscle accounts for a fairly high percentage of body oxygen use. As mentioned

above, this is due to the fact that skeletal muscle accounts for 42% of body mass. The oxygen consumption and mitochondrial content in skeletal muscle are higher in red muscle (more oxidative or slow twitch muscle) than in white muscle (fast twitch muscle), and decreases in the order type I> IIA> IIX fibres (Conley et al, 2007).

RMR contributors can be quantified in terms of coupling to oxygen consumption, ATP turnover, and uncoupling. At the whole body level, in resting state, the mitochondria is responsible for using approximately 90% of mammalian oxygen consumption of which approximately 20% is uncoupled by the mitochondrial proton leak and 80% is coupled to ATP synthesis (Rolfe and Brown, 1997). Of the 80 percent that is coupled to ATP production, protein synthesis accounts for approximately 28%, Na^{+}-K^{+}- ATPase accounts for 19-28%, Ca^{2+}-ATPase accounts for 4-8% (however this value has recently been shown to be an underestimation, as disputed by new and more accurate methods), actinomyosin ATPase accounts for 2-8%, gluconeogenesis accounts for 7- 10%, and ureagenesis accounts for 3%. Furthermore, mRNA synthesis and substrate cycling also contribute. It is important to note, however, that there has been considerable variability in metabolic rate found between individuals but the underlying metabolic processes and specific tissues involved remain unknown.

Variability in Metabolic Rate - Possible Role of Skeletal Muscle:

Studies examining metabolic rate have shown significant variability between individuals. Only a portion of this variability among individuals was accounted for by differences in body weight; fat free mass (FFM) was found to be the best determinant of BMR

and 24 hour energy expenditure but only accounted for 60-80% of the variability between individuals (Persaghin, 2001; Roffey et al, 2006; Widdowson, 1954; Boothby and Sandiford, 1922; Ravussin, 1988). It has been shown that some individuals have BMRs which are >300 kcal/day below or above the value predicted based on their FFM (Bogardus, 1986). These studies examining the variability in metabolism were performed decades ago, and there has yet to be in depth analysis of the possible causes of this variability. To the author's knowledge there are limited studies assessing the relationship between variability in RMR and specific processes which may contribute to this variability within different tissues in the body, especially in human subjects. Furthermore, it is not clear which tissues and organs may account for this variability.

The metabolic rates of brain and kidney tissues are fairly stable and vary little throughout the day. However, the metabolism of skeletal muscle can change quite substantially from rest to maximal physical activity. For example, early reports indicated that approximately 87% of body oxygen consumption is used by skeletal muscle during heavy work in humans and 5% is used by the heart (Wade and Bishop, 1962; McGilvery, 1979). Zurlo et al, in 1990, assessed the importance of skeletal muscle metabolism as a determinant of BMR, SMR and 24 hour energy expenditure (all measured by indirect calorimetry) and compared these measures to forearm oxygen uptake. It was found that adjusted BMR and SMR, expressed as deviations from the predicted values (based on 4 covariates: FFM, fat mass, age and sex), were significantly correlated with resting forearm oxygen uptake. The findings suggested that differences in resting muscle metabolism account for part of the variance in metabolic rate between individuals. However, since these findings, there have been minimal

studies looking into what specific energy requiring processes in the muscle may account for this variability in metabolic rate.

One energy requiring process in skeletal muscle which could potentially account for the variability in whole body metabolic rate is Ca^{2+} handling. The biology of this process will be discussed in more detail later in this chapter. Since the SR Ca^{2+}-ATPase (SERCA) pump is an energy consumer and plays a very large role in Ca^{2+} handling, the investigation of SERCA and its relationship to metabolic rate could prove to be worthwhile. Early studies examined the energy contribution of SERCA based on measurements of the rate of Ca^{2+} efflux from isolated SR vesicles and then the amount of ATP required to reuptake that given amount of Ca^{2+} was calculated with the assumption that there was an optimal 2:1 Ca^{2+}:ATP coupling ratio. This method resulted in an energetic cost of 3.4-8 % of resting muscle metabolism attributable to SERCA activity (Briggs et al, 1992; Hasselbach, 1983). There is now evidence to suggest that this value is underestimated greatly. Another approach that has been used to determine the relative contribution of SR Ca^{2+} cycling to resting energy expenditure in skeletal muscle was to measure the decrease in energy expenditure following exposure of the muscle to chemicals that indirectly inhibit SERCAs by inhibiting Ca^{2+} leakage from SR Ca^{2+} release channels or ryanodine receptors (RyRs). Using this approach with direct calorimetry, Chinet and colleagues found that approximately 12–24% of resting energy expenditure in mouse soleus is related to Ca^{2+} cycling across the SR membrane (Chinet, 1992). A similar study on mouse soleus and extensor digitorum longus (EDL) muscles found that 18–22% of resting energy expenditure in both muscles is related to SR Ca^{2+} uptake (Dulloo, 1994). Given that SERCA activity accounts for a significant percentage of resting energy expenditure in skeletal muscle,

and skeletal muscle metabolism contributes 20-30% of whole body resting metabolic rate, it is possible that differences in SERCA efficiency between different individuals could explain at least part of the variability in whole body RMR between individuals. Therefore, examining the relationship between whole body RMR and the efficiency of SR Ca^{2+} transport in skeletal muscle will be the focus of the present study.

Calcium Handling in Resting Skeletal Muscle:

Calcium plays a role in many different processes which take place in cells within the body. The movement of Ca^{2+} from one compartment in the cell to another has an integral role in signalling various cellular processes. The maintenance of Ca^{2+} gradients across cell membranes is important for maintaining a potential difference across the membrane of excitable cells (Vander, 1990; Henquin, 2009). In skeletal muscle, Ca^{2+} plays a very important role in excitation-contraction coupling, energy expenditure, second messenger signalling, controlling the activities of numerous enzymes, and many other processes (Berchtold, 2000).

Skeletal muscle contraction, referred to as excitation-contraction coupling, and relaxation consist of a series of energy requiring processes. The stimulation of the motor end plate by the neurotransmitter acetylcholine leads to the depolarization of the sarcolemma membrane which propagates along the transverse tubule (t-tubule) into the interior of the muscle cell. This is followed by rapid membrane repolarization. The propagation of the action potential along the t-tubules activates and triggers a conformational change in the voltage sensitive dihydropyrodine receptors, which, in turn, triggers the opening of the RyRs in the SR. Opening of the RyRs results in Ca^{2+} release from the SR and this leads to muscle

contraction. Skeletal muscle relaxation occurs upon the termination of the action potential and the resulting closure of the RyRs, and is induced by the SR Ca^{2+}-ATPase which pumps Ca^{2+} from the cytosol into the SR, ultimately leading to skeletal muscle relaxation.

In skeletal muscle, the regulation of intracellular free Ca^{2+} levels, denoted as $[Ca^{2+}]_{f,}$ is maintained by the RyRs and SERCA pumps found in the membrane of the SR (Dulhunty, 2006). SERCA pumps are 95-110 kDa membrane proteins which are made up of 10 transmembrane helices (M1-10) and 3 cytoplasmic domains (Toyoshima, 2008). These domains consist of the actuator, nucleotide binding and phosphorylation domains. The main isoforms found in adult skeletal muscle are SERCA1a, consisting of 1001 amino acids and found predominately in fast twitch skeletal muscle, and SERCA2a, consisting of 997 amino acids and found predominately in slow twitch skeletal muscle and in the heart (Wu and Lytton, 1993).

During resting conditions, it is well established that SERCA pumps maintain a greater than 10^4-fold Ca^{2+} concentration gradient across the membrane of the SR and are responsible for keeping $[Ca^{2+}]_f$ below a value of 100-200 nM (Toyoshima, 2008). Using energy from the hydrolysis of ATP, SERCAs pump Ca^{2+} from the cytosol into the lumen of the SR. Under optimal conditions, SERCAs hydrolyze 1 mol of ATP to transport 2 mol of Ca^{2+} across the membrane of the SR (Smith, 2002; De Meis, 2001b; Inesi, 1978). However, under certain experimental conditions, partial uncoupling of Ca^{2+} transport from ATP hydrolysis can occur as a result of changes in the reaction cycle of SERCA (Smith, 2002; Mall, 2006; Reis, 2002; Inesi and de Meis, 1989; de Meis, 1998; de Meis, 2000; Arruda, 2003).

SR Ca^{2+} Leak, SERCA Pump Efficiency and Coupling Ratio:

Theoretically, the two major factors which determine the efficiency of SR Ca^{2+} transport (amount of Ca^{2+} transported from the cytoplasm and sequestered in the lumen of the SR per ATP hydrolyzed) in resting skeletal muscle are the rate of Ca^{2+} leakage out of the SR and the efficiency of SERCAs in pumping the Ca^{2+} back into the SR. Fast and slow twitch skeletal muscle have different SR Ca^{2+} leak rates and SERCA coupling ratios; this translates into differences in the efficiency of SERCA pumping and heat production/energy utilization by SERCAs (Reis et al, 2001; Reis et al 2002; Murphy et al, 2009). Theoretically, several factors could influence the rate of SR Ca^{2+} leak in resting skeletal muscle but two primary factors known to influence Ca^{2+} leak are total SERCA content and CSQ content. It is known that there is a higher density of SERCA pumps and a lower [Ca^{2+}] within the SR in fast twitch skeletal muscle because of the higher volume of SR and concentration of CSQ relative to slow twitch skeletal muscle (Murphy et al, 2009). The high density of SERCA pumps likely accounts for the higher Ca^{2+} leak rates found in fast twitch muscle as the SERCA pumps themselves appear to be the major pathway for leakage of Ca^{2+} out of the SR (Inesi and de Meis, 1989; Murphy et al, 2009). Of course, with higher SR Ca^{2+} leak, more ATP are hydrolyzed by SERCA pumps in order to maintain the $>10^4$-fold Ca^{2+} concentration gradient. Therefore, a higher rate of Ca^{2+} leak from the SR in fast twitch muscle could potentially contribute to the lower coupling ratio and hence greater heat production in fast muscle compared to slow muscle (Reis et al, 2001). The high concentration of CSQ in fast twitch muscle is necessary in order to prevent even greater SR Ca^{2+} leak in those muscles (Murphy et al, 2009). Hence, CSQ content could be an important factor in determining the rate of SR Ca^{2+} leak with lower CSQ content leading to

greater SR Ca^{2+} leak. Leakage of Ca^{2+} can also occur through the RyRs, which ultimately will have an effect on the efficiency of SR Ca^{2+} handling (Arruda et al, 2007). Furthermore, a high fat diet which is composed of high amounts of saturated fatty acids has been shown to alter the phospholipid membrane composition in skeletal muscle (Janovska et al, 2010). An altered phospholipid membrane composition of the SR can alter membrane fluidity and, therefore, Ca^{2+} leak rate from the SR (Vangheluwe et al, 2005b). Another study examining Ca^{2+} dependent heat production in both red- and white-fibre muscles from mice found that those fed a high fat diet rich in fish oils had significantly lower Ca^{2+} dependent heat production than other groups fed high fat diets rich in saturated fat (hydrogenated coconut oil) or n-6 polyunsaturated fats (corn oil) and a group fed a low-fat diet (Dulloo et al, 1994). These studies reveal the specific effect of fish oil on muscle-cell energy metabolism through interference with SR Ca^{2+} homeostasis.

As mentioned, the other factor which influences the efficiency of SR Ca^{2+} transport (ie. the coupling ratio) is SERCA pump efficiency. Under optimal conditions, the stoichiometry of SERCA pumps is 2 Ca^{2+}:1 ATP due to the stoichiometry of two Ca^{2+} binding sites and one ATP binding site on each SERCA pump subunit (Smith et al, 2002; Inesi et al, 1978; de Meis, 2001a; MacLennan et al, 1997; Toyoshima and Inesi, 2004). Figure 1 shows the reactions by which SERCA pumps Ca^{2+} into the SR.

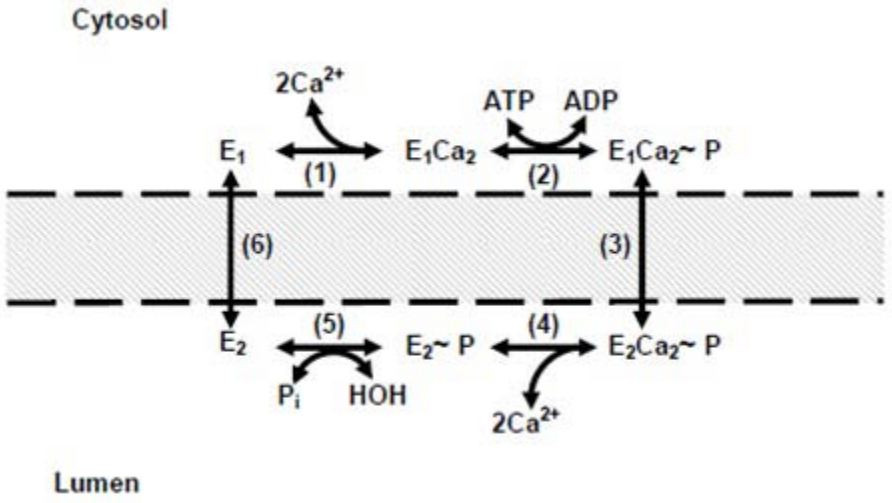

Figure 1: SERCA Reaction Cycle. Note: Figure modified from Inesi, 1985; de Meis and Vianna, 1979.

Two cytoplasmic Ca^{2+} bind (high affinity) to the Ca^{2+} binding sites which are formed by transmembrane helices M4-6 and M8 in the E1 conformation of the SERCA pump (Lee, 2002). ATP then binds to the nucleotide binding domain and is hydrolyzed. This results in the formation of a high energy phosphoprotein intermediate which can be viewed in reactions 1-2. Once the phosphorylation of the SERCA pump has occurred, a resulting conformational change in the cytoplasmic/transmembrane domain occurs due to alterations in the stalk domain of SERCA. These alterations are such that the 2 Ca^{2+} binding sites change to a state of low Ca^{2+} binding affinity and face the lumen, causing the Ca^{2+} ions to be released into the lumen of the SR. This can be viewed in reactions 3-4. The recycling of SERCA from the E2 conformation back to the E1 conformation is completed once dephosphorylation occurs. This can be viewed in reactions 5-6.

The stoichiometry of SERCA pumps has been found to vary under physiological conditions similar to resting skeletal muscle where a Ca^{2+} gradient across the SR membrane is

present. Previous in vitro studies with rabbit fast and slow twitch hind limb skeletal muscle SR vesicles showed that when a Ca^{2+} gradient is present, the Ca^{2+}:ATP stoichiometry could vary between 0.3 and 0.6 for fast twitch, and up to 1.0 for slow twitch skeletal muscle (de Meis, 2001b; Reis et al, 2001; McWhirter et al, 1987; Reis et al, 2002). A reduction in the stoichiometry of SERCA pumps such that less Ca^{2+} is taken up into the SR for every ATP hydrolyzed can occur in 3 ways as a result of changes in the SERCA reaction cycle. These mechanisms can be viewed in figure 2.

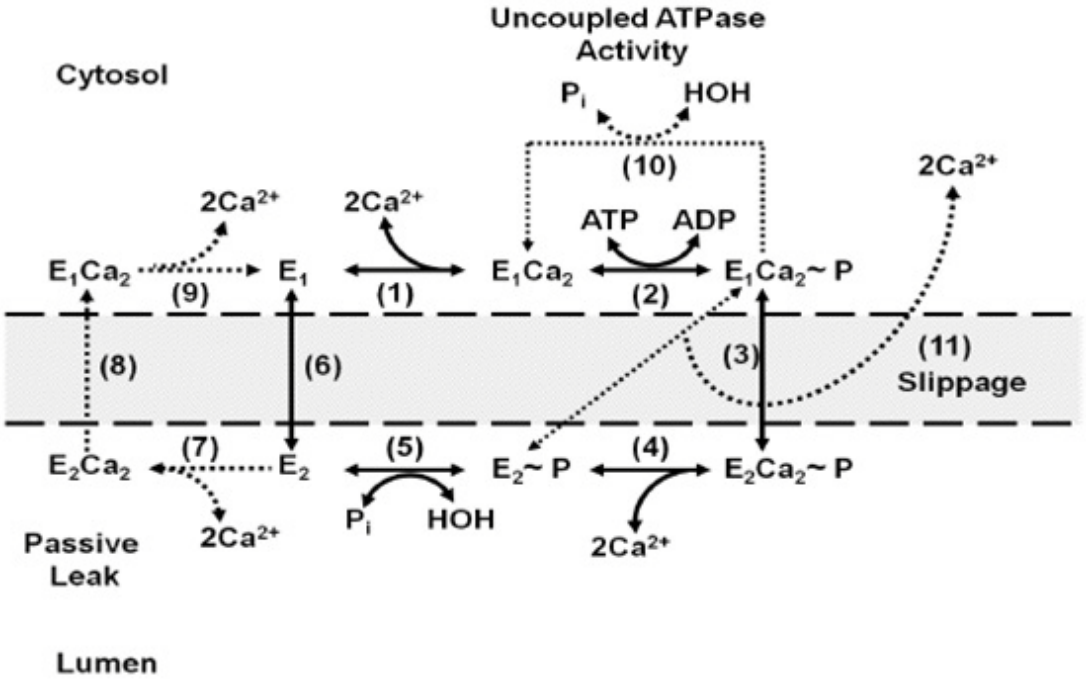

Figure 2: SERCA reaction cycle showing passive leak reactions (7-9), uncoupled ATPase activity (reaction 10) and slippage (reaction 11). Note: Figure modified from de Meis, 2001 and Mall et al 2006.

First, uncoupled Ca^{2+} efflux or passive leak can occur. This is when a high Ca^{2+} concentration in the lumen of the SR promotes the binding of Ca^{2+} to the E2 conformation of the enzyme prior to conversion back to the E1 conformation (Malls et al, 2006; Inesi and de

Meis, 1989; de Meis, 2001a; Berman, 2001). Secondly, uncoupled ATPase activity can occur. This happens when there is an increased concentration of Ca^{2+} in the SR lumen which slows down the forward conformational reaction between the E1Ca2~P and the E2Ca2~P conformations. This leads to an increased number of SERCA pumps which are in the E1Ca2~P state, thus promoting the cleavage of Pi prior to the translocation of Ca^{2+} (de Meis, 2001a; Berman, 2001; Yu and Inesi, 1995). The third mechanism is known as slippage. Slippage occurs when there is a premature release of the Ca^{2+} to the cytoplasmic side of the SR during the conformational change between E1Ca2~P and E2Ca2~P (Smith et al 2002; Malls et al, 2006; Berman, 2001). Slippage is believed to result from the E1Ca2~P conformation having a lower affinity for Ca^{2+} due to increased Ca^{2+} in the lumen and possibly to the presence of proteins which physically interact with the SERCA pumps (discussed below). Regardless of the mechanism, a reduced stoichiometry of SERCA pumps (i.e. <2Ca^{2+}:ATP) would decrease the coupling ratio and could result in a higher RMR, since relatively more ATP would be required to maintain the >10^4-fold Ca^{2+} concentration gradient. Currently, our laboratory cannot directly assess or quantify the stoichiometry of SERCA pumps; however, the IONO ratio can be used to indirectly measure SERCA efficiency. The IONO ratio is the Ca^{2+}-ATPase activity measured with IONO (a Ca^{2+} ionophore)/ Ca^{2+}-ATPase activity without IONO. A lower ratio means that the SR vesicle is more leaky (ie. due to passive leak, slippage and/or uncoupled ATPase activity).

SERCA Isoforms and SERCA Pump Efficiency:

The major SERCA isoforms expressed in skeletal muscle differ with respect to their Ca^{2+} pumping efficiency with SERCA2a being the more efficient isoform, relative to SERCA1a (Reis et al, 2002). Therefore, SERCA2a requires less ATP turnover to pump the amount of Ca^{2+} needed to maintain the $>10^4$-fold Ca^{2+} concentration gradient. Examining the factors that regulate the expression of SERCA isoforms in skeletal muscle may improve our understanding of the relationship between Ca^{2+} handling energetics and whole body metabolic rate. SERCA pumps are encoded by a family of genes, ATP2A1-3, which are highly conserved but localized on different chromosomes (Hovnanian, 2007). The SERCA isoform distribution/diversity is enhanced by alternative splicing of the transcripts, and this occurs mainly at the COOH-terminus (Periasamy, 2006). ATP2A1 is expressed in fast-twitch skeletal muscle and is alternatively spliced to encode for SERCA1a (1001 amino acids, adult) and SERCA1b (1011 amino acids, fetal) (Brandl CJ, 1987; Brandl CJ, 1986). ATP2A2 encodes for SERCA2a (997 amino acids), and is expressed in slow-twitch skeletal muscle and cardiac muscle (MacLennan, 1985; Wuytack, 1995). SERCA isoform distribution exhibits developmental regulation and in adults, SERCA expression can be regulated by neurohumoral factors (Periasamy, 2006; Sayen et al, 1992; van der Linden, 1996).

SERCA expression is both tissue specific as well as developmentally regulated. Isoform switching occurs throughout the process of skeletal muscle cell maturation; however, the regulatory process that is responsible for this is not well understood even though this process is fairly well documented (Periasamy, 2006; Olivetti et al, 1980; Lompre et al, 1991; Hoerter et al, 1981). Studies looking at embryonic development of rats have found that both SERCA2a

and SERCA1b are co-expressed in fetal stages of type II (fast-twitch) skeletal muscle development but are replaced completely by SERCA1a in adult fast-twitch muscle fibres (Anger, 1994). SERCA2a is the predominant isoform expressed in type I (slow-twitch) skeletal muscle in both the fetal and adult stages, however, SERCA2a disappears from other fibre types (Anger, 1994). The function of this isoform switching during development is not well understood.

SERCA expression can also be regulated by neurohormonal factors. Thyroid hormone regulates SERCA expression in a fibre-specific manor (Sayen, 1992; Van der Linden, 1996). Thyroid hormone increases SERCA activity of the SR in skeletal muscle, which in turn increases the energy-turnover associated with Ca^{2+} cycling during rest (Simonides et al, 2000). Studies have found there to be a 2-fold difference in resting O_2 consumption of muscle preparations between hypothyroid and hyperthyroid rats, which could be primarily due to SR Ca^{2+} cycling (van Hardeveld, 1986; Simonides, 1992, Clausen, 1986). These studies also found there to be a triiodothyronine (T3)-dependent increase in SERCA activity. A 2-fold increase in muscle SERCA activity from hypo- to euthyroidism (normal level) was found for slow muscle and a further doubling was observed in the transition to hyperthyroidism. On the other hand in fast muscle, T3 induced a maximal 50 % increase from hypo- to euthyroidism, with little effect in hyperthyroidism. In a study using a rat model to determine changes in SERCA isoform with different levels of thyroid hormone, it was found that hypothyroidism (a state of decreased T4 hormone) produced a large decrease in SERCA1a and SERCA2a mRNA levels in soleus muscle, whereas in EDL muscle it was found that SERCA1a mRNA decreased, and SERCA2a mRNA increased to 175 % of control values (Sayen, 1992). Also occurring with hypothyroidism

is a decrease in SERCA activity. This same study showed that muscle-specific, as well as SERCA gene-specific changes occur with acute administration of T3 to hypothyroid rats. In soleus muscle, T3 had a small effect on SERCA1a and SERCA2a mRNA levels, but in EDL T3 was seen to increase SERCA1a mRNA levels by 3-fold from its hypothyroid level and decrease SERCA2a mRNA to 75 % of control levels. It is important to note that a major inclusion criteria for our study was that the participants could not have either hypo- or hyper-thyroidism, since it has been previously found that RMR in hypothyroid mammals is 70 % of euthyroid (control) values, and hyperthyroidism is 150 % of euthyroid values (van Hadeveld, 1986). Thus although plasma T3 levels were not measured in this study it was assumed that the participants were in a euthyroid state.

Exercise training has also been shown to alter SERCA isoform expression. In a study looking at SERCA isoform expression in human vastus lateralis after 5 weeks of endurance cycling training, a significant down regulation of SERCA2a protein and a tendency ($p=0.055$) to have a lower SERCA1a content resulted (Majerczak, 2008). This was also accompanied by lower plasma thyroid hormone concentration. This reinforces the idea that thyroid hormone is a major regulator of the expression of SERCA isoforms in skeletal muscle. Another study found significant increases in the gastrocnemius SERCA2a mRNA expression after both moderate and high intensity exercise training but no significant changes in SERCA1a expression (Kubo et al, 2003). It should be noted that individuals in the present study had various levels of physical activity, although none of them were taking part in any kind of endurance or fitness training. One of the inclusion criteria was that participants cannot take part in more than 30 minutes of exercise, >3 times per week on average.

Regulation of SERCA Activity and Efficiency by PLN and SLN:

Sarcolipin (SLN) and PLN are known SERCA regulatory proteins which have been shown to physically interact with the transmembrane domain of SERCA molecules (Morita et al, 2008; Bhupathy et al, 2007; Odermatt et al, 1998). Two of these helices (M4 and M6) which make up part of the transmembrane domain also specifically make up part of the Ca^{2+} binding site. Thus, when either SLN or PLN are bound to SERCA, the Ca^{2+} binding affinity is altered which leads to increased slippage and Ca^{2+} being released to the cytosol before it has a chance to be sequestered into the SR lumen.

PLN is a 52 amino acid transmembrane protein that binds with SERCA2a and lowers the apparent Ca^{2+} affinity for the PLN-SERCA2a complex (Simmerman and Jones, 1998). More specifically, dephosphorylated PLN has been shown to interact with SERCA2a and reduce its apparent affinity for Ca^{2+} (Hicks, 1979; MacLennan, 1997). Phosphorylation of PLN removes its inhibition on SERCA and facilitates Ca^{2+} transport into the SR lumen (Lindemann, 1983; Kranias, 1985). One study found that dephosphorylated PLN reduces the affinity of SERCA as well as the apparent efficiency of the Ca^{2+} transport system in cardiac SR, especially at low [Ca^{2+}] (ie. resting muscle) (Frank et al, 2000). Furthermore, the phosphorylation of PLN was shown to enhance the SR Ca^{2+} transport coupling ratio (Frank et al, 2000). A recent study from our laboratory showed that PLN protein is not expressed in mouse skeletal muscle (Tupling et al, 2011); however, PLN protein is abundant in human skeletal muscle where it plays an important role in the regulation of SERCA activity (Damiani et al, 2000; Rose et al, 2006).

SLN, a 31 amino acid protein, has a fairly similar sequence identity and gene structure as PLN (Wawrzynow et al 1992; Odermatt et al, 1997) and is also an inhibitor of SERCAs

(Odermatt et al, 1998; Asahi et al, 2002; Asahi et al, 2003). Like PLN, SLN has also been shown to cause the uncoupling of Ca^{2+} uptake from ATP hydrolysis by the SERCA pumps (Smith et al., 2002; Mall et al., 2006). In two separate *in vitro* studies by the same group, it was found that the presence of SLN in reconstituted membrane vesicles containing SERCA resulted in uncoupled ATP hydrolysis (Smith et al., 2002) and increased the amount of heat released per mol of ATP hydrolyzed (Mall et al., 2006). In a more recent unpublished study from our laboratory, SERCA activity and Ca^{2+} uptake in muscle homogenates from the soleus were compared between SLN-null and wild-type mice under conditions of a Ca^{2+} gradient (Bombardier, 2010 unpublished data). In that study, the calculated transport efficiency (ie. the coupling ratio) was increased by roughly 20% in the SLN-null mice compared with wild type suggesting that SLN causes slippage of SERCA pumps and lowers their efficiency *in vivo.*

The fact that both SLN and PLN have been shown to uncouple ATP from Ca^{2+} transport by SERCA and increase the amount of heat released per mol of ATP hydrolyzed through slippage during the reaction cycle of SERCA means that these regulatory proteins are playing a role in the efficiency of the SERCA pumps, and could ultimately be related to whole body metabolic rate. Currently, our laboratory is in the process of establishing Western blotting procedures for the detection of SLN protein in human skeletal muscle samples. Since this procedure was not available in time for this thesis, SLN protein content could not be examined at this time. However, PLN protein content was assessed for this thesis and future analyses on the samples collected for this thesis will include measurement of SLN protein content.

Objectives:

The primary objective of this thesis was to investigate whether there is a relationship between the efficiency of SR Ca^{2+} transport (assessed by the coupling ratio) and RMR in humans by performing cross-sectional analyses on muscle samples obtained from a group of healthy, weight-stable individuals. Theoretically, the main factors which influence coupling ratio are Ca^{2+} leak and SERCA pump efficiency, so examination of the relationship between RMR and these two factors were carried out. Furthermore, the factors which influence Ca^{2+} leak and SERCA pump efficiency were examined, in order to determine which factors may play a significant role in influencing the coupling ratio and the relationship between coupling ratio and RMR. Two main properties that could influence Ca^{2+} leak are total SERCA expression and CSQ content. The main factors which determine the efficiency of SERCA pumps are slippage, passive leak and uncoupled ATPase activity. Currently, our laboratory is unable to directly assess or quantify the efficiency of SERCA pumps; however, the IONO ratio can be used as a surrogate marker of SERCA efficiency. Furthermore, SERCA isoform distribution (as assessed by SERCA1a/SERCA2a expression) and PLN content, two major SR properties which may influence the efficiency of SERCAs, were also assessed in the present study.

Specific Hypotheses:

It was hypothesized that:

1) Coupling ratio (amount of Ca^{2+} transported into the lumen of the SR from the cytoplasm per ATP hydrolyzed) would be negatively correlated with RMR

2) SR Ca^{2+} leak would be negatively correlated with coupling ratio and positively correlated with RMR

3) IONO ratio would be positively correlated with coupling ratio and negatively correlated with RMR

4) Total SERCA content would be negatively correlated with coupling ratio and positively correlated with RMR

5) CSQ content would be positively correlated with coupling ratio and negatively correlated with RMR

6) The ratio of SERCA1a/SERCA2a expression would be negatively correlated with coupling ratio and positively correlated with RMR

7) PLN content would be negatively correlated with coupling ratio and positively correlated with RMR

CHAPTER TWO: METHODS

Recruitment of Participants:

Recruitment for the study was from the University of Waterloo and from the general Kitchener-Waterloo population. For the first 3 weeks of recruitment, the advertisements stated that the study was looking for individuals who have either a "very fast metabolic rate, who tended to stay at a low weight, or a very slow metabolic rate, who tended to have trouble losing weight". This was done initially in an attempt to recruit a study population with a large spread of RMR values. A sample size of 9 participants was obtained using this strategy. However, 3 weeks into the recruitment, the advertisement was changed to state that the study was looking for "healthy normal weight and overweight individuals". This was done in order to obtain a group of participants with a broad range of BMI and RMR. A sample size of 16 participants was obtained using this strategy. Thus, individuals of all BMI's were accepted into the study. In total, twenty five individuals (5 females and 20 males) were recruited for the study through class announcements and advertisements. Group and individual participant characteristics are presented in the Results and Appendices, respectively.

Study Design:

The participants came in for an introductory session where height, weight, waist and hip circumference, and BMI were assessed. The participants read and signed the Informed Consent letter and filled out a Health Status Form. The purpose of the Health Status Form was to screen the participants for any contraindications for participation in the study. After the introductory session the participants came in on three separate occasions spanning

approximately 3 weeks in total, for different protocols and procedures. On the first day, RMR was measured by indirect calorimetry and body composition was assessed using bioelectrical impedance analysis (BIA). The second session involved measurement of body composition using dual energy x-ray absorptiometry (DXA). However, body composition was only assessed using BIA for the first nine participants that completed the study, because the DXA scanner was not available initially. However, 5 of the participants were able to come in 2 to 3 months after they completed the study to reassess their body composition using a DXA scan. As an alternative for the 4 participants who were not able to come in, DXA values were calculated for these subjects from a regression analysis between BIA and DXA measures from all participants as described below. This was done for participants 2, 5, 6 and 9. The third and final session involved collection of muscle biopsy and blood samples. Blood samples were analyzed for cholesterol (total, LDL and HDL), free fatty acids (FFA), triacylglycerols, glucose and insulin, to verify normal levels for each parameter. Participants were also asked to wear an activity arm band and fill out a 3 day diet and activity logs on their own time. It is important to note that data collected on all females took place during the follicular stage of their menstrual cycles.

The exclusion criteria for the study were as follows: 1) diabetes (type I or II), 2) diagnosed with abnormal thyroid function, such as hyper or hypo-thyroidism, 3) current use of antidepressants, birth control or other medication that may cause weight-gain, 4) smoking or use of illegal drugs, 5) allergies to dental freezing or any other local aesthetic, 6) allergies to rubbing alcohol or iodine, 7) previous leg muscle biopsies, 8) previous abnormal scarring or trouble healing, 9) current participation in physical exercise for more than 30 min/day, 3

times/week. The key inclusion criterion was that the participants were weight stable in the five months prior to starting the study and for the duration of the study. Participants were asked to maintain their current normal diet and activity patterns for the duration of the study. The protocols received clearance by the Office of Research Ethics at the University of Waterloo.

ANALYTICAL PROCEDURES

Diet and Activity Logs and Sensewear Arm Bands:

In order to verify that the participants maintained a state of caloric balance during the study, as they were instructed to do so that no metabolic adaptive processes would be activated that could confound the main results, the participants were each given diet and activity log sheets to record a detailed account of their daily diet and activity for 3 days. The participants were instructed to provide detailed logs of their caloric intake and expenditure, and were given detailed instructions on how to record the intensities and durations of their daily activities. They were asked to record their food intake using measuring cups at the time of the meal and to include all condiments, spices and sauces. Participants recorded the amount and detailed description of the food they were consuming over 1 weekend day and 2 week days, in order to get a measure of the caloric intake each day. The diet log was analyzed using the Food Processor SQL V. 10.8.0 dietary analysis software which provided a detailed analysis of the caloric intake of the participants. Participants recorded the amount their activity levels over 1 weekend day and 2 week days in two categories, activities of daily living and physical activity. The number of hours spent doing each activity was recorded and

analysis was completed to obtain a daily energy expenditure in kcal/day. The energy expenditure (per minute) was computed using both the individual's body weight and the number of metabolic equivalents (METS) required to perform the activity (Ainsworth et al, 2000). Specifically, one MET is equal to 0.0175 kcal/kg/min. Thus, the formula to compute caloric expenditure during the activity is:

Energy Expenditure (kcal/min) = 0.0175 kcal/kg/min/MET * METS * body weight (kg)

In order to obtain an energy expenditure expressed in kcal/day, the energy expenditure in kcal/min was multiplied by the time the activity was performed (in minutes) and resulting energy expenditures for each activity were summed. In addition to the self-reported daily activity, the participants were asked to wear a Sensewear arm band during the same 3 days that the activity log was filled out. The arm band, which was worn on the back of the participant's upper arm (ie. on the triceps muscle) for 3 full days, contains an accelerometer to measure motion and several other sensors to measure electrical conductivity and temperature of the skin and the rate of heat dissipation from the body. The armband data was analyzed using the Sensewear software to provide a quantitative measure of daily energy expenditure, hours spent doing physical activity (and the level of the physical activity), hours spent sleeping, number of steps and METS. The energy balance was determined by subtracting the energy expenditure (quantified from both the activity logs and the Senseware armbands) from the energy intake (quantified from the diet logs) to generate 2 energy balance values that could be compared. Furthermore, the body weight of each participant was measured during 3 sessions over approximately 3 weeks of participation in the study to

determine if participants remained weight-stable throughout the study which should be the case if the participants maintained a state of energy balance during the study.

Resting Metabolic Rate:

RMR was quantified using indirect calorimetry. Resting VO_2 and VCO_2 were measured using the Vmax breath by breath system. The participants were asked to come to the lab between 6:30-8:30 am in a fasted state to have their resting metabolic rate measured. Participants were connected to the Vmax system with a face mask and laid in a still position for 50 minutes while the expired gas concentrations of O_2 and CO_2 were measured. Note that the participant was in a dark room and was told to stay as still as possible for the duration of the test, without falling asleep. The most stable 10 minutes of the test time were selected for analysis and the averages at every 20 seconds were used to determine VO_2 and VCO_2. These values were plugged into the Weir Equation,

$kcal/min = [(3.941*VO_2*1000)+(1.106*VCO_2*1000)]$,

to determine the participants energy expenditure (Weir and De, 1949). The RMR values were then normalized to FFM, since FFM has been shown to be the best predictor of energy expenditure (Ravussin et al, 1981).

Body Composition Measures:

The body composition of the participants was determined using dual energy X-ray absorptiometry (DXA), which provides quantitative measures of lean tissue mass (or fat free mass, FFM) and fat mass (FM) for the whole body and specific regions. The scan was

completed and analyzed by the Medical X-ray Technologist. The main values of interest were the whole body FM and FFM. Due to the fact that the DXA scan was not available during the time that 4 of the participants took part in the study, some calculations for DXA values had to be completed using bioelectrical impedance analysis (BIA). BIA determines the electrical impedance to flow of an electric current which is passed through the tissues of the body via electrodes. This can be used to calculate an estimate of total body water, which can in turn be used to estimate FFM and FM. For the BIA test the participant was connected to the BIA machine by placing 2 electrodes on the participant's right hand and 2 electrodes on their right foot. The participant was then asked to lay supine with their hands placed to the sides of the body. Once the participant was connected, the machine was turned on and the resistance (R_{50}) and reactance (Xc) measures were recorded. These values are plugged into the Kyle Equation,

fatt free mass (FFM) = $-4.104+(0.518Ht^2/R_{50})+(0.231*Wt)+0.130*Xc)+(4.229*sex)$,

where male=1 and female=0, Ht^2 is height squared, Wt is weight (Kyle et al, 2004). This equation was used for the analysis of FFM in this study because of the age group it incorporates and the fact that the participants are healthy individuals (not a clinical population). Fat mass is then calculated by subtracting the participant's fat free mass from their body weight. Individuals were asked to be in a fasted state and to void their bladder prior to the assessment as extra fluid affects the accuracy of the measurements. Every participant in the study had BIA completed.

DXA uses x-rays with two different energy levels; high energy x-rays to measure bone mineral composition and low energy x-rays to measure and differentiate between fat tissue

(FM) and lean tissue (FFM). As mentioned above, since 4 of the participants did not have access to a DXA scan, some calculations for DXA values had to be completed using bioelectrical impedance analysis (BIA). The calculated DXA FM and FFM values were determined using equations based on the line of best fit when BIA and DXA values for FM and FFM were plotted against one another. This approach yielded the following equations:

FM: Y= 0.8579x + 1.766,

FFM: Y=1.138x + (-11.16),

where, x is the value in kg for BIA.

These equations were used to predict DXA values for FM and FFM for the 4 participants that did not have DXA measures of FM and FFM. In order to test the validity of these equations, the actual DXA values for FM and FFM were subtracted from the calculated DXA values for the participants that had measures from both DXA and BIA (see Appendix B).

Biopsy Procedure:

Muscle tissue samples were obtained from the vastus lateralis from one leg with use of the needle biopsy technique. The tissue was obtained by a trained technician using sterile equipment under sterile conditions with the following procedures. A 1 cm incision was made in the skin and fascia and 2 samples were removed using the biopsy needle (approximately 60-100 mg of tissue per sample). The tissue was homogenized using a procedure previously described (Green et al, 2008). Homogenates were frozen in liquid N_2 and stored at -80°C for later analysis. Homogenates were used to measure SERCA activity, SR Ca^{2+} uptake, SR Ca^{2+} leak, and expression of various SR Ca^{2+} regulatory proteins.

Analysis of Cholesterol, FFA, TG, Glucose and Insulin:

A venous blood sample was collected using a closed, sterile vacutainer system. Venous blood sampling was performed only by a trained/licensed technician. One blood sample of approximately 10 ml was taken, and centrifuged at 5000g for 8 min, and the resulting serum was stored at -80°C until further analysis. The blood samples were analyzed for cholesterol (total, LDL and HDL), free fatty acids (FFA), triacylglycerols, glucose and insulin. For cholesterol and triglyceride analysis, a blood sample was sent to LifeLabs. Insulin was analyzed using a Coat-A-Count Insulin kit, using a solid-phase radioimmunoassay procedure (Siemens). FFA were analyzed using a Free Fatty Acids NEFA C Wako 990-75401 procedure using a spectrophotometer (Wako, HR Series NEFA-HR (2)). Blood glucose was also measured using a Glucose monitor stick (Roche, Accu-view).

Expression of SR Ca^{2+} Handling Proteins:

Western blot analyses were used to assess the expression of SERCA1a, SERCA2a, PLN, and CSQ. Sodium dodecyl sulfate (SDS) polyacrylamide gel electrophoresis (PAGE) was performed on samples to separate proteins of interest by size (Laemmli, 1970). Equal quantities of protein were loaded into each well. For the analysis of each of the proteins, 2 gels were run, one containing samples from participant 1-13 and the other containing samples from participants 14-25. A ladder and blank were also loaded into each gel. Due to the large discrepancy in size between the proteins to be measured, different densities and types of gels were used. The density of the gel for SERCA1a, SERCA2a and CSQ was 7.5 % and the density of

the gel for the PLN western blot was 13 %. Following separation of the proteins, they were transferred to a polyvinylidene difluoride membrane (PVDF membrane, Bio-Rad, Canada) using a semi dry transfer unit at 23mV for 45 min (Trans-Blot Cell, Bio-Rad, Canada). After blocking with 5% skim milk in Tris-buffered saline (pH 7.5) for 1 hour at room temperature, the membranes were incubated with the appropriate primary antibodies. SERCA2a analysis was done with a clone 2A7-A1 antibody, PLN analysis was done with a clone 2D12 antibody and CSQ analysis was done with a clone VIIID12 antibody (Pierce Antibodies). SERCA1a analysis was done as previously described (Zubrzycka-Gaarn, 1984). After washing in Tris-buffered saline 0.1% Tween, the membranes were treated with the appropriate secondary antibody for 1 hour. The membranes were then washed again and the signals were detected with an enhanced chemiluminescence kit (Amersham Pharmacia Biotech, Piscataway, NJ) using a bio-imaging system and densitometric analysis performed using the GeneSnap software. All proteins were normalized to α-actin.

SERCA Activity:

Homogenates were used to determine the Ca^{2+}-ATPase activity using a spectrophotometric assay developed by Simonides & Van Hardeveld (1990) and modified by Duhamel et al to accommodate a 96-well plate (Duhamel et al., 2004). A reaction buffer (200 mM KCl, 20 mM HEPES (pH 7.0), 15 mM $MgCl_2$, 1 mM EGTA, 10 mM NaN3, 5 mM ATP and 10 mM PEP) containing 18 µL of both lactate dehydrogenase (LDH) and pyruvate kinase (PK), as well as homogenate were added to test tubes containing 15 different concentrations of Ca^{2+}, ranging between 7.6 and 4.7 pCa units in the presence and absence of the Ca^{2+} ionophore

A23817. In the absence of the ionophore, Ca^{2+} accumulates inside the SR vesicle and causes back-inhibition of SERCA pumps, which is more relevant to the physiological system found in skeletal muscle. The ionophore allows the Ca^{2+} ions to be transported across the SR membrane, and thus makes the SR more 'leaky'. This results in less back-inhibition of the SERCA pumps to occur. Aliquots of 100 µl were transferred in duplicate to a clear bottom 96-well plate, and NADH was added to start the reaction. The plate was read at a wavelength of 340 nm for 30 min at 37°C. Cyclopiazonic acid (CPA), a highly specific SERCA inhibitor (Seidler et al, 1989), was used to determine background activity which is then subtracted from the total Ca^{2+}-ATPase activity measured in muscle homogenate. All activity data were then plotted against the negative logarithm of $[Ca^{2+}]_f$ (pCa) using basic statistatical software (GraphPad PrismTM version 4) to determine maximal SERCA activity (Vmax), and EC50 (the concentration of Ca^{2+} needed to elicit 50 % of the maximum Ca^{2+}-ATPase activity). The IONO ratio, which was used as a surrogate marker of SERCA pump efficiency, was calculated as Ca^{2+}-ATPase activity with IONO/ Ca^{2+}-ATPase activity with no IONO. The IONO ratio reflects the amount of slippage, passive leak and uncoupled ATPase activity because if there is a high amount of slippage occurring, then even in the absence of the ionophore the SR vesicles will fill with Ca^{2+} relatively more slowly. This slowed filling of Ca^{2+} would result in less back-inhibition and thus the SERCA activity will be closer to the SERCA activity measured in the presence of the ionophore.

SR Ca^{2+} Uptake, Ca^{2+} leak and Coupling Ratio:

Muscle homogenates were used to determine SR Ca^{2+} uptake using the Ca^{2+} fluorophore, indo-1 as has been described in detail previously (Duhamel et al, 2007). Fluorescence signals produced by Indo-1 were collected on a dual emission wavelength spectrofluorometer (RatiomasterTM system, Photon Technology International, Birmingham, NJ). Two ml of reaction buffer (200 mM KCl, 20 mM HEPES, 10mM NaN_3, 5 µM TPEN, 5 mM oxalate and 15mM $MgCl_2$, pH 7.0 at 37 °C) were added to a four sided cuvette and mixed with 1.5 µM Indo-1. Then 3 µl of $CaCl_2$ were added to achieve an initial $[Ca^{2+}]_f$ between 3 and 3.5 µM. Prior to the addition of homogenate (approx. 500 µg protein), data collection was initiated using Felix software (Photon Technology International, Birmingham, NJ), and then ATP (5mM) was added to initiate Ca^{2+} uptake. Measurements of Ca^{2+} uptake in the muscle homogenates were made with the Ca^{2+} precipitating anion, oxalate. The curve ($[Ca^{2+}]_f$ versus time) was generated and linear regression performed on values ranging ±100nM at $[Ca^{2+}]_f$ of 500 nM and 1500 nM and the rate of Ca^{2+} uptake determined by differentiating the linear fit curve and expressed as µmoles/g protein/min. Ca^{2+} leak was assessed by the addition of CPA to the above protocol. The coupling ratio was determined by dividing SR Ca^{2+} uptake/Ca^{2+}-ATPase activity, at a matching pCa value which ranged between 5.96 and 6.74 for each participant.

Statistical Analysis:

Statistical analysis was performed using Graph Pad Prism software. The relationships between RMR and SR Ca^{2+} handling properties and between coupling ratio and other SR

properties were examined using the Pearson product-moment correlation coefficient. A one-way repeated measures ANOVA was used to determine whether the participant body weights fluctuated significantly over the course of the study.

CHAPTER THREE: RESULTS

Since this is a correlational study, data reported in the results section will be primarily group means and standard deviations (SD) and r^2 values. Individual data for each of the participants, as well as supplementary data can be found in the Appendix.

Participant Characteristics:

A total of 25 participants were recruited for the present study. Of these, 6 were females and 19 were males. Participant values for weight, height, BMI, and waist and hip circumference were collected on 3 different occasions to ensure that all participants were weight stable throughout the duration of the study. The participant descriptive characteristics mean values are presented in Table 2. Individual participant descriptive characteristics are also presented in Appendix A.

Table 2: Participant Descriptive Characteristics

Weight	Height	BMI	Hip Circumference	Waist Circumference	Age	RMR
72.8	174.6	23.9	99.0	81.4	22.2	29.9
(21)	(8.0)	(6.2)	(9.1)	(6.2)	(3.6)	(3.4)

Data are means ± (SD). Weight is expressed in kg, height is expressed in cm, BMI is expressed In kg/m^2, waist and hip circumference are expressed in cm, age is expressed in years and RMR is expressed in kcal/kg lean/day. Abbreviations: BMI, body mass index; RMR, resting metabolic rate.

A frequency plot of values for BMI can be found in Figure 3. Our recruitment strategy resulted in a study population which is slightly oversampled at the low/lean end of BMI with 12% (3/25) of the participants considered underweight (i.e. BMI<18.5), 52% (13/25)

considered normal weight (i.e. BMI 18.5 – 24.9), 20% (5/25) considered overweight (i.e. BMI 25.0 – 29.9), 8% (2/25) considered obese class I (i.e. BMI 30.0 – 34.9) and 8% (2/25) considered obese class II (i.e. BMI 35.0 – 39.9) according to the Health Canada issued guidelines for body weight classification in adults (Katzmarzyk and Mason, 2006). According to Statistics Canada 2007-2009, the distribution of BMI for 18 to 39 year old men was found to be 44.2 % normal weight, 36.2 % overweight and 18.4 % obese class I, II, and III. The distribution of BMI for 18 to 39 year old women was found to be 5.0 % underweight, 52.4 % normal weight, 22.9 % overweight and 19.7 % obese class I, II, and III.

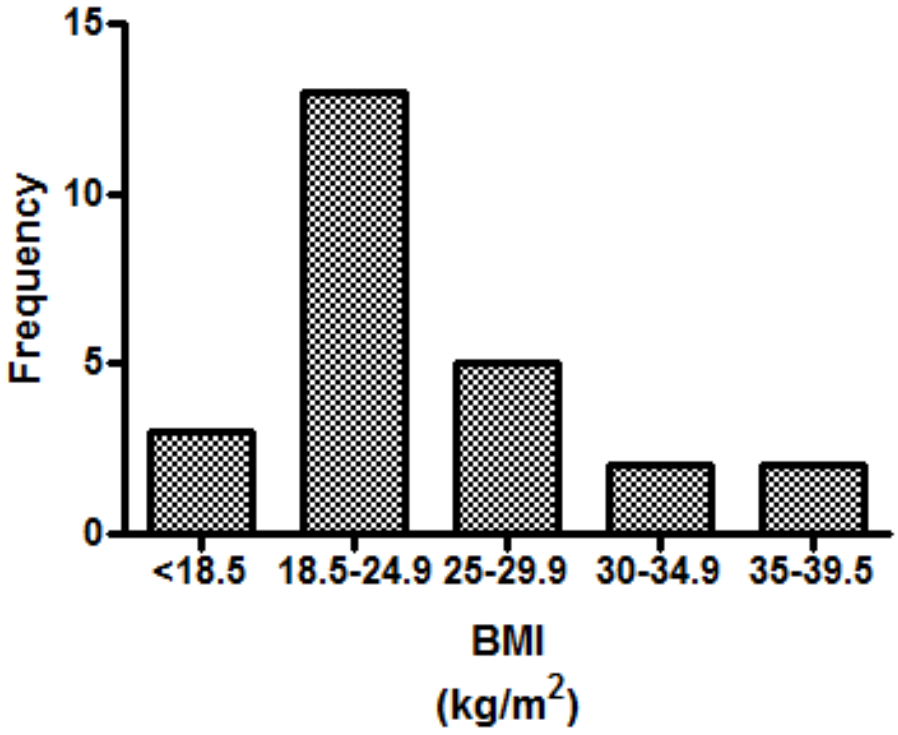

Figure 3: Frequency Plot for BMI (kg/m^2). Abbreviation: BMI, body mass index.

DXA Body Compositional Measures:

DXA scans were only completed for 23 of the 27 participants in this study due to the fact that 4 participants did not have access to the DXA scanner at the time of their participation in the study. Therefore, a computed DXA value was completed for these 4 subjects using the calculation described in the methods section. The mean values for the DXA scan body compositional measures are presented in Table 3 and the individual participant values can be found in Appendix B.

Table 3: DXA Body Compositional Measures.

FM	FFM	%Fat	%Lean	Lean mass/Ht^2	Appendicular lean mass/Ht^2
18.0	50.0	24.0	71.4	9.0	17.8
(11)	(12)	(9.0)	(9.1)	(2)	(3.1)

Data are means $\pm$ SD. FM is expressed in kg, FFM is expressed in kg, %Fat is expressed as a percentage of total body mass, %Lean is expressed as a percentage of total body mass, lean mass/Ht^2 is expressed in kg/m^2 and appendicular lean mass/Ht^2 is expressed in kg/m^2. Abbreviations: FM, fat mass; FFM, fat free mass; Ht, height.

Energy Balance Assessment Using Diet and Activity Log Data:

At the time of this study, participants reported that they had been weight stable for a period of at least 5 months and they were instructed to maintain their habitual diet and physical activity levels throughout the study. Participants had their weight measured each time they came in for a study session and it was found that there were no significant differences in weight between all 3 measures for all individual participants spanning a period of approximately 3 weeks as assessed by one way repeated ANOVA ($p=0.13$). Thus, body

weight was stable over the course of the study which suggests that participants were in a weight and energetic steady state. Therefore, it can be assumed that the study measurements were not influenced by acute changes in energy balance.

Diet and Activity logs were also completed by each of the participants over 3 days in order to verify the assumption that energy balance (intake – expenditure) of the participants was maintained over the course of the study. The mean daily caloric intake and expenditure data for the participants can be found in Table 4 and the individual participant values can be found in Appendix C.

Table 4: Diet and Activity Log Data.

Day 1:			Day2:			Day 3:			Average
Intake	Expen	Balance	Intake	Expen	Balance	Intake	Expen	Balance	Balance
2503	3084	-581	2881	2957	-215	2198	3095	-897	-564
(987)	(1119)	(1210)	(3120)	(978)	(3442)	(753)	(1011)	(920)	(1500)

Data were collected over a 3 day period (1 weekend and 2 week days) for both diet and activity logs in order to determine the energy balance of the participants. A description of the diet and activity logs can be found in the Methods section. Data are means $\pm$ SD. Caloric intake, expenditure and balance are expressed in kcal/day. The average balance is the energy balance over a 3 day period in kcal. Abbreviations: Expen., expenditure.

The mean calorie intake for a 3 day period was found to be 2527 $\pm$ 1180 kcal and the mean caloric energy expenditure for a 3 day period was found to be 3046 $\pm$ 1010 kcal (Appendix C). The goal was to have the participants in a state of energy balance for the duration of the study. Based on the diet and activity logs, the participants had a net negative daily energy balance of -564 $\pm$ 1500 kcal on average. However, these logs can be inaccurate depending on how vigilant the participants are in filling them out correctly. Studies have

shown that participants tend to under-report their energy intake and over-report their energy expenditure through physical activity (Garriquet, 2008; Scaqlius, 2009).

Energy Balance Assessment Using Sensewear Arm Band Energy Expenditure Data:

Daily energy expenditure of the participants was also assessed using Sensewear arm bands as described in the Methods. The mean daily caloric expenditure data for the participants from the Sensewear arm band recordings can be found in Table 5 and the individual participant values can be found in Appendix C. An average energy balance of 42.6$\pm$2045 kcal over a two day period was demonstrated (Appendix 6). There was found to be a statistically significant difference between energy balance values generated from the activity logs versus the sensewear armband ($p = 0.007$). This also suggests that the activity log likely over-estimated the energy expenditure. Assessment of energy expenditure with the Sensewear arm band is described in the Methods section. The Sensewear data likely quantifies energy expenditure more accurately than activity logs since it better reflects body weight measurements and verifies that participants maintained energy balance during the study period (Mackey, 2011).

Table 5: Sensewear Data:

Total Energy Expenditure: Day 1	Day 2	Average METS: Day 1	Day 2	Energy Balance Day 1	Day 2	Average Energy Balance
2759	2720	1.6	1.5	-21.6	629.5	42.6
(586)	(596)	(0.3)	(0.3)	(961)	(3580)	(2045)

Data are in means ± SD. Energy Balance is energy intake (assessed from diet log) - Sensewear armband energy expenditure. Total daily energy expenditure is expressed in kcal, Average METS is the MET values averaged over ~24 hours, Duration on Body is the number of hours the armband was recording values of the body (it is not water proof, thus could not be worn in the shower), and energy balance is 'energy intake (as assessed by the analysis of the diet log, shown in the first table in Appendix C) – total energy expenditure (assessed by the armband). Energy expenditure and balance are expressed in kcal/day. Abbreviations: METs, metabolic equivalents.

Cholesterol, FFA, TG, Glucose and Insulin:

The participant blood metabolite and hormone mean values are presented in Table 6. Individual blood metabolite and hormone values are also presented in Appendix D. Blood measures were taken in order to verify that the participants did not have any abnormal blood values, such as high insulin or blood glucose levels, and to get baseline values to characterize the health status of the participants. The majority of participant blood metabolite and hormone values were in the normal/healthy range, with the exception of approximately 2 participants being slightly over the desired range in each of the blood measures (see Appendix D) (Canadian Diabetes Association, 2008; Insulin Coat-A-Kit; NEFA C Wako 990-75401). Note that different participants were over the desired range for various blood metabolite and hormone measures. The participants who were just slightly above the normal/healthy range were in the borderline category (ie. did not have un-healthy values) and were included in all of the analyses.

Table 6: Cholesterol, TG, FFA, Glucose and Insulin.

Cholesterol	LDL	HDL	Cholesterol/HDL Ratio	Triglycerides	FFA	Glucose	Insulin
3.94	2.25	1.29	3.14	0.90	0.40	4.65	8.23
(0.8)	(0.7)	(0.3)	(0.8)	(0.6)	(0.3)	(0.5)	(5.5)

Data are means ± SD. Cholesterol, LDL, HDL, triglycerides, and glucose are expressed in mmol/L. FFA is expressed in mEq/L and insulin is expressed in µlU/ml. Descriptions of blood analysis techniques can be viewed in the Methods section. Abbreviations: LDL, low density lipoprotein; HDL, high density lipoprotein; FFA, free fatty acids.

Relationship Between RMR and Fat Free Mass:

FFM was assessed using the DXA scanner and RMR was calculated based on a standard equation (see `Methods' section for details) using values from a Vmax breath by breath system. RMR is strongly dependent on body size and body composition (Ravussin et al, 1981; Poehlman, 1992; Cunningham, 1980; Poehlman, 1993; Ravussin, 1986). Thus, to compare individuals differing in body size and composition, it is necessary to remove their confounding influence, or to normalize metabolic rate for differences in body weight (BW) or FFM. The relationships between RMR (kcal/day) and both BW (kg) and FFM (kg) for our study population were assessed using the Pearson product-moment correlation coefficient (Fig. 4). As expected, a significant strong positive correlation was found between RMR and both BW (Fig. 4A) and FFM (Fig. 4B). Although the relationship between BW and RMR tended to be slightly stronger than the relationship between FFM and RMR in this study, it is generally accepted that lean body tissues (i.e. FFM) have the highest metabolic activity relative to non-lean tissues (i.e. FM) and it is common to normalize RMR to FFM both in clinical and research settings (Poehlman, 1992; Cunningham, 1980; Poehlman, 1993; Ravussin, 1986; Himms-

Hagen J, 1997; Keys, 1973; Tzankoff, 1977). In a hallmark study in this field, it was reported that FFM was the best predictor of energy expenditure and explains more of the variability in RMR between individuals than body mass (Ravussin et al, 1981). Therefore, RMR was normalized to FFM in the present study; however, it should be noted that normalization of RMR to BW produces similar results with respect to the relationship between RMR and Ca^{2+} handling properties (data not shown). Finally, as seen in Figure 4, participants recruited for this study tended to be over sampled at the low end of FFM and RMR but there is a large spread of RMR values, which ranged from 985 kcal/day to 2479 kcal/day, with a fairly continuous distribution. Thus, the Pearson product-moment correlation coefficient was used to assess the relationship between RMR and the SR Ca^{2+} handling properties.

A)

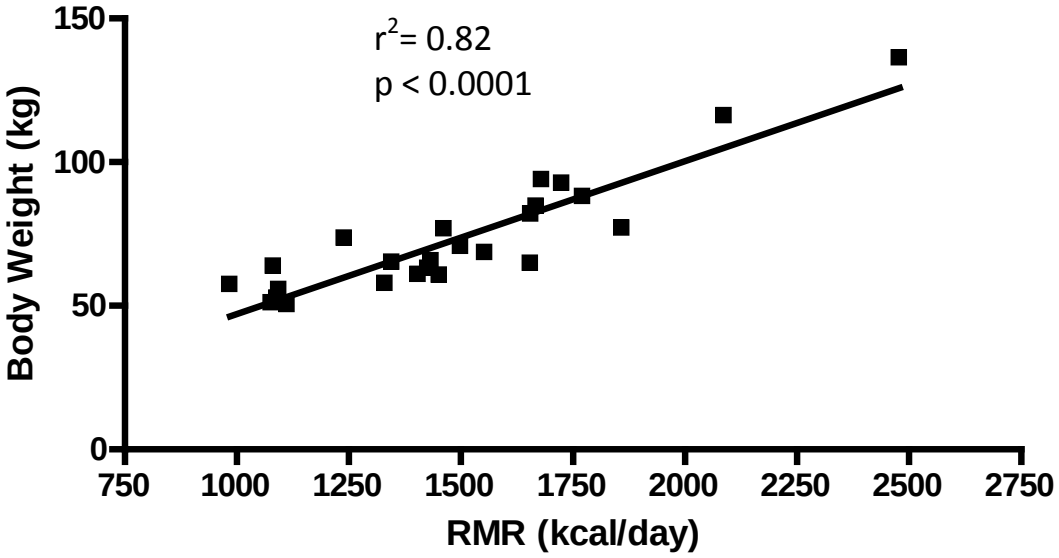

B)

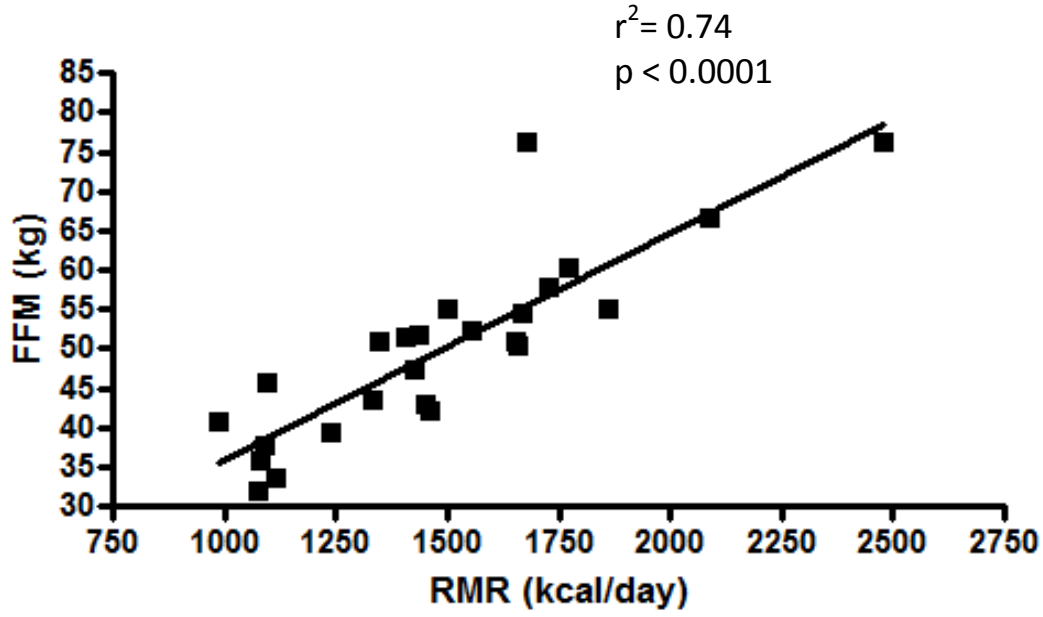

Figure 4: Correlation of RMR (kcal/day) and Body Weight (kg) (A) and RMR (kcal/day) and FFM (kg) (B). The correlation coefficient (r^2) is 0.82 ($p<0.0001$) for A, and the r^2 is 0.74 ($p< 0.0001$) for B. VO_2 and VCO_2 values were collected using a Vmax breath by breath gas collection system, and then RMR was calculated using the Weir equation as described in the Methods section. Abbreviations: RMR, resting metabolic rate; FFM, fat free mass.

Ca^{2+}Handling Properties in Skeletal Muscle:

SR Ca^{2+} handling properties were assessed *in vitro* in muscle homogenates. Values for Ca^{2+}-ATPase activity (Vmax and EC50) and IONO ratio (at Vmax) were determined using a Ca^{2+}-ATPase activity assay and values for Ca^{2+} uptake and leak were determined using a Ca^{2+} uptake assay (see Methods section). The apparent coupling ratio was calculated by dividing Ca^{2+} uptake (μmol/g protein/min) by Ca^{2+}-ATPase activity (μmol/g protein/min) at a matching pCa value which ranged between 6.74 and 5.96, which is just above resting pCa and thus simulates resting conditions as close as possible. The participant mean values for the SR Ca^{2+} handling properties are presented in Table 7. Individual participant SR Ca^{2+} handling properties are presented in Appendix E-G. All values for the SR Ca^{2+} handling properties are comparable to published values from our laboratory (Duhamel et al, 2007; Holloway et al, 2005; Green et al, 2000; Duhamel et al, 2005; Tupling et al, 2003) and others (Leppik et al, 2004; Li et al, 2002; Ortenblad et al, 2000).

Table 7: Ca^{2+}Handling Properties in Skeletal Muscle.

Vmax	EC50	IONO Ratio	Coupling Ratio	Ca^{2+} Leak
200.44	5.15	8.00	0.13	0.42
(43.10)	(0.19)	(2.6)	(0.1)	(0.3)

Data are presented in means ± SD. Vmax was assessed with IONO and is expressed in μmol/g protein/min , IONO ratio is assessed at Vmax, EC50 is expressed in *pCa*, Ca^{2+} uptake is expressed in μmol/g protein/min, Ca^{2+} leak is expressed in μmol/g protein/min, and the coupling ratio is Ca^{2+} uptake/ Ca^{2+}-ATPase activity. Abbreviations: EC50, $[Ca^{2+}]_f$ concentration to elicit 50 % of maximal Ca^{2+}-ATPase acitivty; IONO, Ca^{2+} Ionophore; IONO ratio, Ca^{2+}-ATPase acitivty with IONO/ Ca^{2+}-ATPase acitivty with no IONO.

Expression of PLN, CSQ and SERCA Isoforms:

Expression (via densitometry) of PLN, CSQ and SERCA isoforms was determined using Western Blot analysis procedures which are described in the Methods section. Mean values for expression on PLN, CSQ and SERCA isoforms are presented in Table 8 and individual values can be found in Appendix H. Expression of PLN is reported as the PLN monomer since it is the monomer that physically binds to SERCA molecules and, presumably, causes reduced SERCA pump efficiency. Note, that all values for protein expression are normalized to α-actin. Figure 5 shows the Western Blots for PLN, CSQ and SERCA isoforms on all participants. As explained earlier, expression of these SR proteins could influence the coupling ratio and may thus be associated with RMR.

Table 8: Expression of PLN, CSQ and SERCA Isoforms.

PLN (monomer)	CSQ	SERCA1a	SERCA2a	SERCA1a/SERCA2a Ratio	SERCAtotal
0.35	3.50	4.80	4.46	1.32	9.26
(0.4)	(1.2)	(1.7)	(1.9)	(0.74)	(2.6)

Data are presented in means $\pm$ SD All proteins are analyzed with Western Blot techniques and are normalized to α-actin. Densities of the various proteins are expressed in arbitrary units. Abbreviations: PLN, phospholamban; CSQ, calsequestrin; SERCA, sarco(endo)plasmic reticulum Ca^{2+}-ATPase.

Relationship between RMR and Ca^{2+} Handling Properties:

The primary objective of this study was to determine if RMR is associated with skeletal muscle SR Ca^{2+} transport efficiency in humans. SR Ca^{2+} transport efficiency was quantified by measuring the coupling ratio as described in the Methods. A lower coupling ratio would reflect a lower efficiency of SR Ca^{2+} transport. Individual values for coupling ratios can be viewed in Appendix G. The relationship between RMR and coupling ratio was assessed using

the Pearson product-moment correlation coefficient (Figure 6). There was a weak but significant negative correlation between RMR and coupling ratio (r^2= 0.21, p =0.024). As hypothesized, participants with the lowest coupling ratios tended to have higher RMRs than the participants who had the highest coupling ratios.

Given the relationship between RMR and coupling ratio, it was of interest to determine the relationship between RMR and other Ca^{2+} handling properties that have been shown to influence coupling ratio as this could provide some insight into the underlying factors that explain the relationship between RMR and coupling ratio. Theoretically, coupling ratio is determined by SR Ca^{2+} leak and the efficiency of the SERCA pumps. SR Ca^{2+} leak was measured in the absence of SERCA pump activity and, therefore, quantifies the rate of resting Ca^{2+} leak through RyR and other Ca^{2+} channels. The efficiency of the SERCA pumps was assessed indirectly by measuring the IONO ratio as described in the Methods.

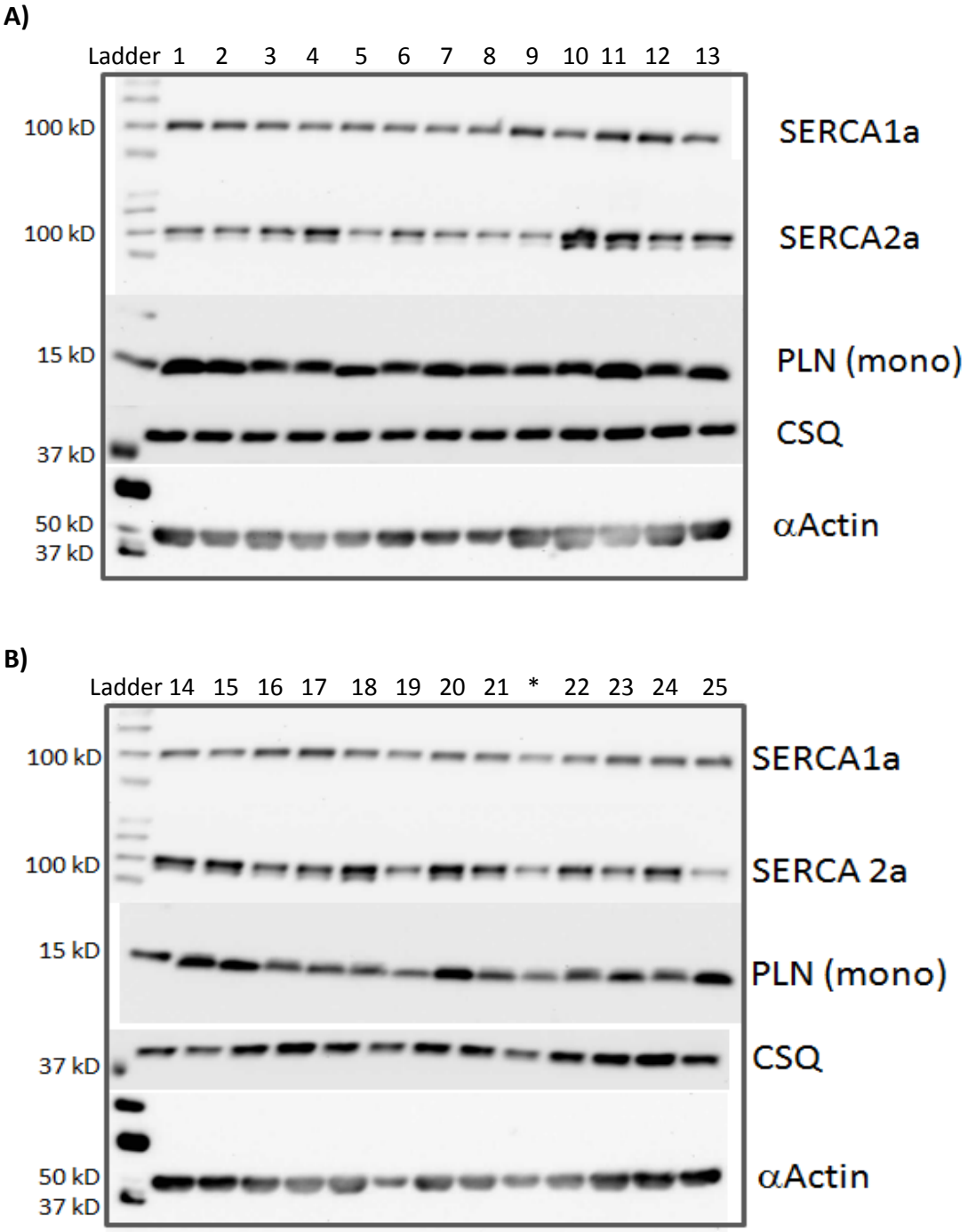

Figure 5: Western Blots for SERCA1a, SERCA2a, PLN and CSQ. Data are shown for participants 1-13 (a) and 14-27 (b). α-actin was used as a loading control. The loading control sample from only one of the membranes is shown. Note that * is indicating that this participant was not assessed in the study due to the fact that their homogenate contained a large amount of blood, which results in inaccurate measures of SR Ca^{2+} handling properties. Densities of the various proteins are expressed in arbitrary units. Abbreviations: PLN, phospholamban; CSQ, calsequestrin; SERCA, sarco(endo)plasmic reticulum Ca^{2+}-ATPase; kD, kilodalton.

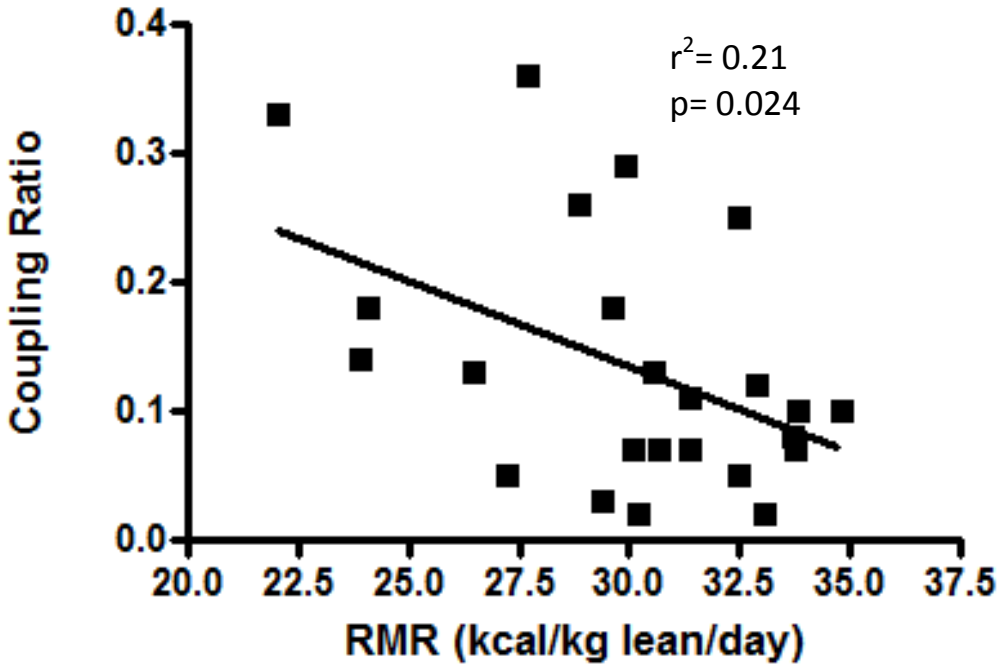

Figure 6: Correlation of RMR (kcal/kg lean/day) and Coupling Ratio. The correlation coefficient is -0.21 (p =0.024). Coupling ratio is Ca^{2+} uptake/Ca^{2+}-ATPase Activity. Abbreviations: RMR, resting metabolic rate.

RMR was found not to be significantly correlated with SR Ca^{2+} leak (r^2=0.061, p=0.24) (Figure 7). Theoretically, total SERCA content and CSQ expression are two properties that influence SR Ca^{2+} leak. Those who have increased total SERCA expression would be expected to have a higher RMR due to more Ca^{2+} leakage from the SERCA pump and those with lower CSQ may be expected to have a higher RMR due to higher free Ca^{2+} levels inside the SR which would increase the drive for SR Ca^{2+} leak (Inesi and de Meis, 1989; Murphy et al, 2009). However, since there was no relationship found between RMR and SR Ca^{2+} leak, no significant

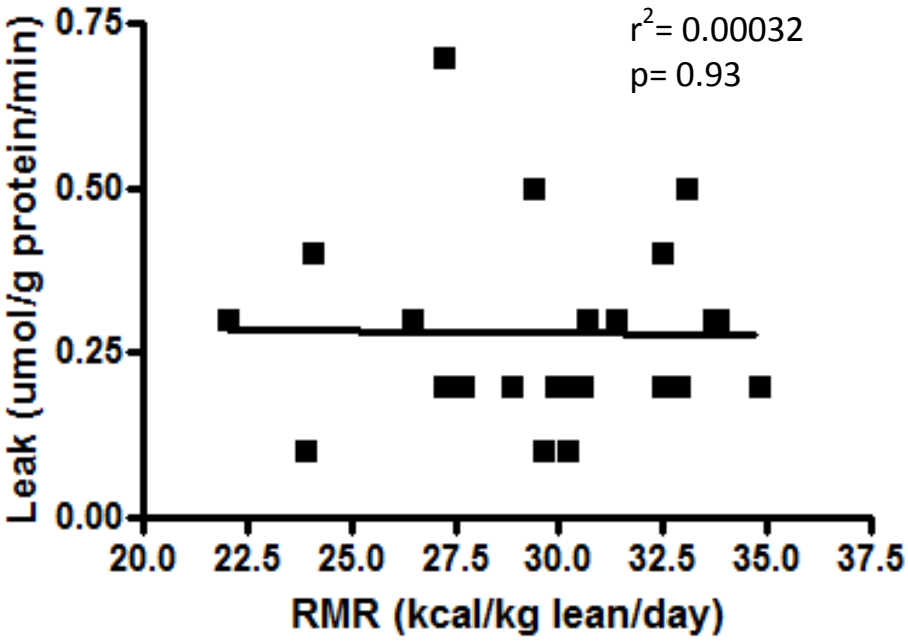

Figure 7: Correlation of RMR (kcal/kg lean/day) and Ca^{2+} Leak (uM/g protein/min). The correlation coefficient is 0.061, p =0.24. Ca^{2+} leak was assessed by completion of a Ca^{2+}uptake assay as described in the Methods section. Abbreviations: RMR, resting metabolic rate.

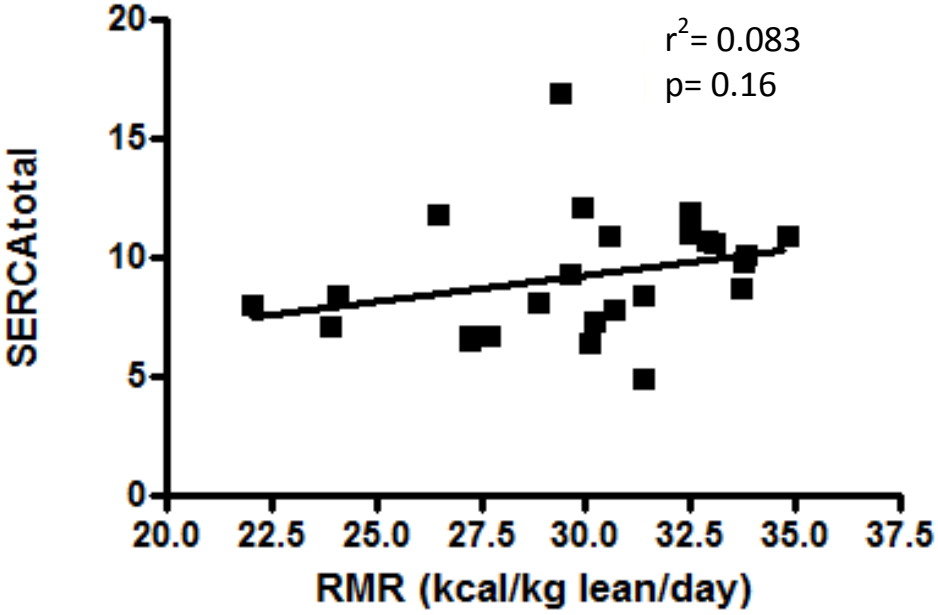

Figure 8: Correlation between RMR (kcal/kg lean/day) and total SERCA. Total SERCA is SERCA1a + SERCA2a. SERCA expression is normalized to α-actin. SERCA expression is protein density expressed in arbitrary units. Abbreviations: RMR, resting metabolic rate; SERCA, sarco(endo)plasmic reticulum Ca^{2+}-ATPase.

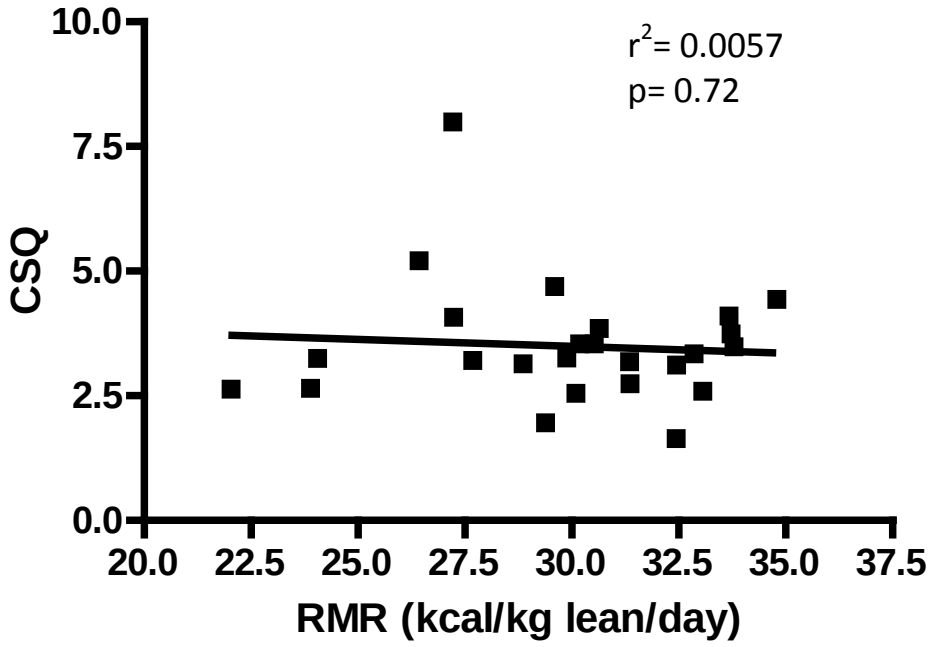

Figure 9: Correlation of RMR (kcal/kg lean/day) and CSQ. The correlation coefficient is 0.057, p =0.72. CSQ content was assessed using Western Blot Techniques and was normalized to α-actin. CSQ expression is protein density expressed in arbitrary units. Abbreviations: RMR, resting metabolic rate; CSQ calsequestrin.

relationship between RMR and total SERCA or CSQ contents would be expected in this study. Not surprisingly then, neither total SERCA content (r^2=0.083, p=0.16, Figure 8) nor CSQ content (r^2=0.0057, p=0.72, Figure 9) were found to be significantly related to RMR.

These results suggest that SERCA efficiency rather than SR Ca^{2+} leak may have a larger influence on the relationship between RMR and coupling ratio. However, the non-significant results of the correlational analysis between RMR and IONO ratio did not support that hypothesis (r2=0.027, p=0.43) (Figure 10). It has been shown that SERCA1a is less efficient

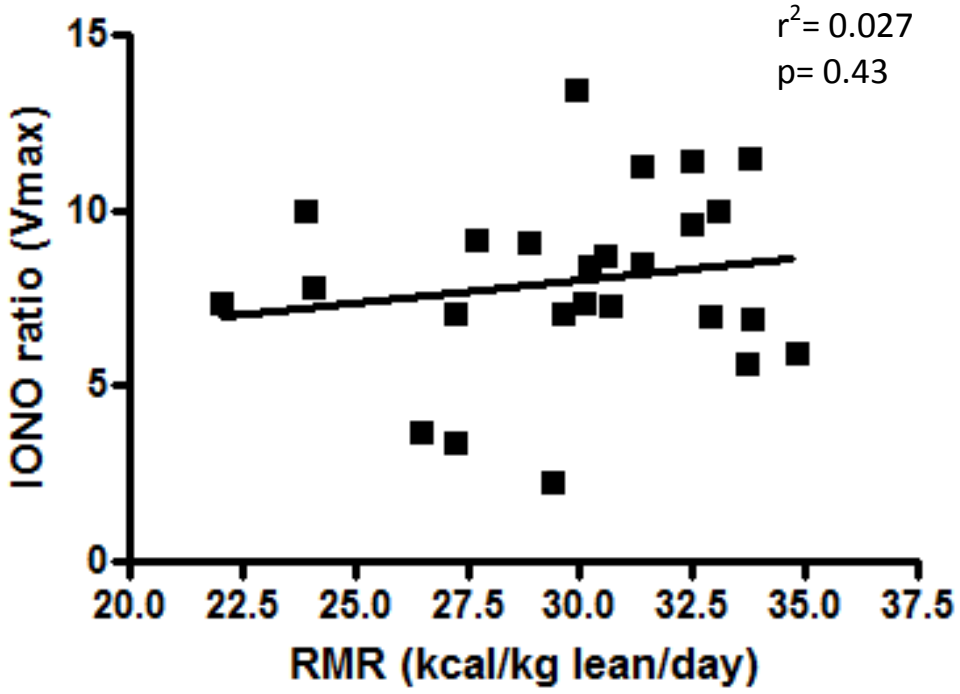

Figure 10: Correlation of RMR (kcal/kg lean/day) and IONO ratio. The IONO ratio was assessed at Vmax and is the ratio of the Ca^{2+}-ATPase activity with IONO/ Ca^{2+}-ATPase activity without IONO. Abbreviations: IONO, Ca^{2+} ionophore; RMR, resting metabolic rate; Vmax, maximal Ca^{2+}-ATPase activity.

than SERCA2a (Reis et al, 2002) and that PLN reduces the apparent efficiency of SERCA Ca^{2+} handling (Frank et al, 2000). However, since there was no relationship found between RMR and IONO ratio in this study, it would not be expected that SERCA isoform distribution (as assessed by SERCA1a/SERCA2a expression) or PLN content would be related to RMR. The correlation for RMR and SERCA1a/SERCA2a can be seen in Figure 11. Surprisingly, there was a weak but significant positive correlation between RMR and SERCA1a/SERCA2a (r^2=0.18, p=0.04). This means that those participants with higher RMRs tended to have a higher expression of SERCA1a relative to SERCA2a. On the other hand, PLN (monomer) expression was not related to RMR (r^2= 0.044, p=0.32, Figure 12).

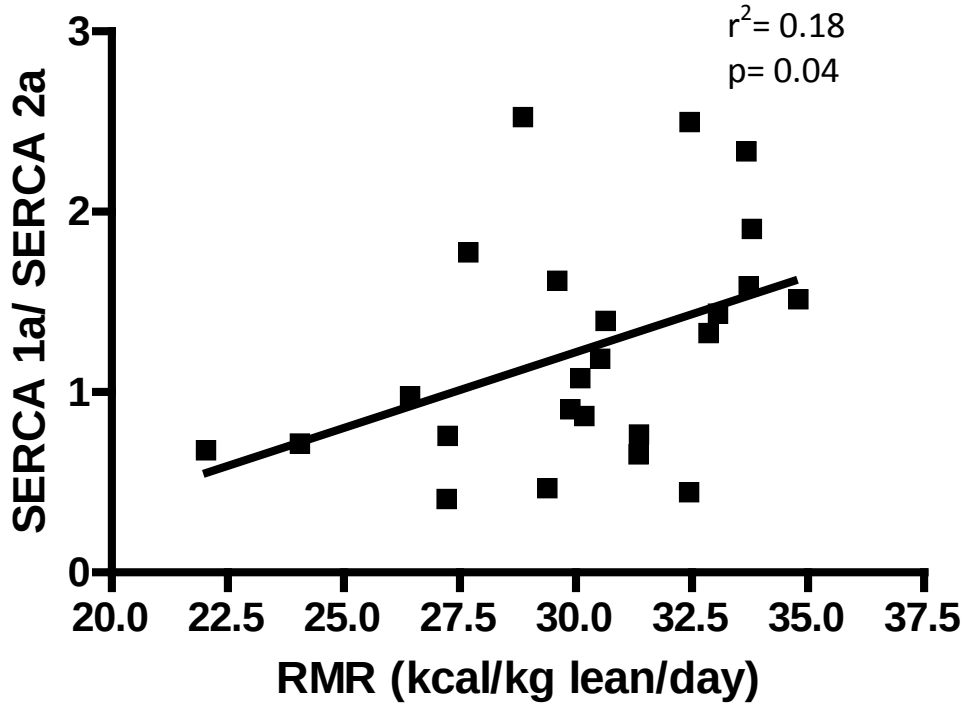

Figure 11: Correlation of RMR (kcal/kg lean/day) and SERCA1a/SERCA2a Ratio. SERCA isoform expression is normalized to α-actin. The correlation coefficient is 0.18, p=0.04. Note that there was one outlier which had to be removed. SERCA expression is protein density expressed in arbitrary units. Abbreviations: RMR, resting metabolic rate; SERCA, sarco(endo)plasmic reticulum Ca^{2+}-ATPase.

Relationship Between Coupling Ratio and Other SR Ca^{2+} Handling Properties:

Given that no relationships were found between RMR and either SR Ca^{2+} leak or SERCA pump efficiency, or the other SR Ca^{2+} handling properties that have been known to play a role in influencing the coupling ratio, it was an important next step to assess whether these SR Ca^{2+} handling properties are in fact related to coupling ratio, as we and others have assumed from interpreting results of previous studies.

A higher relative amount of SR Ca^{2+} leak would result in a lower coupling ratio and thus less efficient SR Ca^{2+} handling (Inesi and de Meis, 1989; Murphy et al, 2009). However, our analyses revealed no significant relationship between coupling ratio and SR Ca^{2+} leak (r^2=0.099, p=0.13) (Figure 13). Increased CSQ content is known to result in a lower free [Ca^{2+}] within the SR, and thus would likely result in less SR Ca^{2+} leak out of the SR which would be expected to result in a higher coupling ratio (Murphy et al, 2009). However, there was no significant relationship found between CSQ content and coupling ratio (r^2=0.00082, p=0.89) (Figure 14). It is also important to assess the relationship between coupling ratio and total SERCA content, since SERCA pumps themselves have been shown to be a pathway for Ca^{2+} leak out of the SR (Inesi and de Meis, 1989; Murphy et al, 2009). Thus, it would be expected that increased total SERCA would lead to a lower coupling ratio due to increased Ca^{2+} leakage from the SR. However, this was not the case, as there was no significant relationship found between coupling ratio and total SERCA content (r^2=0.00046, p=0.92) (Figure 15).

A lower IONO ratio is reflective of a 'leaky' SR which would equate to lower SR Ca^{2+} transport efficiency. Thus, it would be expected that the lower the IONO ratio the lower the relative coupling ratio would be. However, there was no relationship found between coupling ratio and IONO ratio (r^2=0.085, p=0.17) (Figure 16). Theoretically, a higher SERCA1a to SERCA2a ratio would result in a lower coupling ratio since the SERCA1a isoform is relatively less efficient than SERCA2a and this would lead to less efficient SR Ca^{2+} handling. Although SERCA1a/SERCA2a was significantly correlated to RMR, surprisingly SERCA1a/SERCA2a was not found to be significantly related to coupling ratio (r^2=0.085, p=0.18) (Figure 17).

Theoretically, a higher PLN content would lead to a lower relative coupling ratio due to the fact that PLN reduces the apparent efficiency of SERCA Ca^{2+} handling (Frank et al, 2000). However, there was no relationship found between coupling ratio and PLN content (r^2=0.0042, p=0.76) (Figure 18).

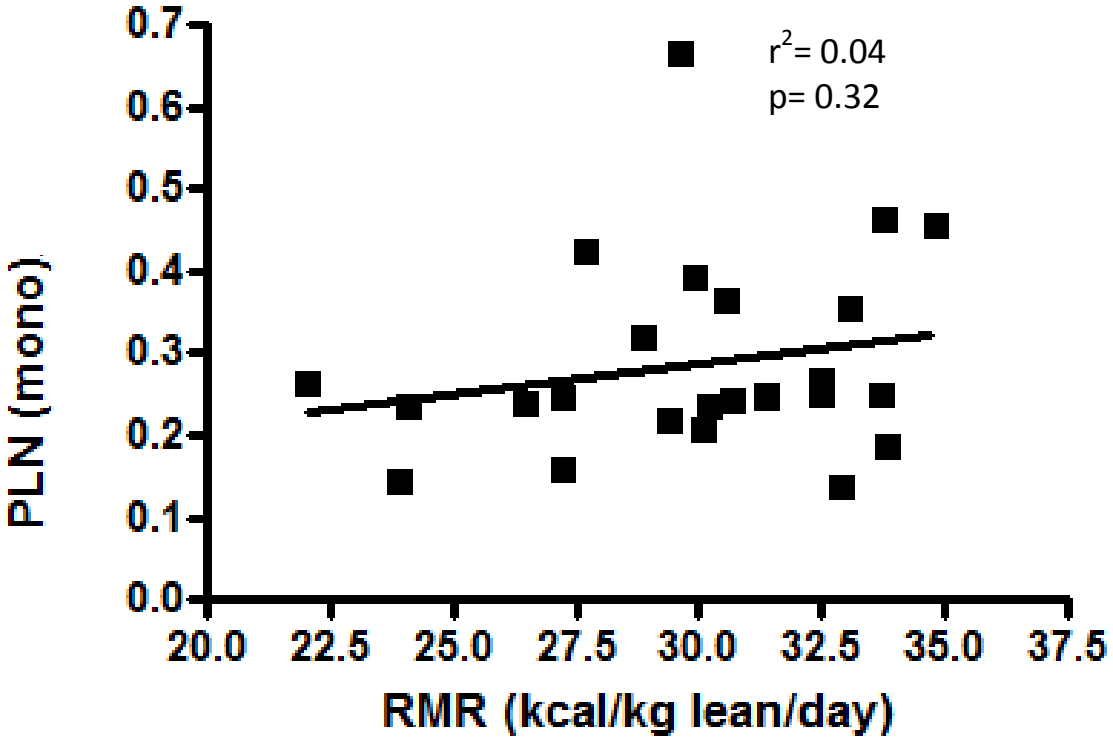

Figure 12: Correlation of RMR (kcal/kg lean/day) and PLN (monomer) Expression. PLN expression is normalized to αActin. The correlation coefficient is 0.044, p=0.32. PLN expression is protein density expressed in arbitrary units. Abbreviations: RMR, resting metabolic rate; PLN, phospholamban.

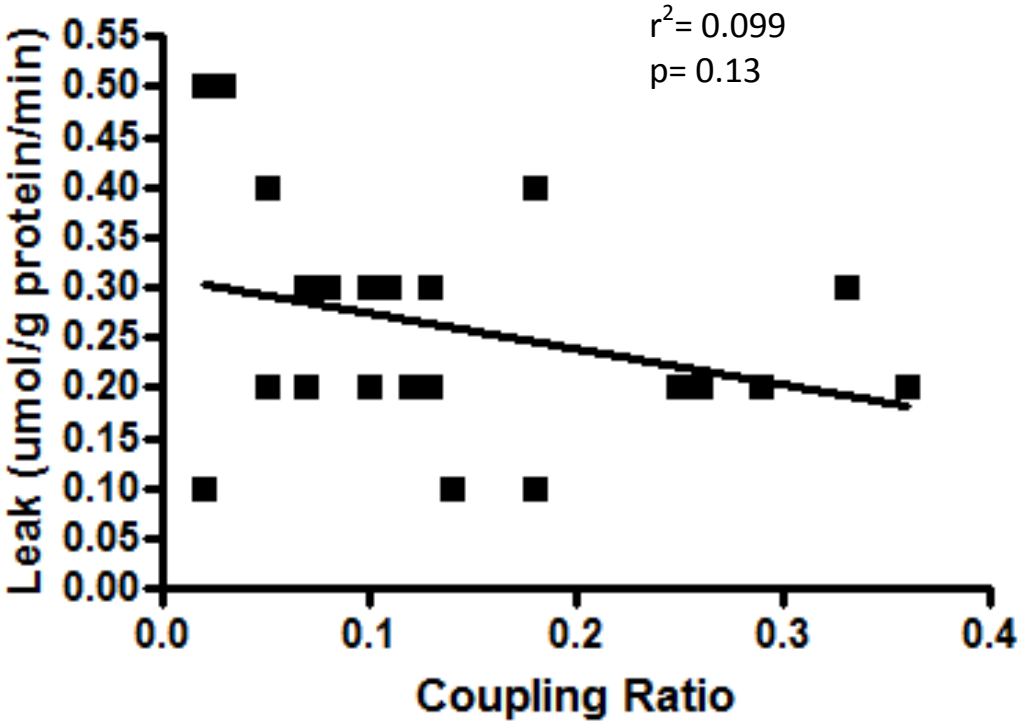

Figure 13: Coupling Ratio and Ca^{2+} Leak. Ca^{2+} Leak is measured in μmol/g protein/min.

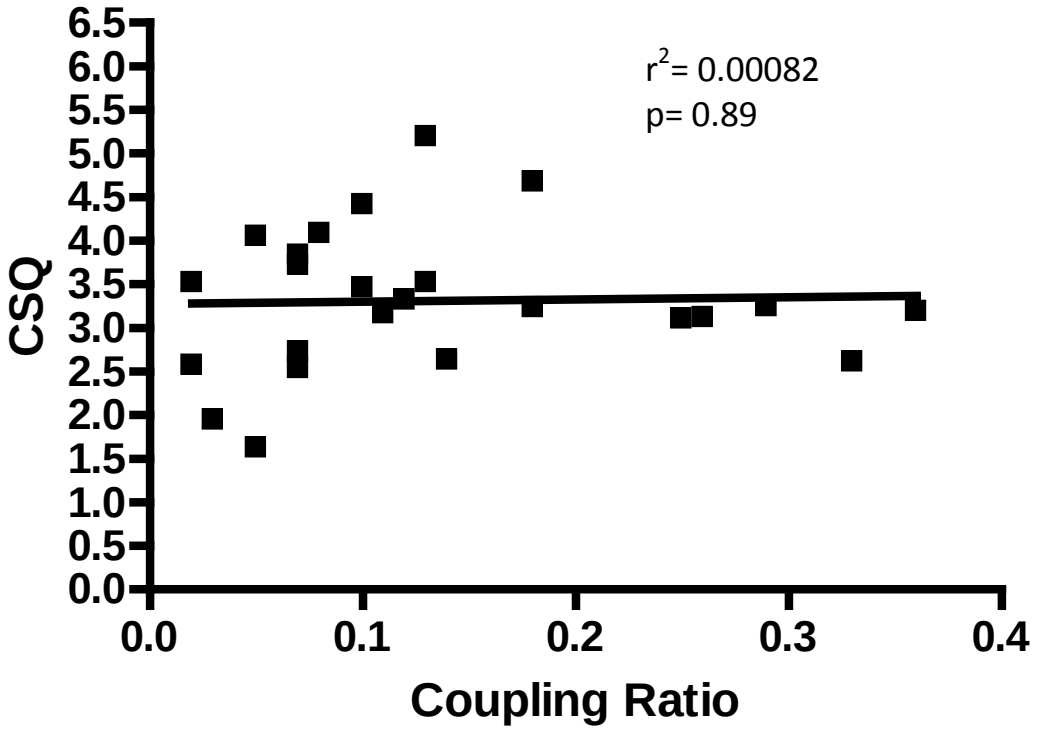

Figure 14: Coupling Ratio and CSQ. CSQ content is assessed with Western Blot techniques and is normalized to α-actin. CSQ expression is protein density expressed in arbitrary units. Abbreviations: CSQ, calsequestrin.

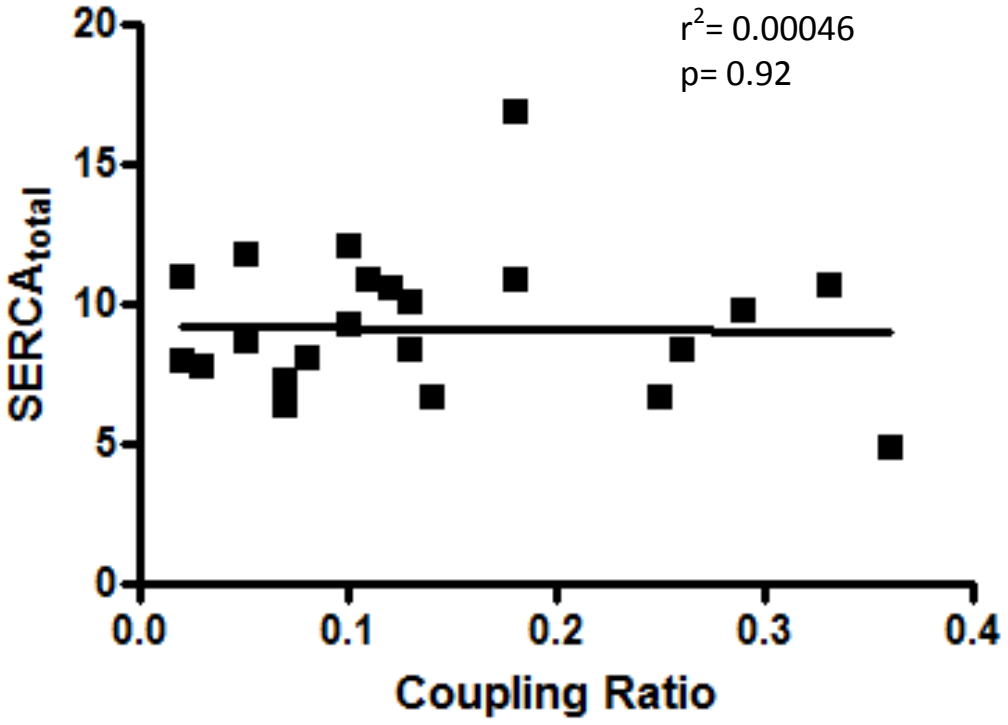

Figure 15: Coupling Ratio and Total SERCA. SERCA total is SERCA1a + SERCA2a. SERCA isoforms were assessed using Western Blot techniques and are normalized to α-actin. SERCA expression is protein density expressed in arbitrary units. Abbreviations: SERCA, sarco(endo)plasmic reticulum Ca^{2+}-ATPase.

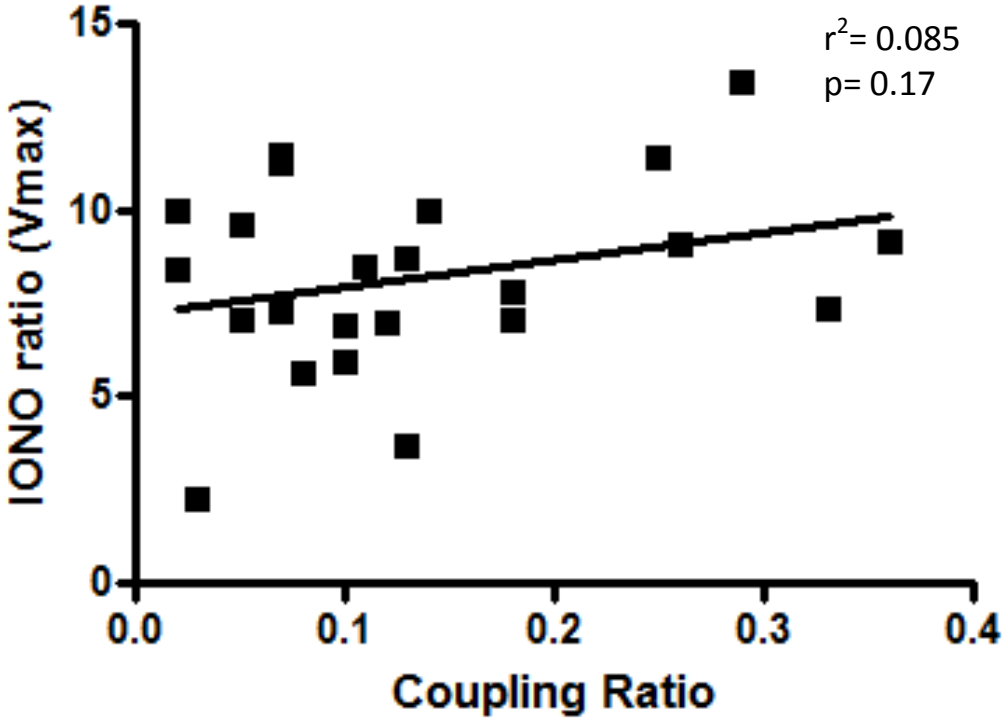

Figure 16: Coupling Ratio and IONO Ratio. IONO ratio is Ca^{2+}-ATPase activity with IONO/ Ca^{2+}-ATPase activity with no IONO and is assessed at Vmax. Abbreviations: IONO, Ca^{2+} ionophore.

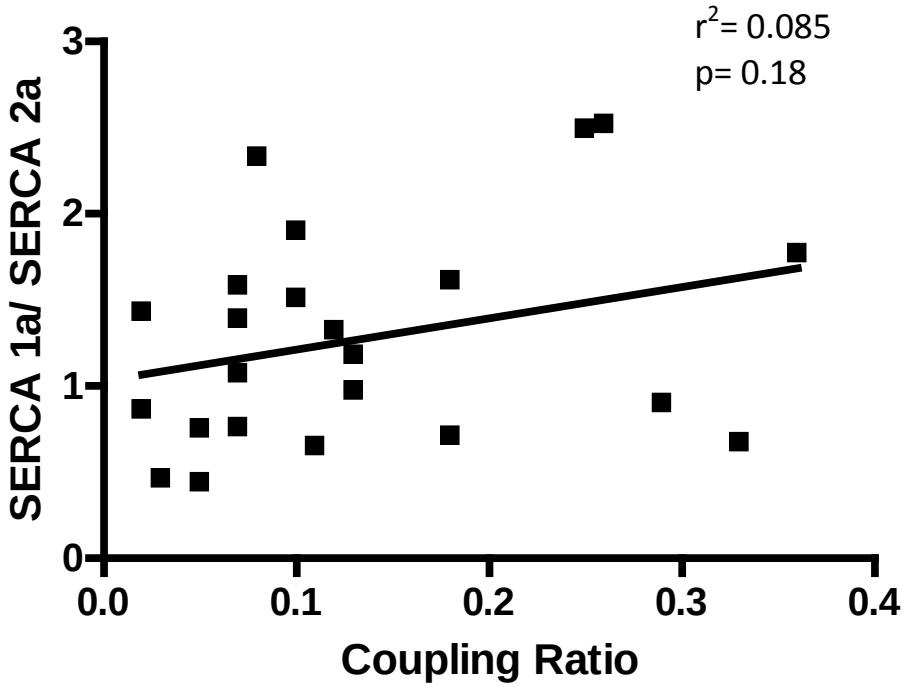

Figure 17: Coupling Ratio and SERCA Distribution. SERCA1a and SERCA2a are assessed using Western Blot techniques and are normalized to α-actin. SERCA expression is protein density expressed in arbitrary units. Abbreviations:SERCA, sarco(endo)plasmic reticulum Ca^{2+}-ATPase.

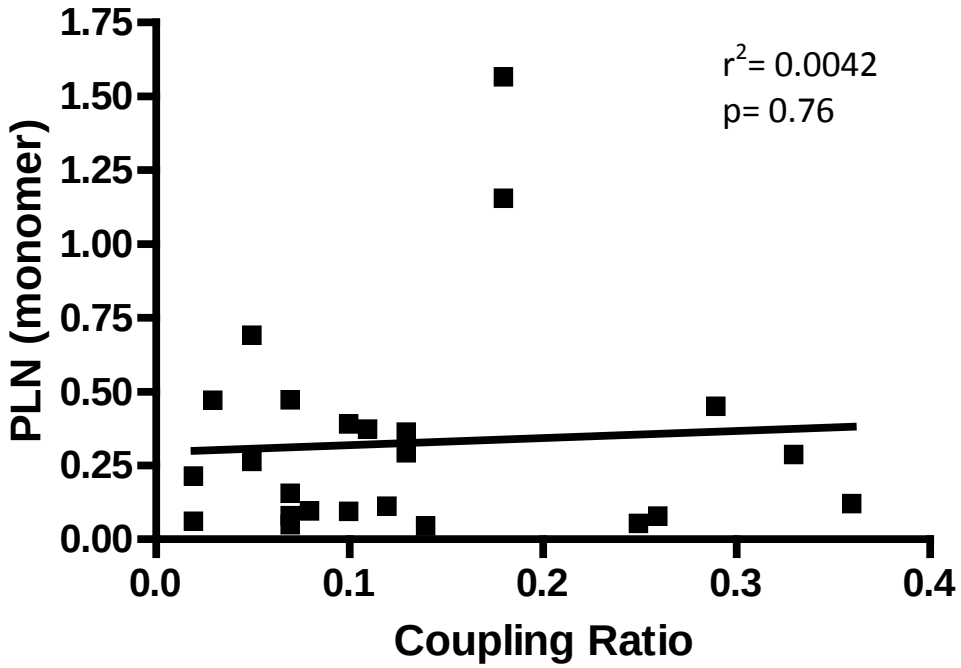

Figure 18: Coupling Ratio and PLN Content. PLN (monomer) content is assessed using Western blot techniques and is normalized to α-actin. PLN expression is protein density expressed in arbitrary units. Abbreviations: PLN, phospholamban.

CHAPTER FOUR: DISCUSSION

In the present study, cross-sectional analyses were completed on skeletal muscle samples obtained from a group of healthy, weight-stable individuals to determine whether RMR is related to skeletal muscle SR Ca^{2+} transport efficiency. RMR was determined using a breath by breath system, and correlated with various SR Ca^{2+} handling measures. The primary SR Ca^{2+} handling property that represented the SR Ca^{2+} transport efficiency was the coupling ratio, which was calculated from measurements of homogenate SR Ca^{2+} uptake and Ca^{2+}-ATPase activity (i.e. Ca^{2+} uptake/Ca^{2+}-ATPase activity). It was also of interest to examine the relationship between RMR and other Ca^{2+} handling properties which have been shown to influence the coupling ratio. Specifically, it was of interest to assess SR Ca^{2+} leak and SERCA pump efficiency (as assessed by IONO ratio), as these properties are theoretically the main determinants of coupling ratio. It was hypothesized that RMR would be negatively correlated to coupling ratio; positively correlated to SR Ca^{2+} leak; and negatively correlated to IONO ratio. The main finding of the study, as hypothesized, was that a weak but significant negative relationship between RMR and coupling ratio exists, such that as RMR increases, coupling ratio decreases (r^2= 0.21, p =0.024) (Figure 6). However, in contrast to the hypotheses, RMR was not found to be significantly related to either SR Ca^{2+} leak or IONO ratio and, unexpectedly, these properties were also not associated with the coupling ratio. Overall, based on these findings, the significance of any relationship between RMR and skeletal muscle SR Ca^{2+} transport efficiency in humans remains uncertain. However, the subtle relationship observed between coupling ratio and RMR in this study warrants further examination.

Correlational analysis was used to assess the relationships between RMR and SR properties, which appears to be appropriate based on the continuous spread of RMR data observed in our study population. Nevertheless, it is important to recognize that the study population was over-sampled at the low end of BMI and RMR, partly due to the recruitment procedures that were employed and partly due to random selection of the participants who volunteered for the study. Therefore, it is possible that the results of this study may not be generalizable to a larger population including individuals with higher BMIs and RMRs. However, to account for differences in BMI/body weight between participants, RMR is usually normalized to body weight or FFM in kg, which takes into account the lean tissue mass differences of each individual. Interestingly, in the present study body mass and FFM were correlated to RMR with very similar r^2 values, showing that normalizing RMR to either body mass or FFM may have been appropriate. However, FFM is generally considered to be the best predictor of energy expenditure and explains more of the variability in RMR between individuals than body mass explains (Ravussin et al, 1981; Poehlman, 1992; Cunningham, 1980; Poehlman, 1993; Ravussin, 1986). Therefore the RMR data reported in the present study and used for the correlational analyses were expressed normalized to FFM (kcal/kg).

Completion of a health status form was completed to rule out any contraindications to participation in the study. Measurements of blood lipids, glucose and insulin were taken in order to verify that the participants fell within a normal range. No participants were allowed to take part in the study if they had a medical condition or were taking medications which may have altered the results of the study in any way. The participants were also required to fill out a 3 day diet and activity log which provides information on the energy balance of the

individuals. The goal was to have the participants in a state of energy balance for the duration of the study, as well as five months prior to the study. Valid energy intake and expenditure data from self-reported diet and activity logs requires that participants are very vigilant in accurately filling out the logs. It is well established that participants tend to under-report their energy intake and over-report their energy expenditure through physical activity (Garriquet, 2008; Scaqlius, 2009). These methodological limitations associated with diet and activity logs likely explain why some of the participants in this study reported energy balance values that were up to plus or minus 2000 kcal/day (Appendix C).

The Sensewear data likely quantifies energy expenditure more accurately than activity logs since it better reflects body weight measurements and verifies that participants maintained energy balance during the study period (Mackey, 2011). A study examining evaluation of total energy expenditure (TEE) using both doubly labelled water and the Sensewear armband found no significant difference in TEE values between the two methods (Mackey, 2011). In support of the view that the energy balance results from the diet and activity logs or the sensewear arm bands are inaccurate, body weight of the participants was measured on 3 separate occasions over the course of the study and there were no significant differences observed between time points. Thus, the weight of the participants was stable for the duration of the study indicating that the participants must have maintained energy balance during the study. For the purpose of obtaining accurate results, it is important that adaptive thermogenesis is not occurring in any of the participants for the duration of the study.

Relationship Between RMR and Coupling Ratio:

The main research question was whether or not a relationship exists between RMR and Ca^{2+} transport efficiency (i.e. coupling ratio) in skeletal muscle in humans. It was hypothesized that RMR would be negatively correlated with coupling ratio. Although, only a relatively weak inverse relationship was found (r^2= 0.21), it was statistically significant (p=0.024) as hypothesized (figure. 6). The relationship between RMR and coupling ratio was not expected to be a strong relationship given that many organs other than skeletal muscle and many different cellular processes contribute to RMR. This finding is also particularly noteworthy given the small sample size used for this study. Under optimal conditions, the coupling ratio is 2 Ca^{2+}:1 ATP, due to the stoichiometry of two Ca^{2+} binding sites and one ATP binding site on each SERCA pump subunit (Smith et al, 2002; Inesi et al, 1978; de Meis, 2001a; MacLennan et al, 1997; Toyoshima and Inesi, 2004). A lower coupling ratio means that there is less Ca^{2+} transported into the lumen of the SR from the cytoplasm per ATP hydrolyzed relative to the amount of Ca^{2+} transported into the SR under optimal 'stoichiometric' conditions. Previous in vitro studies with rabbit fast and slow twitch hind limb skeletal muscle SR vesicles showed that when a Ca^{2+} gradient is present the coupling ratio could vary between 0.3 and 0.6 for fast twitch, and up to 1.0 for slow twitch skeletal muscle (de Meis, 2001b; Reis et al, 2001; McWhirter et al, 1987; Reis et al, 2002). The values for coupling ratio in the present study range from 0.02 to 0.36, which are fairly close to the values stated above, considering a mixed skeletal muscle (vastus lateralis) was studied in humans in the present study. It should be noted that all values for the SR Ca^{2+} handling properties, including coupling ratio values, are comparable to published values from our laboratory (Duhamel et al, 2007;

Holloway et al, 2005; Green et al, 2000; Duhamel et al, 2005; Tupling et al, 2003) and others (Leppik et al, 2004; Li et al, 2002; Ortenblad et al, 2000).

The relationship between RMR and coupling ratio observed in this study likely reflects the fact that individuals who have a lower coupling ratio would require higher ATP turnover by the SERCA pumps under resting conditions in order to pump the needed amount of Ca^{2+} into the SR to maintain the >10^4-fold Ca^{2+} concentration gradient that exists in resting muscle. The next logical question was to determine which factors that influence the coupling ratio are important for the relationship between coupling ratio and RMR. The main factors that play a role in the coupling ratio are SR Ca^{2+} leak and SERCA pump efficiency (Frank et al, 2000; Reis et al, 2001; Reis et al 2002; Murphy et al, 2009). Assessing these factors thus leads to a better understanding of which SR properties may be influencing the relationship seen between RMR and coupling ratio.

RMR and SR Ca^{2+} Leak:

SR Ca^{2+} leak results in a greater demand on SERCAs to pump Ca^{2+} back into the SR lumen from the cytosol. If we assume a constant SERCA pump efficiency, then the more Ca^{2+} leaking out of the SR, the more hydrolysis of ATP must occur in order to maintain the Ca^{2+} gradient across the SR in resting muscle. Of the several factors which could influence SR Ca^{2+} leak, total SERCA content and CSQ content are thought to be of primary importance. For example, there is a higher density of SERCA pumps and a lower [Ca^{2+}] within the SR in fast twitch skeletal muscle because of the higher volume of SR and concentration of CSQ relative to slow twitch skeletal muscle (Murphy et al, 2009). The high density of SERCA pumps likely

accounts for the higher SR Ca^{2+} leak rates found in fast twitch muscle as the SERCA pumps themselves appear to be the major pathway for leakage of Ca^{2+} out of the SR (Inesi and de Meis, 1989; Murphy et al, 2009). Therefore, higher rates of SR Ca^{2+} leak from the SR in fast twitch muscle could account for the lower coupling ratio and hence greater heat production in fast muscle compared to slow muscle, due to increased ATP hydrolysis by SERCA pumps (Reis et al, 2001). Therefore, it was hypothesized that RMR would be positively correlated with both SR Ca^{2+} leak and total SERCA content. High concentrations of CSQ in fast muscle are thought to be necessary in order to prevent even higher rates of SR Ca^{2+} leak and heat production (Murphy et al, 2009). This would be consistent with the hypothesis that CSQ content would be negatively correlated with SR Ca^{2+} leak and thus positively correlated with RMR. However, given that no significant relationship was found between RMR and SR Ca^{2+} leak in this study, it was actually not surprising to find that neither total SERCA content or CSQ content were significantly related to RMR either. These findings lead to the conclusion that SR Ca^{2+} leak is not a significant underlying factor involved in the relationship between RMR and coupling ratio which suggests that SERCA pump inefficiency may be the primary factor contributing to this relationship in humans.

RMR and SERCA Pump Efficiency:

A reduction in the coupling ratio as a result of altered SERCA pump efficiency, such that less Ca^{2+} is taken up into the SR for every ATP hydrolyzed, can occur as a result of passive leak, uncoupled ATPase activity and slippage. SERCA pump efficiency in skeletal muscle has been shown to be influenced by SERCA isoform expression as well as the presence of PLN.

SERCA2a is the more efficient SERCA isoform relative to SERCA1a (Reis et al, 2002), but it is unknown if the differences in efficiency between SERCA1a and SERCA2a are due to differences in passive leak, uncoupled ATPase activity, slippage or a combination of more than one of those uncoupling reactions. PLN has been shown to reduce the apparent efficiency of SERCA Ca^{2+} handling (Frank et al, 2000) probably by causing increased slippage of SERCA pumps as has been demonstrated for SLN (Smith et al, 2002; Mall et al, 2006), a structural and functional homologue of PLN (MacLennan, 2004). Of particular significance for this study, dephosphorylated PLN exerts its effects on SERCA efficiency under conditions that would exist in resting skeletal muscle (ie. at low [Ca^{2+}]) (Frank et al, 2000). Therefore, it was hypothesized that individuals with higher relative PLN expression would have a lower coupling ratio, due to less efficient SERCA pumping, and a higher relative RMR as a result.

SERCA pump efficiency is defined as the fraction of free energy derived from ATP hydrolysis by the pump that is converted to osmotic energy which is used to drive ion transport with the remainder of free energy being released as heat. The amount of heat released per mol of ATP hydrolyzed by SERCA pumps can be measured with a calorimeter (Mall et al, 2006). This technique is not available in our laboratory however, so the IONO ratio is used as a surrogate marker of SERCA efficiency. A lower relative IONO ratio indicates that the SR vesicle is more leaky (ie. more slippage, passive leak and uncoupled ATPase activity occurring) and thus SR Ca^{2+} transport is less efficient. In contrast to the hypothesis, there was no relationship found between RMR and IONO ratio in this study (r^2=0.027, p=0.43) (Figure 10). Consistent with this finding was the fact that PLN was also not significantly correlated with RMR (r^2= 0.044, p=0.32) (Figure. 12). On the other hand, a weak but significant positive

correlation between RMR and SERCA isoform distribution was observed, such that RMR tended to increase as the ratio of SERCA1a/SERCA2a increased (r^2=0.18, p=0.04) (Figure 11). Although this later finding supports the original hypothesis, the interpretation is complicated since the relationship between SERCA isoform expression and RMR should reflect isoform differences in SERCA efficiency, yet IONO ratio, which is thought to be a marker of SERCA efficiency, was not related to RMR. One possibility is that SERCA isoform expression is strongly related to some other factor that influences RMR independent of coupling ratio and IONO ratio. Another possibility is that the IONO ratio is not a very valid marker of SERCA efficiency so that SERCA isoform expression could actually be an important factor that influences the relationship between coupling ratio and RMR. To help clarify these results, it was important to test the assumption that coupling ratio is indeed related to the various SR Ca^{2+} handling properties, including IONO ratio and SERCA isoform distribution.

Relationship Between Coupling Ratio and SR Ca^{2+} Handling Properties:

As mentioned earlier, a higher relative amount of SR Ca^{2+} leak should result in a lower coupling ratio (Inesi and de Meis, 1989; Murphy et al, 2009); however, surprisingly there was no relationship found between coupling ratio and SR Ca^{2+} leak in skeletal muscle homogenates prepared from human vastus lateralis (r^2=0.099, p=0.13) (Figure 13). This finding supports the conclusion that SR Ca^{2+} leak is not an influential factor involved in the relationship between RMR and coupling ratio. Furthermore, assuming that the sensitivity of the methods used in this study to measure coupling ratio and SR Ca^{2+} leak was sufficiently

high, it also strongly suggests that SERCA pump efficiency, rather than SR Ca^{2+} leak, is the major determinant of coupling ratio.

Increased CSQ content is known to result in a lower [Ca^{2+}] within the SR, and thus would likely result in less Ca^{2+} leak out of the SR (Murphy et al, 2009). This should result in a higher coupling ratio, however, there was no relationship found between CSQ content and coupling ratio (r^2=0.0057, p=0.72) (Figure 14). The relationship between coupling ratio and total SERCA content is also important to assess, since SERCA pumps themselves have been shown to be a pathway for Ca^{2+} leak out of the SR (Inesi and de Meis, 1989; Murphy et al, 2009). Having a higher relative total SERCA content would theoretically lead to a lower coupling ratio due to relatively more SR Ca^{2+} leak. There was also no significant relationship found between coupling ratio and total SERCA content (r^2=0.00046, p=0.92) (Figure 15). These findings further support the finding that SR Ca^{2+} leak is not a significant factor which modulates the relationship seen between coupling ratio and RMR.

A major methodological assumption is that IONO ratio is a valid surrogate measure for SERCA pump efficiency. If that is true and if SERCA pump efficiency is the major determinant of coupling ratio as suggested by the lack of relationship observed between SR Ca^{2+} leak and coupling ratio, then IONO ratio should be significantly correlated with coupling ratio. As mentioned above, a lower IONO ratio reflects an SR vesicle that is relatively more leaky to Ca^{2+}, presumably due to greater passive leak, slippage and/or uncoupled ATPase activity. Thus, it would be expected that the coupling ratio would decrease as IONO ratio decreases but this was not the case; there was no relationship found between coupling ratio and IONO ratio (r^2=0.085, p=0.17) (Figure 16). This finding points out a possible weakness in the

assumption that IONO ratio is a valid measure of SERCA pump efficiency. It may be that a limitation to the present study is that it is not possible, due to methodological constraints, to assess the contribution of SERCA pump efficiency to the relationship between RMR and coupling ratio.

To further examine this, PLN content and SERCA distribution, two main factors which determine SERCA pump efficiency, were assessed. Theoretically, a higher PLN content would lead to a lower relative coupling ratio due to the fact that PLN reduces the apparent efficiency of SERCA Ca^{2+} handling (Frank et al, 2000). However, there was no significant relationship found between coupling ratio and PLN content (r^2=0.0042, p=0.76) (Figure 17). Theoretically, a higher SERCA1a to SERCA2a ratio would result in a lower coupling ratio since the SERCA1a isoform is relatively less efficient than SERCA2a and this would lead to less efficient SR Ca^{2+} handling. Importantly, a significant negative correlation between SERCA1a/SERCA2a and coupling ratio would lend support to the view that efficiency differences between the SERCA isoforms could at least partly explain the significant positive relationship that was observed between SERCA1a/SERCA2a and RMR. However, there was found to be no significant relationship between coupling ratio and SERCA1a/SERCA2a ratio (r^2=0.085, p=0.18) (Figure 17). The lack of any relationships between coupling ratio and other SR properties measured in this study, that have been reported to play a role in determining coupling ratio, highlights the need to establish more sensitive and direct methods for measuring SERCA efficiency and SR Ca^{2+} leak. The fact that there was no relationship seen between coupling ratio and SERCA isoform distribution but there was a relationship seen between RMR and SERCA isoform distribution suggests that SERCA isoform distribution may only be indirectly associated with

RMR which could occur if SERCA isoform distribution was associated with some other metabolic mechanism taking place in skeletal muscle that does influence RMR directly.

Regulation of SERCA Isoform Distribution:

Examining the factors that play a role in expression of SERCA isoforms in skeletal muscle may lead to increased understanding of why there was a relationship seen between RMR and SERCA distribution, but not coupling ratio and SERCA distribution. Details pertaining to the regulation of SERCA isoform expression were covered in the Introduction. Recall that SERCA isoform distribution can be regulated by development and aging, neurohormonal factors, and exercise training. Development and aging would not be playing a role in the present study since the participants were all similar in age, being approximately 22 years on average. With respect to exercise training, individuals in the present study had various levels of physical activity, although none of them were taking part in any kind of endurance or fitness training. One of the inclusion criteria was that participants cannot take part in more than 30 minutes of exercise, >3 times per week on average. Some participants stated that they fit this inclusion criteria, but then listed more than 30 minutes of exercise, >3 times per week, on their activity log. This theoretically could influence SERCA expression, however, it is not likely that the amount of physical activity the participants were taking part in would cause any significant alterations in SERCA isoform distribution.

SERCA expression is strongly regulated by neurohormonal factors, such as thyroid hormone levels. The genes encoding SERCA1a and SERCA2a are transcriptionally regulated by T3 with most studies showing increased SERCA1a expression and decreased SERCA2a

expression with increases in T3, especially in slow-twitch muscle fibres (Simonides et al, 2001). Although plasma T3 levels were not measured in this study it was assumed that the participants were in a euthyroid state as this was a requirement for participation in the study. Nevertheless, it is likely that SERCA isoform expression differences between participants could be related to differences in thyroid hormone levels. This could possibly explain why RMR was positively correlated with SERCA1a/SERCA2a but there was no relationship between coupling ratio and SERCA1a/SERCA2a, because thyroid hormone can influence RMR through other mechanisms that are independent of SERCA gene expression.

In adult humans the thyroid hormone accelerates energy expenditure, and shown in many hypo- and hyperthyroidism studies (Oppenheimer et al, 1987). In patients with severe hypothyroidism, total body energy expenditure has been shown to fall as much as 50 %, and in thyrotoxic patients, it can be increased by approximately 50 %, which totals a 3-fold induction over a hypothyroid baseline (Bianco et al, 2005). Thyroid hormone levels have been shown to play a role in adaptive thermogenesis. Adaptive thermogenesis is a mechanism involved in regulating energy expenditure by increasing the heat production during prolonged periods of excess energy intake (i.e. high fat diet; Levine et al., 1999) or cold exposure (Lowell and Spiegelman, 2000). This can occur in skeletal muscle through the uncoupling of protons from the electron transport chain by membrane bound uncoupling proteins (UCPs), resulting in the conversion of osmotic energy into heat (Lowell and Spiegelman, 2000). An increase in the levels of mRNAs for uncoupling protein 2 (UCP2) and 3 (UCP3) have been shown to occur with hyperthyroidism (Gong et al, 1997). Administration of T3 to rodents has been shown to lead to increased expression of UCP2 and UCP3 in heart and skeletal muscle (Gong et al, 1997;

Lanni et al, 1997; Lanni et al 1999). In the transition from hypo- to hyper-thyroidism, increases in UCP3 mRNA expression occur in skeletal muscle as well as in mitochondrial uncoupling activity (Lanni et al, 1999). Furthermore, T3 has been shown to regulate UCP2 and UCP3 mRNA expression in human skeletal muscle and adipose tissue both *in vivo* and *in vitro* (Barbe et al, 2001). In the same study it was found that the increase in T3 levels that occurred following T3 injection was associated with an increase in RMR, thus pointing towards a role for UCP3 in the effect of T3 on resting metabolism (Barbe et al, 2001). These findings highlight the alternative mechanism, besides SERCA isoform expression, which can explain the effects of thyroid hormone on RMR, since thyroid hormone can influence RMR through other mechanisms that are independent of SERCA gene expression.

Limitations:

With any human study, there are limitations to how well controlled the study is. For example, although there were strict inclusion criteria regarding the amount of activity per week the individuals took part in, the medical conditions affecting hormone levels, RMR or skeletal muscle physiology, and medications taken, it is not possible to control for the numerous factors and hormone interactions that can occur in different individuals which may have affected the results of the study. It was not in the scope of this study to examine the thyroid hormone levels of the participants since these individuals did not have any thyroid conditions and the main objective of the study was to investigate the relationship between SR Ca^{2+} handling variables and RMR (and not as much causation of any of the findings); however,

it may be helpful in future studies to assess to the levels of thyroid hormone to determine if differences are modulating the results seen.

The limited accuracy of assessing energy balance through diet and activity logs is another limitation to the study. Although diet and activity log analysis was not a primary aim of the study, the participants should be roughly in a state of energy balance and weight stability for the duration of the study. It was clear that some of the participants were not very thorough in filling out their logs, and as a result their calculated daily caloric intake and expenditures are questionable. The participants were all weight stable throughout the study however. In future studies, it would be helpful to have a more detailed analysis of both caloric intake and expenditure, in order to ensure a steady state metabolism for the duration of the study. This could be done by having the participants stay in the laboratory for the duration of the study (ie. an 'in-participant' study) in order to strictly monitor their caloric intake, and the use of doubly labelled water to assess energy expenditure. Another limitation is that FFM had to be calculated (as described in the methods section) for 4 of the individuals because they did not have access to a DXA scanner at the time of their completion of the study. This is not a major limitation however because FFM was only used to characterize the participants, and was not a primary measure in the study. Furthermore, because of the selection method used initially to gather a sample population that had a large spread of RMRs, there was an over-sampling of participants with a low BMI, although for the primary variable studied, RMR, there was a good spread/continuous data achieved. For any human study, it is also important to have a fairly large sample size, so that the power can be higher. The sample size was limited to 25 participants for this thesis due to the time constraints and resources available.

It was found that a limitation of this study was likely that the IONO ratio may not be an accurate method to assess the SERCA pump efficiency and thus may not accurately assess the relationship between SERCA pump efficiency and coupling ratio. A future study could use a gold standard method (ie. direct calorimetry) to assess the role of slippage, passive leak, and uncoupled ATPase activity on the relationship between coupling ratio and RMR. This would involve analysis of SERCA pump efficiency by measuring the heats of reaction of the Ca^{2+}-ATPase with ATP using isothermal calorimetry (Mall et al, 2006; Smith et al, 2002). Another limitation is that SLN and phosphorylated-PLN were not assessed in the present study. Phosphorylation of PLN removes its inhibition on SERCA and facilitates Ca^{2+} transport into the SR lumen and thus enhances the SR Ca^{2+} transport coupling ratio (Frank et al, 2000; indemann, 1983; Kranias, 1985). Like PLN, SLN has also been shown to cause the uncoupling of Ca^{2+} uptake from ATP hydrolysis by the SERCA pumps (Smith et al., 2002; Mall et al., 2006). In two separate *in vitro* studies by the same group, it was found that the presence of SLN in reconstituted membrane vesicles containing SERCA resulted in uncoupled ATP hydrolysis (Smith et al., 2002) and increased the amount of heat released per mol of ATP hydrolyzed (Mall et al., 2006). These specific measures could influence the relationship between coupling ratio and RMR, and thus should be assessed in a future study.

Future Studies:

The present study only looked at the role of SR Ca^{2+} handling in RMR under steady-state conditions. A future study examining diet-induced thermogenesis would be an important next step to see how the SR Ca^{2+} handling system may adapt to changes in diet.

Thus, in addition to the future directions/studies mentioned in the Conclusions and Limitations sections, other future studies could examine a similar primary research question, but with a much larger sample population and more measures to explain the relationships found between RMR and SR Ca^{2+} handling variables which may include looking at thyroid hormone levels, and adaptive thermogenesis measures such as UCP levels. To have more control numerous variables and to minimize the error of the study, it would be ideal to have an 'in-participant' study, where the individuals are in the lab for the duration of the study (ie sleeping, eating, doing activities of daily living) in the lab facilities. This study would have a large sample population, and would take baseline measures of all the variables which have been measured in the present study. Then the participants would all be given a high fat diet for a number of weeks, and post high fat diet measures would be taken on all the variables. The aim of this study would be to look at whether there were any differences in expression or levels of major SR Ca^{2+} handling variables and changes in RMR, and how these correlate. For example, one primary question may be 'are individuals who have a higher relative expression of PLN at baseline more protected from high fat diet-induced weight gain due to less efficient Ca^{2+} handling systems'. This type of study would allow more accurate measures of activity levels and diet during the study, would provide more control, and would provide more insight on the relationship between SR Ca^{2+} handling properties, RMR and whether any energy imbalance that are occurring or leading to weight gain are modulated by differences in levels of these given variables.

Conclusion and Significance of Findings:

The findings of the present study demonstrate that there is a weak but significant negative correlation between coupling ratio and RMR, such that as coupling ratio decreases, RMR increases. It was not expected to be a strong relationship given that many cellular processes contribute to RMR, so this finding is particularly noteworthy, especially given the small sample size. The two main factors which influence the coupling ratio, SR Ca^{2+} leak and SERCA pump efficiency (as assessed by IONO ratio), showed no significant relationship to either coupling ratio or RMR. Furthermore, two major factors that determines SR Ca^{2+} leak, namely total SERCA and CSQ content, were also not significantly related to coupling ratio or RMR. These findings lead to the conclusion that SR Ca^{2+} leak is not influencing the relationship seen between coupling ratio and RMR. Therefore, coupling ratio and IONO ratio were strongly expected to be related but were not found to be, suggesting that the IONO ratio may not be a valid surrogate measure of SERCA pump efficiency. Further studies will need to be completed to determine whether the main factors directly influencing SERCA pump efficiency, slippage, passive leak and uncoupled ATPase activity, are related to RMR.

The other factors which influence the SERCA pump efficiency, PLN content and SERCA isoform distribution, showed no significant relationship with coupling ratio. PLN content was not related to RMR, however, SERCA isoform distribution was significantly related to RMR, such that as SERCA1a/SERCA2a ratio increase, RMR increases. It is likely that SERCA isoform expression differences are the result of thyroid hormone levels, which also increases RMR, likely independent of differences in SR Ca^{2+} handling energetics/efficiency. Due to the small sample size and the fact that there was a weak relationship between coupling ratio and RMR,

it is not surprising that there were no significant relationships between other SR Ca^{2+} handling variables and RMR. The influence of these SR Ca^{2+} handling variables could be minimal enough that a small sample size would not be significant enough to show any relationship between the various SR properties and RMR, due to the numerous other cellular mechanisms that could be influencing RMR. Therefore, overall, the findings of the present study do not rule out the possibility that the relationship between RMR and coupling ratio is physiologically and clinically significant in humans, and if so, further work is required to determine what the underlying mechanisms are that explain this relationship in order to determine potential therapeutic targets for the treatment of various metabolic diseases.

Since SERCA activity accounts for at least 18-24 % of resting energy expenditure in skeletal muscles, and since skeletal muscle metabolism contributes 20-30% of whole body resting metabolic rate, the differences in SERCA efficiency between different individuals could manifest in differences in relative whole body RMR, such that those with less efficient SR Ca^{2+} handling systems tend to have a higher RMR due to an increased energy turnover for SR Ca^{2+} handling for a given amount of time. In contrast, those with more efficient SR Ca^{2+} handling systems tend to have lower relative RMRs, and thus may be more prone to diet induced weight gain, or inability to maintain a desired weight, due to the accumulation of relatively small energy imbalances over time. The finding that coupling ratio is negatively related to RMR could pose significance to the field because it could lead to the development of more studies which examine SR Ca^{2+}handling energetics as a means of prevention and/or treatment for obesity. For example, in those with less efficient SR Ca^{2+} handling systems, prescribing something which could increase the coupling ratio, could lead to increased RMR, and thus

result in a more balanced energy level over time. This could have implications for prevention of diseases which result from a negative energy balance, such as type II diabetes. Further studies would have to be done to determine which SR Ca^{2+} handling properties are influencing the relationship between coupling ratio and RMR, in order to target possible obesity prevention/treatment strategies which could work on the SR Ca^{2+} handling system.

References:

Ainsworth BE, Haskell WL, Whitt MC, Irwin ML, Swartz AM, Strath SJ, O'Brien WL, Bassett DR, Schmitz KH, Emplaincourt PO, Jacobs DR, Leon AS. Compendium of physical activities: an update of activity codes and MET intensities. *Med Sci Sports Exerc*. 32(9): S498-504, 2000.

Altman, P.L., Dittmer D.S. *Biological Handbooks: Metabolism*. Bethesda: FASEB, 1968.

Anger M, Samuel JL, Marotte F, Wuytack F, Rappaport L, Lompre AM. In situ mRNA distribution of sarco(endo)plasmic reticulum Ca^{2+}-ATPase mRNA isoform during ontogeny in the rat. *J Mol Cell Cardiol.* 26: 101-102, 1994.

Arruda AP, Nigro M, Oliveira GM, de Meid L. Thermogenic activity of the Ca2+-ATPase from skeletal muscle heavy sarcoplasmic reticulum: the role of ryanodine Ca2+ channel. *Biochemica et Biophysica Acta*. 1498-1505, 2007.

Arruda AP, daSilva WS, Carvalho DP and deMeis L. Hyperthyroidism increases the uncoupled ATPase activity and heat production by the sarcoplasmic reticulum Ca^{2+} ATPase. *Biochem. J.* 375: 753-760, 2003.

Asahi M, Kurzydlowski K, Tada M, MacLennan D.H. Sarcolipin inhibits polymerization of phospholamban to induce superinhibition of sarco(endo)plasmic reticulum Ca^{2+}-ATPases (SERCAs). *J. Biol. Chem.* 277: 26725-26728, 2002.

Asahi M, Sugita Y, Kurzydlowski K, de Leon S, Tada M, Toyoshima C, MacLennan D.H. Sarcolipin regulates sarco(endo)plasmic reticulum Ca^{2+}-ATPase (SERCA) by binding to transmembrane helices alone or in association with phospholamban. *Proc. Natl. Acad. Sci.* 100: 5040-5045, 2003.

Aschoff, J, Gunther B, Kramer K. Energiehausfaul and temperature-regulation. *Urban & Schwarzeberg*. 1971.

Barbe P, Larrouy D, Boulanger C, Chevillotte E, Viguerie N, Thalamas C, Oliva Trastoy M, Roques M, Vidal H, Lanqin D. Triiodothyronine-mediated up-regulation of UCP2 and UCP3 mRNA expression in human skeletal muscle without coordinated induction of mitochondrial respiratory chain genes. *FASEB J*. 15(1): 13-15, 2000.

Barclay CJ, Woledge RC, Curtin NA. Energy turnover for Ca^{2+} cycling in skeletal muscle. *J. Muscle. Res. Cell. Motil.* 28: 259-274, 2007.

Berchtold M.W, Brinkmeier , Muntener M. Calcium ion in skeletal muscle: Its crucial role for muscle function, plasticity, and disease. *Physiol. Rev.* 80: 1215-1265, 2000.

Berman M.C. Slippage and uncoupling in P-type cation pumps; implications for energy transduction mechanisms and regulation of metabolism. *Biochem. Biophys. Acta.* 1513: 95-121, 2001.

Berry MN, Gregory RB,Grivell AR, Henly DC, Phillips JW, Wallace PG, Welch GR. The thermodynamics regulation of celluar metabolism and heat production. In: *Energy Tranformations in cells and organisms*. Germany: Georg Thieme Verlag. 18-27, 1989.

Bhupathy P, Babu G.J, Periasamy M. Sarcolipin and phospholamban as regulators of cardiac sarcoplasmic reticulum Ca2+ATPase. *J. Mol. Cell. Cardio.* 42: 903-911, 2007.

Bianco AC, Maia AL, de Silva W, Christoffolete MA. Adaptive activation of thyroid hormone and energy expenditure. Bioscience reports. 25: 191-208, 2005.

Blaxter K. Energy metabolism in animals and man. *Cambridge, UK Cambridge Univ*. Press, 1989.

Boothby W, Sandiford I. Summary of the basal metabolism data on 8,614 subjects with special reference to the normal standards for the estimation of the basal metabolic *rate. J. Biol. Chem*. 54: 783-803, 1922.

Bogardus C, Lilioja S, Ravussin E, Abbott W, Zawadzki JK, Young A, Knowler W, Jacobowits R, Moll P.P. Familial dependence of the resting metabolic rate. *N. Engl. J. Med*. 315: 96-100, 1986.

Bombardier E. The role of sarcolipin in calcium handling and obesity. Unpublished PhD Thesis, University of Waterloo. 2010.

Brandl CJ, deLeon S, Martin DR, MacLennan DH. Adult forms of the Ca^{2+}ATPase of sarcoplasmic reticulum. Expression in developing skeletal muscle. *J Biol Chem*. 262: 3768-3774, 1987.

Brandl CJ, Green NM, Korczak B, MacLennan DH. Two Ca^{2+} ATPase genes: homologies and mechanistic implications of deduced amino acid sequences. *Cell*. 44: 597-607, 1986.

Brown GC, Brand, MD. Changes in permeability of protons and other cations at high proton motive force in rat liver mitochondria. *Biochem J*. 234: 75-81, 1986.

Canadian Diabetes Association. Canadian diabetes association 2008 clinical practice guidelines for the prevention and management of diabetes in Canada. *Canadian Journal of Diabetes*. 32: supplement 1, 2008.

Chinet A, Decrouy A, Even PC. Ca^{2+}-dependent heat production under basal and near-basal conditions in the mouse soleus muscle. *J. Physiol.* 455: 663-678, 1992.

Clausen T, Van Hardeveld C, Everts M.E. Significance of cation transport in control of energy metabolism and thermogenesis. *Physiol Rev*. 71: 733-774, 1991.

Conley K, Amara CE, Jubrias S, Marcinek DJ. Mitochondrial function, fibre types and ageing: new insights from human muscle *in vivo. Exp Physiol*. 92(2): 333-339, 2007.

Cunningham JJ. A reanalysis of the factors influencing basal metabolic rate in normal adults. *Am J Clin Nutr*. 33:2372-4, 1980.

Damiani E, Sacchetto R, Margreth A. Variation of phospholamban in slow-twitch muscle sarcoplasmic reticulum between mammalian species and a link to the substrate specificity of endogenous Ca^{2+} - calmodulin dependent protein kinase. *Biochem. Biophys. Acta*. 501: 231-241, 2000.

de Meis L, Vianna AL. Energy interconversion by the Ca^{2+} ATPase transport ATPase of sarcoplasmic reticulum. *Annu. Rev. Biochem.* 48: 275-292, 1979.

de Meis L. Control of heat produced during ATP hydrolysis by the sarcoplasmic reticulum Ca^{2+}-ATPase in the absence of a Ca2+ gradient. *Biochem. Biophys. Res. Commun.* 243: 598-600, 1998.

de Meis L. ATP synthesis and heat production during Ca^{2+} efflux by sarcoplasmic reticulum Ca^{2+}ATPase. *Biochem. Biophys. Res. Commun.* 276: 35-39, 2000.

de Meis L. Uncoupled ATPase activity and heat production by the sarcoplasmic reticulum Ca^{2+}-ATPase: Regulation by ADP. *J. Biol. Chem.* 276: 25078-25087, 2001a.

de Meis L. Role of the sarcoplasmic reticulum Ca^{2+}-ATPase on heat production and thermogenesis. *Biosci. Rep.* 21: 113-137, 2001b.

de Meis L. Ca2+-ATPases (SERCA): Energy transduction and heat production in transport ATPases. *J. Membr. Biol.* 188: 1-9, 2002.

Duhamel TA, Stewart RD, Tupling AR, Ouyang J, Green HJ. Muscle sarcoplasmic reticulum calcium regulation in humans during consecutive days of exercise. *J Appl Physiol*. 103(4): 1212-20, 2001.

Duhamel TA, Green H, Sandiford s, Perco J, Ouyang J. Effects of progressive exercise and hypoxia on human muscle sarcoplasmic reticulum function. *J. Appl Physiol*. 97: 188-196, 2004.

Duhamel TA, Green HJ, Perco JG, Ouyang J. Metabolic and sarcoplasmic reticulum Ca^{2+} cycling responses in human muscle 4 days following prolonged exercise. *Can J Physiol Pharmacol*. 83(7): 643-55, 2005.

Duhamel TA, Stewart RD, Tupling AR, Ouyang J, Green HJ. Muscle sarcoplasmic reticulum calcium regulation in humans during consecutive days of exercise and recovery. *J Appl Physiol*. 103(4): 1212-20, 2007.

Dulhunty A.F. Excitation-countraction coupling from the 1950`s into the new millennium. *Clin Exp Pharmacol Physiol*. 33(9): 763-772, 2006.

Dulloo AG, Decrouy A, Chinet A. Suppression of Ca^{2+}-dependent heat production in mouse skeletal Muscle by high fish oil consumption. *Metabolism*. 43: 931-934, 1994.

Field J, Beldingg H, Martin A. An analysis of the relation between basal metabolism and summated tissue respiration in the rat. *Cell Comp Physiol*. 14: 143-155, 1939.

Folke B, Neil E. Quantitative role of brown adipose tissue in thermogenesis. *Circulation*. 1971.

Frank K, Tilgmann C, Shannon TR, Bers D, Kranias EG. Regulatory Role of Phospholamban in the Efficiency of Cardiac Sarcoplasmic Reticulum Ca^{2+} Transport. *Biochem.* 39*:* 14176–14182, 2000.

Fromme T, Klingenspor M. Uncoupling protein 1 expression and high-fat diets. *Am J Physiol Regul Integr Comp Physiol*. 300(1): R1-8, 2011.

Gambke B, Lyons GE, Haselgrove J, Kelly AM, Rubinstein NA. Thyroidal and neural control of myosin transitions during development of rat fast and slow muscles. *FEBS Lett*. 156(2): 335-339, 1983.

Garriquet D. Under-reporting of energy intake in the canadian community health survey. *Health Rep*. 19(4): 37-45, 2008.

Garriquet D. Impact of identifying plausible respondents on under-reporting of energy intake in the canadian community health survey. *Health Rep*. 19(4): 47-55, 2008.

Gianni D, Chan J, Gwathmey JK, del Monte F, Hajjar RJ. SERCA2a in heart failure: role and therapeutic prospects. *J Bioenerg Biomembr*. 37: 275-80, 2005.

Gong DW, He Y, Karas M, Reitman M. Uncoupling protein-3 is a mediator of thermogenesis regulated by thyroid hormone, beta3-adrenergic agonists, and leptin. *J Biol Chem*. 272(39): 24129-32, 1997.

Green HJ, Duhamel TA, Stewart RD, Tupling AR, Ooyang J. Dissociation between changes in muscle Na+-K+-ATPase isoform abundance and activity with consecutive days of exercise and recovery. *Am J Physiol Endocrinol Metab*. 294: E761-767, 2008.

Green HJ, Jones S, Ball-Burnett M, Fraser I. Early adaptations in blood substrates, metabolites and hormones to prolonged exercise training in man. *Can. J. Physiol. Pharmacol.* 69: 1222-1229, 1991.

Green HJ, Roy B, Grant S, Tupling AR, Otto C, Pipe A, McKenzie D, Ouyang J. Effects of a 21-day expedition to 6,194 m on human skeletal muscle SR Ca^{2+}-ATPase. *High Alt Med Biol*. 1(4): 301-10, 2000.

Hamalainen N, Pette D. Myosin and SERCA isoform expression in denervated slow-twitch muscle of euthyroid and hyperthyroid rabbits. *J Muscle res Cell*. 22: 453-57, 2001.

Hawkins C, Xu A, Narayanan N. Comparison of the effects of fluoride on the calcium pumps of cardiac and fast skeletal muscle sarcoplasmic reticulum: evidence for tissue- specific qualitative difference in calcium-induced pump conformation. *Biochemica. Biophysica. Acta.* 1191: 231-243, 1994.

Henquin JC. Regulation of insulin secretion: a matter of phase control and amplitude modulation. *Diabetologia.* 52: 739-751, 2009.

Hicks MJ, Shiqekawa M, Katz AM. Mechanism by which cyclic adenosine 3':5'-monophosphate-dependent protein kinase stimulates calcium transport in cardian sarcoplasmic reticulum. *Cir Res*. 44(3): 384-91, 1979.

Himms-Hagen J. On raising energy expenditure in ob/ob mice. *Science.* 276: 1132-1133, 1997.

Holloway GP, Green HJ, Duhamel TA, Ferth S, Moule JW, Ouyang J, Tupling AR. Muscle sarcoplasmic reticulum Ca^{2+} cycling adaptations during 16 h of heavy intermittent cycle exercise. *J Appl Physiol*. 99(3): 836-43, 2005.

Homsher E, Kean C.J. Skeletal muscle energetics and metabolism. *Annu. Rev. Physiol.* 40: 93-131, 1978.

Homsher E. Muscle enthalpy production and its relationship to actinomyosin ATPase. *Annu. Rev. Physiol.* 46: 672-690, 1987.

Hoerter J, Mazet F, Vassort G. Perinatal growth of the rabbit cardiac cell: possible implications for the mechanism of relaxation. *J Mol Cell Cardiol*. 13: 725-740, 1981.

Hovnanian A. SERCA pumps and human diseases. *Biochem*. 45: 337-363, 2007.

Inesi G, Kurzmack M, Verjoversuski-Almeida S. ATPase phosphorylation and calcium ion translocation in the transient state of sarcoplasmic reticulum activity. *Ann. N.Y. Acad. Sci.* 307: 224-227, 1978.

Inesi G. Mechanism of Ca^{2+} transport. *Annu. Rev. Physiol.* 47: 573-601, 1985.

Inesi G, de Meis L. Regulation of steady state filling in sarcoplasmic reticulum: Roles of back-inhibition, leakage, and slippage of the calcium pump. *J. Biol. Chem.* 264: 5929-5936, 1989.

Janovska A, Hatzinikolas G, Mano M, Wittert GA. The effect of dietary fat content on phospholipid fatty acid profile is muscle fibre-type dependent. *Am. J. Physiol.* 2010.

Jansky L. Adaptability of heat production mechanisms in homeotherms. *Acta univ Carol Ciol*. 1: 1-91, 1965.

Kadambi V, Ponniah S, Harrer JM, Hoit B, Dorn G.W, Walsh R, Kranias E.G. Cardiac-specific overexpression of phospholamban alters calcium kinetics and resultant cardiomyocyte mechanics in transgenic mice. *J. Clin. Invest.* 97: 533-539, 1996.

Katzmarzyk PT, Mason C. Prevalence of class I, II and II obesity in Canada. *CMAJ*. 174(2): 156-7, 2006.

Keys A, Taylor HL, Grande F. Basal metabolism and age of adult man. *Metab. Clin. Exp*. 22: 579-587, 1973.

Klingenspor M. Cold-induced recruitment of brown adipose tissue thermogenesis. *Exp Physiol*. 88: 141-148, 2003.

Kranias EG, Garvey JL, Srivastava RD, Solaro RJ. Phosphorylation and function modifications of sarcoplasmic reticulum and myofibrils in isolated rabbit hearts stimulated with isoprenaline. *Bichem J*. 226(1): 113-21, 1985.

Kubo H, Libonati JR, Kendrick ZV, Paolone A, Gaughan JP, Houser SR. Differential effects of exercise training on skeletal muscle SERCA gene expression. *Med Sci Sports Exerc*. 35 (1): 27-31, 2003.

Kyle U, Bosaeus I, De Lorenzo AD, Deurenberg P, Elia M, Gomez JM, Heitmann BL, Kent-Smith L, Melchior JC, Pirlich M, Scharfetter H, Schols A, Pichard C, Composition of the ESPEN Working Group. Bioelectrical impedance analysis – part I: review of principles and methods. *Clinical Nutrition*. 23: 1226-1243, 2004.

Lakatta EG. Aging of the adult heart. *Physiology and pathophysiology of the heart*, 3rd Ed. San Diego: Adademic Press. P. 701-718, 1995.

Lambertson C. Elements of normal renal function. *Medical Physiology (11th Ed)*. 1961.

Lanni A, De Felice M, Lombardi A, Moreno M, Fleury C, Ricquier D, Goglia F. Induction of UCP2 mRNA by thyroid hormones in rat heart. *FEBS Lett*. 418(1-2): 171-4, 1997.

Lanni A, Beneduce L, Lombardi A, Moreno M, Boss O, Muzzin P, Giacobina JP, Goglia F. Expression of uncoupling protein-3 and mitochondrial activity in the transition from hypothyroid to hyperthyroid state in rat skeletal muscle. *FEBS Lett*. 444(2-3): 250-4, 1999.

Lee, A.G. A calcium pump made visible. *Curr. Opin. Struct. Biol.* 12: 547-554, 2002.

Leijendekker WJ, van Hardeveld C, and Elzinga G. Heat production during concentration in skeletal muscle of hypothyroid mice. *Am J Physiol Endocrinol Metab*. 253: E214-E220, 1987.

Leppik JA, Aughey RJ, Medved I, Fairweather I, Carey MF, McKenna MJ. Prolonged exercise to fatigure in humans impairs skeletal muscle Na^+-K+-ATPase activity, sarcoplasmic reticulum Ca^{2+} release, and Ca^{2+} uptake. *J Appl Physiol*. 97(4): 1414-23, 2004.

Levine J, Eberhardt N and Jensen M. Role of non-exercise activity thermogenesis in resistance to fat gain in humans. *Science*. 283: 212-214, 1999.

Li JL, wang XN, Fraser SF, Carey WF, Wrigley TV, McKenna MJ. Effects of fatigue and training on sarcoplasmic reticulum Ca^{2+} regulation in human skeletal muscle. *J Appl Physiol*. 92 (3): 912-22, 2002.

Lindemann J, Jones LR, Hathaway DR, Henry BG, Watanabe AM. Beta-adrenergic stimulation of phospholamban phosphorylation and Ca^{2+}-ATPase activity in guinea pig ventricles. *J Biol Chem*. 258(1): 464-71, 1983.

Lompre AM, Lambert F, Lakatta EG, Schwartz K. Expression of sarcoplasmic reticulum Ca2+ ATPase and calsequestrin genes in rat heart during ontogenic development and aging. *Circ Res*. 69" 1380-1388, 1991.

Lompre AM, Anger M, Lambert D. Sarco(endo)plasmic reticulum calcium pumps in the cardiovascular system: function and gene expression. *J Mol Cell Cardiol*. 26: 1109-1121, 1994.

Lowell BB and Spiegelman BM. Towards a molecular understanding of adaptive thermogenesis. *Nature*. 404: 652-660, 2000.

Mackey DC, Manini TM, Schoeller DA, Koster A, Glynn NW, Goodpaster BH, Satterfield S, Newman AB, Harris TB, Cummings SR. Validation of an armband to measure daily energy expenditure in older adults. J *Gerontol A Biol Sci Med Sci*. [Epub ahead of print], 2011.

MacLennan DH, Brandl CJ, Korczak B, Green NM. Amino acid sequence of Ca^{2+} + Mg^{2+} dependent ATPase from rabbit muscle sarcoplasmic reticulum, deduced from its complementary DNA sequence. *Nature*. 316: 696-700, 1985.

MacLennan D.H, Rice W.J, Green N.M. The mechanism of Ca^{2+} transport by sarco(endo)plasmic reticulum Ca^{2+}-ATPases. *J. Biol. Chem.* 272: 28815-28818, 1997.

MacLennan DH, Asahi M, Tupling AR. The regulation of SERCA-type pumps by phospholamban and sarcolipin. *Ann. NY. Acad. Sci*. 986: 472-487, 2003.
MacLennan DH. Interactions of calcium ATPase with phospholamban and sarcolipin: structure, physiology and pathophysiology. *J Muscle Res Cell Motil*. 25(8): 600-1, 2004.

Mahmmoud YA. Capsaicin stimulates uncoupled ATP hydrolysis by sarcoplasmic reticulum calcium pump. *J. Biol. Chem.* 283: 21418-21426, 2008.

Mazerczak J, Karasinski J, Zoladz JA. Training induced decrease in oxygen cost of cycling in accompanied by down-regulation of SERCA expression in human vasus lateralis muscle. *Journal of Physiology and Pharmacology.* 59(3): 589-602, 2008.

Mall S, Broadbridge R, Harrison SL, Gore MG, Lee A, East JM. The presence of sarcolipin results in increased heat production by Ca2+-ATPase. *J. Biol. Chem.* 281: 36597-36602, 2006.

McArdle W, Katch K, Katch V.L. *Exercise Physiology (2nd ed.*). Philadelphia, PA: Lea & Febiger. 1986.

McGilvery R.W. *Biochemistry: A Functional Approach*. Philadelphia, PA: Saunders. 1979.

McWhirter J.M, Gould G.W, East J, Lee A.G. Characterization of Ca^{2+}uptake and release by vesicles of skeletal-muscle sarcoplasmic reticulum. *Biochem. J.* 245: 731-738, 1987.

Morita T, Hussain D, Asahi M, Tsuda T, Kurzydlowski K, Toyoshima C, MacLennan D.H. Interaction sites among phospholamban, sarcolipin, and the sarco(endo)plasmic reticulum Ca^{2+}-ATPase. *Biochem. Biophys. Res. Commun.* 369: 188-194, 2008.

Murphy R.M, Larkins N, Mollica J, Beard N.A, Lamb G.D. Calsequestrin content and SERCA determine normal and maximal Ca^{2+} storage levels in sarcoplasmic reticulum of fast- and slow- twitch fibres of rat. *J. Physiol.* 587: 443-460, 2009.

Nozais M, Lompre AM, Janmot C, D'Albis A. Sarco(endo)plasmic reticulum Ca2+ pump and metabolic enzyme expression in rabbit fast-type and slow-type denervated skeletal muscles. A time course study. *Eur J Biochem*. 238: 807-812, 1996.

O'Brien PJ, Shen H, Weiler J, Mirsalimi M, Julian R. Myocardial Ca-sequestration failure and compensatory increase in Ca^{2+}-ATPase with congestive cardiomyopathy: Kinetic characterization by a homogenate microassay using real-time ratiometric indo-1 spectrofluorometry. *Mol. Cell. Biochem.* 102: 1-12, 2001.

Odermatt A, Becker S, Khanna V.K, Kurzydlowski K, Leisner E, Pette D, MacLennan D.H. Sarcolipin regulates the activity of SERCA1, the fast-twitch skeletal muscle sarcoplasmic reticulum Ca^{2+}-ATPase. *J. Biol. Chem.* 273: 12360-12369, 1998.

Olivetti G, Anversa P, Loud AV. Morphometric study of early postnatal development in the left and right myocardium of the rat: tissue composition, capillary growth and sarcoplasmic reticulum. *Circ res*. 46: 519-522, 1980.

Oppenheimer JH, Schwartz HL, Mariash CN, Kinlaw WB, Wong W, Freake HC. Advances in out understanding of thyroid hormone action at the cellular level. *Endocr. Rev*. 8: 288-308, 1987.

Ortenblad N, Lunde PK, Levin K, Andersen JL, Pedersen PK. Enhanced sarcoplasmic reticulum Ca^{2+} release following intermittent sprint training. *Am J Physiol Regul Integr Comp Phy siol*. 279(1): R152-60, 2000.

Ottenheijm C, Fong C, Vangheluwe P, Wuytack F, Babu G.J, Periasamy M, Witt C.C, Labeit S, Granzier H. Sarcoplasmic reticulum calcium uptake and speed of relaxation are depressed in nebulin-free skeletal muscle. *FASEB. J.* 22: 2912-2919, 2008.

Owen O.E, Reichard GA, Boden G, Patel M, Trapp VE. Interrelationships among key tissues in the utilization of metabolic substrate. *Adv. Mod. Nutr*. 2: 517-550, 1978.

Periasamy M and Kalyanasundaram A. SERCA pump isoforms: their role in calcium transport and disease. *Muscle Nerve*. 35: 430-442, 2006.

Perseghin G. Pathogenesis of obesity and diabetes mellitus: insights provided by indirect calorimetry in humans. *Acta Diabetol*. 38: 7-21, 2001.

Pette D, Vrbova G. Adaptation of mammalian skeletal muscle fibers to chronic electrical stimulation. *Rev Physiol Biochem Pharmacol*. 120: 115-202, 1992.

Poehlman ET, Berke EM, Joseph JR, Gardner AW, Katzman-Rooks SM, Goran MI. Influence of aerobic capacity, body composition, and thyroid hormones on the age-related decline in resting metabolic rate.
Metabolism. 41 :915-21, 1992.

Poehlman El, Goran MI, Gardner AW, et al. Metabolic determinants of the decline in resting metabolic rate in aging females. *Am J Physiol*. 267:E450-55, 1993.

Ravussin E, Burnard B, Schutz Y, Jequier E. Twenty-four-hour energy expenditure and resting metabolic rate in obese, morbidly obese, and controls. *Am. J. Clin. Nutr*. 35: 566-573, 1981.

Ravussin E, Lillioja 5, Anderson TE, Christin L, Bogardus C. Determinants of 24-hour energy expenditure in man. *J Clin Invest*. 78: 1568-78, 1986.

Ravussin E, Lilioja S, Knowler L, Christin D, Freymond D, Abbott WG, Boyce V, Howard B, Bogardus C. Reduced rate of energy expenditure as a risk factor for body-weight gain. *N. Engl. J. Med*. 318: 467-472, 1988.

Reis M, Farage M, de Souza A, de Meis L. Correlation between uncoupled ATP hydrolysis and heat production by the sarcoplasmic reticulum Ca2+-ATPase: coupling effect of fluoride. *J. Biol. Chem.* 276: 42793-42800, 2001.

Reis M, Farage M, de Meis L. Thermogenesis and energy expenditure: control of heat production by the Ca2+-ATPase of fast and slow muscle. *Mol. Mem. Biol.* 19: 301-310, 2002.

Roffey DM, Byrne NM, Hills AP. Day-to-day variance in measurement of resting metabolic rate using ventilated-hood and mouthpiece and nose-clip indirect calorimetry systems. *Journal of Parental and Enternal Nutrition*. 30(5): 426-432, 2006

Rolfe D, Brown G. Cellular energy utilization and molecular origin of standard metabolic rate in mammals. *Physiological Reviews*. 77 (3): 731-758, 1997.

Rose A, Kiens B, Richter EA. Ca^{2+}-calmodulin dependent protein kinase expression and signalling in skeletal muscle during exercise. *J. Physiol*. 574: 889-903, 2006.

Sayen MR, Rohrer DK, Dillmann WH. Thyroid hormone response of slow and fast sarcoplasmic reticulum Ca^{2+} ATPase mRNA in striated muscle. *Mol Cell Endocrinol*. 87: 9287-9341, 1992.

Scagliusi FB, Ferriolli E, Pfrimer K, Laurano C, Cunha CS, Gualano B, Louenco BH, Lancha AH. Characteristics of women who frequently under report their energy intake: a doubly labelled water study. *Eur J Clin Nutr*. 63(10)1192-9, 2009.

Schmidt-Nielsen K. Scaling: why is animal size so important? *Cambridge, UK: Cambridge Press*. 1984.

Schrauwen P, Hasselink MK. The role of uncoupling protien 3 in fatty acid metabolism: protection against lipotoxicity. *Proc. Nutri. Soc*. 63: 287-292, 2004.

Schulte L, Peters D, Taylor J, Navarro J, Kandarian S. Sarcoplasmic reticulum Ca^{2+} pump expression in denervated skeletal muscle. *Am J Physiol*. 267: C617-C622, 1994.

Schutz Y. The basis of direct and indirect calorimetry and their potentials. *Diabetes Metab.* Rev. 11: 383-408, 1995.

Seidler W, Jona I, Vegh M, Martonosi A. Cyclopiazonic acid is a specific inhibitor of the Ca2+-ATPase of sarcoplasmic reticulum. *J. Biol. Chem.* 264: 17816-17823, 1989.

Simmerman H.K, Jones L.R. Phospholamban: protein structure, mechanism of action, and role in cardiac function. *Physiol. Rev.* 78: 921-947, 1998.

Simonides WS, Thelen M, van der Linden CG, Muller A, van Hardeveld C. Mechanism of thyroid-hormone regulated expression of the SERCA genes in skeletal muscle: implications for thermogenesis. *Bioscience Reports*. 21(2): 139-154, 2001.

Smith WS, Broadbridge R, East JM, Lee AG. Sarcolipin uncouples hydrolysis of ATP from accumulation of Ca^{2+} by the Ca^{2+}-ATPase of skeletal muscle sarcoplasmic reticulum. *Biochem. J.* 361: 277-286, 2002.

Song Q, Young K, Chu G, Gulick J, Gerst M, Grupp I, Robbins J, Kranias E. Overexpression of phospholamban in slow-twitch skeletal muscle is associated with depressed contractile function and muscle remodelling. *FASEB Journal*. 10.1096⁄fj.03-1058fje, 2004.

Statistics Canada. Body composition of Canadian adults 2007-2009. *Canadian health measures survey*. 2007-2009.

Thomas PE, Ranatunga KW. Factors affecting muscle fiber transformation in cross-reinnervated muscle. *Muscle Nerve*. 16(2): 193-199, 1993.

Toyoshima C, Nakasako M, Nomura H, Ogawa H. Crystal structure of the calcium pump of sarcoplasmic reticulum at 2.6 A resolution. *Nature.* 405: 647-655, 2000.

Toyoshima C, Inesi G. Structural basis of ion pumping by Ca^{2+}-ATPase of the sarcoplasmic reticulum. *Annu. Rev. Biochem.* 73: 269-292, 2004.

Toyoshima C. Structural aspects of ion pumping by Ca^{2+}-ATPase of sarcoplasmice reticulum. *Arch Biochem Biophys.* 476: 3-11, 2008.

Tupling AR, Green H, Senisterra G, Lepock J, McKee N. Ischemia-induced structural change in SR Ca^{2+}-ATPase is associated with reduced enzyme activity in rat muscle. *Am. J. Physiol.* 281: R1681-1688, 2001.

Tupling A.R, Asahi M, MacLennan D.H. Sarcolipin overexpression in rat slow twitch muscle inhibits sarcoplasmic reticulum Ca2+ uptake and impairs contractile function. *J. Biol. Chem.* 277: 44740-44746, 2002.

Tupling AR and Green H. Silver ions induce Ca^{2+} release from the SR in vitro by acting on the Ca^{2+} release channel and the Ca^{2+} pump. *J. Appl. Physiol.* 92: 1603-1610, 2002.

Tupling AR, Green HJ, Roy BD, Grant S, Ouyang J. Paradoxical effects of prior activity on human sarcoplasmic reticulum Ca^{2+}-ATPase response to exercise. *J Appl Physiol*. 95(1): 138-44, 2003.

Tupling AR, Gramolini O, Duhamel A, Kondo H, Asahi M, Tsuchiya SC, Borrelli MJ, Lepock JR, Otsu K, Hori M, MacLennan H, Green H. HSP70 binds to the fast-twitch skeletal muscle Sarco (endo)plasmic reticulum Ca^{2+}-ATPase (SERCA1a) and prevents thermal inactivation. *J. Biol. Chem*. 279: 52382 – 52389, 2004.

Tupling A.R, Hussain D, Trivieri M.G, Bapu G, Backx P, Periasamy M, MacLennan D.H, Gramolini A.O. Improvement of Ca2+ transport and muscle relaxation in skeletal muscle from sarcolipin null mice. *FASEB J* 22(Meeting Abstracts). 962.934, 2008.

Tupling AR, Combardier E, Gupta SC, Hussain D, Vigna C, Bloemberg D, Quadrilatero J, Trivieri MG, Babu GJ, Backx PH, Periasamy M, Maclennan DH, Gramolini AO. Enhanced Ca2+ transport and muscle relaxation in skeletal muscle from sarcolipin-null mice. *Am J Physiol Cell Physiol*. [Epub ahead of print], 2011.

Tzankoff SP, Norris AH. Effects of muscle mass decrease on age-related BMR changes. *J Appl. Physiol*. 43: 1001-1006, 1977.

van Hardeveld C, Simonides WS. Effect of the thyroid status on the sarcoplasmic reticulum in slow skeletal muscle of the rat. *Cell Calcium*. 7(3): 147-60, 1986.

van Hardeveld C, Simonides WS. *Surviving hypoxia*. CRC Press, Boca Raton, Fl. Pp. 111-127, 1986.

Van Hardeveld C, Clausen T. *Intracellular calcium regulation.* Machester University Press, machester, UK. Pp. 355-365, 1986.

Vander E.J, Sherman J.H, Luciano D.S. *Human physiology: The mechanisms of body function*. 5th ed. McGraw Hill publishing, Toronto. pp 158-635, 1990.

Van der Linden CG, Simonides WS, Muller S, van der Laarse WJ, Vermeulen JL, Zuidwijk MJ. Fiber-specific regulation of Ca^{2+}-ATPase isoform expression by thyroid hormone in rat skeletal muscle. *Am J Physiol*. 271: C1908-C1919, 1996.

Vaugheluwe P, Raeymaekers L, Dode L, Wuytack F. Modulating sarco(endo)plasmic reticulum Ca^{2+} ATPase 2 (SERCA2) activity: cell biological implications. *Cell. Calcium.* 38: 291-302, 2005b.

Wade O.L., Bishop J. Cardiac output and regional blood flow. *Blackwell Scientific Publications, Oxford, UK*. 1962.

Wawrzynow A, Theibert J.L, Murphy C, Jona I, Martonosi A, Collins J.H. Sarcolipin, the "proteolipid" of skeletal muscle sarcoplasmic reticulum, is a unique, amphipathic, 31-residue peptide. *Arch. Biochem. Biophys.* 298: 620-623, 1992.

Weicher H, Feraudi M, Hagele H, Plato R. Electrochemical detection of catecholamines in urine and plasma after separation with HPLC. *Clin. Chim. Acta.* 141: 17-25, 1984.

Weir V, DE J. New methods for calculating metabolic rate with special reference to protein metabolism. *J. Physiol*. 109: 1-9, 1949.

Wieser, W. Energy allocation by addition and by compensation: an old principle revisited. Energy Transformations in Cells an old principle revisited. *Energy Transformations in Cells and Organisms*. 98-105, 1989.

Widdowson E, Edholm O, McCance R. The food intake and energy expenditure of cadets in training. *Br. J. Nutr.* 8: 147-155, 1954.

Wu K.D, Lytton J. Molecular cloning and quantification of sarcoplasmic reticulum Ca(2+)-ATPase isoforms in rat muscles. *Am. J. Physiol.* 264: C333-C341, 1993.

Wu X, Patki A, Lara-Castro C, Cui X, Zhang K, Walton RG, Osier M, Gadbury G, Allison D, Martin M, Garvey T. Genes and biochemical pathways in human skeletal muscle affecting resting energy expenditure and fuel partitioning. *J Appl Physiol*. 110: 746-755, 2011.

Wuytack F, Dode L, Baba-Aissa F, Raeymaekers L. The SERCA3-type of organellar Ca^{2+} pumps. *Biosci Rep*. 15: 299-306, 1995.

Yu X, Inesi G. Variable stoichiometric efficiency of Ca2+ and Sr2+ transport by the sarcoplasmic reticulum ATPase. *J. Biol. Chem.* 270: 4361-4367, 1995.

Zhang S-J, Anderson DC, E. SM, Westerblad H, Katz A. Cross bridges account for only 20% of total ATP consumption during submaximal isometric contraction in mouse fast-twitch skeletal muscle. *Am. J. Physiol.* 291: C147-C154, 2006.

Zorratti M, Favaron M, Pietrobon D, Azzone GF. Intrinsic uncoupling of mitochondrial proton pumps 1. Non-ohmic conductance cannot account for the non-linear dependence of static head respiration on ∇ µH+. *Biochemistry*. 25: 760-767, 1986.

Zubrzycka-Gaarn E, Phillips L, MacLennan DH. Monoclonal antibodies to the Ca2+ + Mg2+-dependent ATPase of skeletal muscle sarcoplasmic reticulum cross-reactivity with ATPase isozymes and other Ca2+-binding proteins. *Prog Clin Biol Re.s* 168: 19-23, 1984.

Zurlo F, Larson K, Bogardus C, Ravussin E. Skeletal muscle metabolism is a major determinant of resting energy expenditure. *Journal of Clinical investigations*. 86: 1423-1427, 1990.

Appendix A

Participant Characteristics:

Participant	Weight (kg)	Height (cm)	BMI (kg/m^2)	Waist (cm)	Hip (cm)	Sex	Age (years)	RMR (kcal/kg lean/ day)
1	76.9	181	23.47	81.7	105	male	21	33.74
2	52.5	174	17.14	68.2	91.2	male	22	28.88
3	50.3	168	17.82	68.8	89.3	female	19	33.08
4	60.8	172	20.55	72.2	88	male	20	27.26
5	50.9	162.8	19.2	65.2	93.7	female	22	33.69
6	63.7	174.2	20.99	86.5	102.6	female	19	30.12
7	57.7	172	19.5	76.7	92.4	male	29	30.66
8	64.7	182.6	19.4	75.7	92.5	male	20	32.47
9	55.5	170.6	19.07	70	87.2	male	21	23.91
10	57.3	181.2	17.05	75.1	91.5	female	22	24.08
11	68.4	181.2	20.85	74.5	92.7	male	20	29.62
12	60.6	165.4	22.12	78.5	89.4	male	28	33.81
13	73.4	167.8	26.07	87.1	105.8	female	31	31.38
14	87.9	169.2	30.7	90.8	105.8	male	28	29.41
15	136.2	188	38.54	123.1	128.6	male	23	32.46
16	84.5	173.2	28.17	92.8	101.3	male	25	30.54
17	76.7	160.4	29.81	92.2	113.6	female	20	34.81
18	93.8	182.2	28.26	89.1	110.2	male	23	22.06
19	81.8	166.4	29.5	94.3	105.5	male	22	32.88
20	116	179.2	36.12	106.1	118.2	male	21	31.37
21	62.9	181	19.2	75.2	94.2	male	18	30.20
22	92.6	166.4	33.44	103.2	111.1	male	20	29.9
23	65	178.4	20.42	72.6	93.1	male	25	26.45
24	70.6	189.2	19.7	73.8	97.7	male	19	27.24
25	65.5	182.6	19.64	76.3	93.6	male	18	27.7
Average	**72.8**	**174.6**	**23.9**	**81.4**	**99.0**		**22.2**	**29.91**
Standard Deviation	**201**	**7.97**	**6.2**	**6.2**	**9.1**		**3.6**	**3.35**

Weight is expressed in kg, height is expressed in cm, BMI is expressed in cm, age is expressed in years, RMR is normalized to FFM (expressed as kcal/kg lean/day). RMR was calculated using the Weir equation (see Methods) using VO_2 and VCO_2 values collected using a breath by breath indirect calorimetry system.

Appendix B

Body Composition Measures

DXA Body Compositional Measures:

Participant	Fat Mass (kg)	Fat Free Mass (kg)	% Fat	% Lean	Lean Mass/Ht^2 (kg/m^2)	Appendicular Lean Mass/Ht^2 (kg/m^2)
1	11.99	55.12	17.20	78.86	8.78	17.9
2	10.61	37.76	20.73	73.80	12.49	N/A
3	15.09	33.65	29.80	66.48	5.42	12.6
4	8.56	51.53	13.70	82.24	8.92	18.3
5	12.40	31.97	25.00	64.42	12.03	N/A
6	16.88	35.93	27.23	57.94	12.62	N/A
7	11.30	43.42	19.80	76.29	6.94	15.3
8	8.25	50.98	13.30	82.16	7.39	16.1
9	5.90	45.75	10.92	84.61	15.68	N/A
10	13.22	40.89	23.40	72.44	5.95	13.3
11	12.87	52.45	18.90	77.19	8.24	16.8
12	14.29	42.96	24.20	72.61	7.81	16.4
13	28.16	39.52	40.20	56.38	6.11	14.9
14	19.43	60.26	23.40	72.61	10.7	22.2
15	50.71	76.36	38.60	58.19	10.3	22.5
16	24.19	54.62	29.50	66.69	8.82	19.2
17	28.15	42.03	38.80	57.90	8.12	17.3
18	16.16	76.17	16.90	79.43	10.9	24
19	25.37	50.38	32.40	64.34	9.13	19.3
20	42.59	66.55	37.84	59.13	9.28	21.5
21	12.01	47.24	19.40	76.47	7.01	15.2
22	30.95	57.72	33.90	63.18	10.7	22.1
23	9.34	50.90	14.90	80.95	7.83	16.8
24	11.63	55.05	16.70	79.04	7.44	16.2
25	9.11	51.78	14.40	81.64	7.54	16.2
Average	**18.0**	**50.0**	**24.0**	**71.4**	**9.0**	**17.8**
Standard Deviation	**11**	**12**	**9**	**9.1**	**2**	**3.1**

Fat mass is expressed in kg, fat free mass is expressed in kg, %fat and %lean are expressed as percentages of whole body weight, Ht^2 is height squared, lean mass/Ht^2 is the total FFM in the body/height squared (expressed as mg/m^2), appendicular lean mass/Ht^2 is the sum of the arm and leg lean tissue masses/height squared (expressed in kg/m^2).

Data for Calculation of FM and FFM using DXA and BIA Body Composition Measures:

Part.	FM (BIA)	FM (DXA)	Calculated FM	DXA – DXA Calc (FM)	FFM (BIA)	FFM (DXA)	Calculated FFM	DXA – DXA Calc (FFM)
1	16.62	11.99	16.03	-4.04	60.48	55.12	57.66	-2.54
2	10.31	-	10.61	-	42.99	-	37.76	-
3	12.67	15.09	12.63	2.46	37.48	33.65	31.49	2.16
4	7.50	8.56	8.20	0.37	53.90	51.53	50.18	1.34
5	12.40	-	12.40	-	37.90	-	31.97	-
6	17.62	-	16.88	-	41.38	-	35.93	-
7	9.61	11.30	10.01	1.29	47.02	43.42	42.35	1.07
8	11.41	8.25	11.55	-3.31	52.39	50.98	48.46	2.52
9	4.82	-	5.90	-	50.01	-	45.75	-
10	15.19	13.22	14.79	-1.57	42.11	40.89	36.77	4.13
11	12.74	12.87	12.70	0.17	56.26	52.45	52.86	-0.41
12	10.82	14.29	11.05	3.24	49.78	42.96	45.49	-2.53
13	28.73	28.16	26.42	1.74	44.67	39.52	39.67	-0.15
14	23.57	19.43	21.99	-2.56	64.33	60.26	62.04	-1.78
15	55.36	50.71	49.26	1.45	80.84	76.36	80.84	-4.48
16	23.03	24.19	21.53	2.67	61.47	54.62	58.79	-4.16
17	32.48	28.15	29.63	-1.48	44.22	42.03	39.16	2.87
18	24.04	16.16	22.39	-6.24	69.79	76.17	68.22	7.95
19	25.86	25.37	23.95	1.42	55.94	50.38	52.50	-2.12
20	49.77	42.59	44.47	-1.88	66.23	66.55	64.20	2.34
21	12.21	12.01	12.42	-0.23	50.69	47.24	46.53	0.71
22	34.11	30.95	31.03	-0.08	58.49	57.72	55.40	2.31
23	11.45	9.34	11.59	-2.24	53.55	50.90	49.78	1.12
24	14.00	11.63	13.78	-2.15	56.60	55.05	53.25	1.79
25	10.95	9.11	11.16	-2.05	54.55	51.78	50.92	0.87
Average	**19.18**	**18.0**	**18.22**	**-0.14**	**52.91**	**50.0**	**49.05**	**0.15**
SD	**12.4**	**11**	**10.6**	**4.0**	**10.3**	**12**	**11.7**	**3**

The calculated FM and FFM were determined using the equations base on the line of best fit when BIA and DXA values for FM and FFM were plotted against one another. The equations for calculated DXA were: FM: Y= 0.8579x + 1.766, FFM: Y=1.138x + (-11.16), where, x is the value in kg for BIA. The DXA-DXA Calc (FM) is the resulting value from the calculation: FM assessed by DXA – Calculated FM (based on the above equation). The DXA-DXA Calc (FFM) is the resulting value from the calculation: FFM assessed by DXA – Calculated FFM (based on the above equation). Abbreviation: Part, participant; SD, standard deviation.

Appendix C

Energy Balance Analysis

Caloric Intake, Expenditure and Balance (kcal):

Part.	Day 1: Intake	Expen	Diff.	Day2: Intake	Expen	Diff.	Day 3: Intake	Expen	Diff.	Avg Diff.
1	5406	3066	2339	2311	3000	752	2293	3058	-766	775
2	2298	1690	608	2866	1905	1038	2109	1828	281	642
3	1535	1909	-375	1704	1928	-168	1339	1872	-534	-359
4	2281	4001	-1721	1818	4038	-2559	1505	4376	-2871	-2383
5	1419	2006	-588	1842	2006	-176	1461	2010	-550	-438
6	2512	2595	-83	2243	2313	-877	3253	3120	132	-276
7	2526	2799	-273	17368	2342	15236	2036	2133	-96	4955
8	1786	2925	-1139	3719	2799	743	3034	2976	58	-112
9	1669	2400	-731	2072	2220	-544	1077	2617	-1539	-938
10	1750	2302	-552	2800	2461	579	1745	2221	-476	-150
11	2696	2365	331	1488	2510	-1062	1937	2550	-612	-448
12	3192	2765	427	1547	2221	-457	2067	2004	63	11
13	1848	2573	-725	1291	2778	-2137	1452	3428	-1977	-1613
14	1970	3362	-1392	3030	3396	-371	2958	4301	-443	-735
15	3701	6886	-3185	2952	6217	-3122	3779	6074	-2295	-2867
16	3078	3052	26	3887	3629	302	1875	3584	-1710	-461
17	1668	4212	-2544	1201	3076	-2914	1886	4115	-2229	-2562
18	2902	4555	-1654	2707	4073	-927	1910	3634	-1724	-1435
19	1780	3393	-1613	1619	3328	-1705	2124	3324	-1200	-1506
20	1821	4275	-2455	1716	4226	-2645	2740	4360	-1621	-2240
21	1401	2216	-815	1862	2224	-790	3401	2652	749	-285
22	4529	4147	393	2097	3826	-2317	3605	4414	-809	-911
23	3281	2860	422	2544	2256	156	1778	2389	-611	-11
24	2606	2368	238	1304	2643	-1444	1399	2748	-1349	-852
25	2915	2380	82	2535	2521	38	2193	2497	-303	90
Avg	**2503**	**3084**	**-581**	**2881**	**2957**	**-215**	**2198**	**3095**	**-897**	**-564**
SD	**987**	**1119**	**1210**	**3120**	**978**	**3442**	**753**	**1011**	**917**	**1499**

Energy intake, expenditure and energy difference (or balance, as assessed by 'Intake – Expenditure') are expressed as Intake, Expen, and Diff, respectively, and are in kcal/day (for day 1-3). The Average Diff is the average difference (or energy balance) over the 3 days and is expressed in kcal. Data taken from diet and activity logs. Abbreviation: Part, participant; Avg, Average; SD, standard deviation.

Sensewear Armband Data:

Part	Total Energy Expen:		Avg METS:		Duration on Body:		Energy Balance		Avg Energy Balance
	Day 1	Day 2	Day 1	Day 2	Day 1	Day 2	Day 1	Day 2	
1	-	-	-	-	-	-	-	-	-
2	-	-	-	-	-	-	-	-	-
3	1917	1752	1.6	1.5	23:42	23:35	-382	-48	-215
4	2718	2862	1.8	1.9	23:54	23:49	-437	-1044	-740.5
5	-	-	-	-	-	-	1419	1842	-
6	-	-	-	-	-	-	2512	2243	-
7	1950	1887	1.4	1.4	24:00	23:53	576	15481	8028.5
8	2219	2291	1.5	1.5	23:44	23:51	-433	1248	497.5
9	-	-	-	-	-	-	1669	2072	-
10	2504	2541	1.8	1.9	23:32	22:27	-754	259	-247.5
11	2699	2668	1.6	1.6	23:34	23:34	-3	-1180	-591.5
12	3771	4057	1.6	1.8	23:36	23:16	-579	-2510	-1544.5
13	1957	2906	1.1	1.7	24:00	22:42	-109	-1615	-862
14	3264	3205	1.6	1.5	23:46	24:00	-1294	-175	-734.5
15	3070	3788	1.9	1.3	11:30	21:24	631	-836	-102.5
16	2954	2199	1.5	1.1	23:44	23:15	124	1688	906
17	2206	2641	1.2	1.4	23:41	23:26	-538	-1440	-989
18	3093	2984	1.4	1.3	23:38	24:00	-191	-277	-234
19	2524	2678	1.3	1.4	23:33	23:42	-744	-1059	-901.5
20	2912	3129	1.1	1.1	23:40	23:02	-1091	-1413	-1252
21	2754	2741	1.8	1.8	23:18	23:51	-1353	-879	-1116
22	4117	2560	1.9	1.2	24:00	23:38	412	-463	-25.5
23	2818	2072	1.8	1.3	23:45	23:46	463	472	467.5
24	2980	-	1.8	-	23:50	-	-374	1304	465
25	-	-	-	-	-	-	-	-	-
Avg	**2759**	**2720**	**1.6**	**1.5**			**-21.6**	**629.5**	**42.6**
SD	**586**	**596**	**0.3**	**0.3**			**961**	**3580**	**2045**

Note: Energy Balance is energy intake (assessed from diet log) - Sensewear armband energy expenditure. Total daily energy expenditure is expressed in kcal, Average METS is the MET values averaged over ~24 hours, Duration on Body is the number of hours the armband was recording values of the body (it is not water proof, thus could not be worn in the shower), and energy balance is 'energy intake (as assessed by the analysis of the diet log, shown in the first table in Appendix C) – total energy expenditure (assessed by the armband). Abbreviations: Part, participant; Avg, average; SD, standard deviation; Expen, expenditu

Appendix D

Cholesterol, FFA, TG, Glucose and Insulin:

Participant Blood Cholesterol and TG Data:

Participant	Cholesterol (mmol/L)	LDL (calculated) (mmol/L)	HDL (mmol/L)	Cholesterol/HDL Ratio (mmol/L)	Triglycerides (mmol/L)
1	3.63	2.04	1.31	2.8	0.62
2	2.62	1.24	1.16	2.3	0.48
3	3.05	1.62	1.18	2.6	0.56
4	4.23	2.52	1.44	2.9	0.59
5	3.7	1.81	1.61	2.3	0.62
6	5.53	2.05	1.84	3	1.41
7	3.49	2.14	0.92	3.8	0.95
8	4.01	2.57	1.12	3.6	0.7
9	4.63	2.64	1.61	2.9	0.83
10	4.92	3.24	1.42	3.5	0.58
11	2.79	1.6	0.95	2.9	0.53
12	4.9	3.22	1.04	4.7	1.4
13	3.1	1.68	1.17	2.6	0.54
14	4.03	1.85	1.52	2.7	1.46
15	3.46	1.9	1.15	3	0.9
16	5.43	3.67	1.1	4.9	1.46
17	3.08	1.64	1.34	2.3	0.23
18	4.48	2.43	1.87	2.4	0.4
19	3.39	1.67	1.5	2.3	0.48
20	4.57	1.98	1.25	3.7	2.94
21	3.13	1.68	1.17	2.7	0.62
22	4.76	2.79	1.03	4.6	2.07
23	4.36	2.69	1.32	3.3	0.76
24	2.94	1.54	1.07	2.7	0.73
25	4.33	2.97	1.11	3.9	0.54
Average	**3.94**	**2.25**	**1.29**	**3.14**	**0.90**
Standard Deviation	**0.84**	**0.7**	**0.3**	**0.8**	**0.6**

Cholesterol is expressed in mmol/L, LDL is expressed in mmol/L, HDL is expressed in mmol/L, cholesterol/HDL ratio is expressed in mmol/L, and triglycerides are expressed in mmol/L.

Participant Blood FFA, Glucose and Insulin Data:

Participant	Glucose (mmol/L)	FFA (mEq/L)	Insulin (μlU/ml)
1	4.3	0.753	5.98
2	4.2	0.229	6.68
3	4.7	0.481	5.62
4	3.1	0.123	5.01
5	5.2	0.246	3.58
6	4.2	0.348	7.89
7	4.4	0.365	6.26
8	4.8	1.183	5.89
9	4.8	1.141	9.75
10	4.4	0.198	3.78
11	4.6	0.231	5.95
12	4.2	0.164	N/A
13	4.6	0.168	9.66
14	4.6	0.296	7.79
15	4.9	0.239	29.3
16	5.3	0.228	6.91
17	4.2	N/A	2.62
18	5.3	0.055	8.11
19	4.7	0.412	9.36
20	5.5	0.502	10.00
21	4.6	0.172	7.42
22	5.2	0.498	19.68
23	4.6	0.262	6.761
24	4.6	0.798	6.57
25	5.3	0.566	6.90
Average	**4.65**	**0.40**	**8.23**
Standard Deviation	**0.51**	**0.3**	**5.5**

Glucose is expressed in mmol/L, FFA is expressed in mEq/L, and insulin is expressed in μlU/ml.

Normal Blood Metabolite and Hormone Values:

A)

Cholesterol (mmol/L)	LDL (calculated) (mmol/L)	HDL (mmol/L)	Cholesterol/HDL Ratio (mmol/L)	Triglycerides (mmol/L)
<5.2	<3.4	>1.6	<3.5	<2.3

B)

Glucose (mmol/L)	FFA (mEq/L)	Insulin (μlU/ml)
3.8-5.5	0.1-0.6	Median of 7.8

Cholesterol, LDL, HDL, cholesterol/HDL ratio, triglycerides and glucose expressed in mmol/L. FFA expressed in mEq/L and insulin expressed in μlU/ml. Insulin values from study of 126 serum samples provided by the Coat-A-Kit, which yielded a median of 7.8 μlU/ml with 95% of the results being 29.4 μlU/ml or less. Values from Canadian Diabetes Association, Insulin Coat-A-Kit and NEFA C Wako 990-75401.

Appendix E

Ca^{2+}-ATPase Assay Data

Participant Values for Ca^{2+}-ATPase, IONO Ratio, Vmax, and EC50:

Participant	Vmax with IONO (μM/mg protein/min)	EC50 (nM)	IONO Ratio (at Vmax)	Ca^{2+}-ATPase Activity with IONO (μM/mg protein/min)
1	301.2	5.65	11.50	16
2	236	5.78	9.11	7.2
3	174.3	5.63	10.02	12.8
4	241.3	5.63	7.09	8.5
5	168.5	5.42	5.62	12.1
6	164.8	5.70	7.39	8.7
7	146.8	5.44	7.27	7.9
8	193.9	5.42	11.41	2.6
19	208.3	5.63	10.01	7.3
10	162.9	5.05	7.79	4.5
11	219.8	5.64	7.09	6.6
12	215.5	5.50	6.91	3.9
13	197.1	5.62	11.26	11.2
14	170.7	5.37	2.27	19.9
15	162.1	5.42	9.65	11.3
16	181.5	5.27	8.68	6.6
17	329.4	5.29	5.96	33.9
18	155.6	5.19	7.37	2.1
19	191.4	5.72	6.99	9.8
20	162.9	5.45	8.48	19.1
21	207.7	5.71	8.41	22.3
22	207.9	5.75	13.41	4.4
23	197.5	5.71	3.67	15.9
24	191.4	5.54	3.39	9.5
25	222.6	5.34	9.16	2.4
Average	**200.44**	**5.15**	**8.00**	**10.66**
Standard Deviation	**43.10**	**0.19**	**3**	**7.36**

Ca^{2+}-ATPase Activity is assessed with IONO and is expressed in μM/mg protein/min, IONO ratio is Ca^{2+}-ATPase activity with IONO/ Ca^{2+}-ATPase activity with no IONO and is assessed at Vmax, Vmax is assessed with IONO and expressed in μM/mg protein/min, and EC50 is the Ca^{2+} concentration when the Ca^{2+}-ATPase activity is 50% of Vmax (and is expressed in nM). . A description of the Ca^{2+}-ATPase assay is found in the Methods section.

Appendix F

Ca^{2+} Uptake and Leak Assay Data

Participant Values for Ca^{2+} Uptake and Leak:

Participant	Ca^{2+} Uptake (μM/g protein/min)	Ca^{2+} Leak (μM/g protein/min)
1	1.0	0.3
2	1.8	0.3
3	0.3	0.5
4	0.4	0.4
5	0.9	0.2
6	0.6	0.2
7	0.5	0.3
8	0.6	0.2
9	1.0	0.1
10	0.8	1.1
11	1.2	0.3
12	0.4	0.4
13	0.8	0.3
14	0.6	0.6
15	0.5	0.6
16	0.8	0.5
17	3.2	0.4
18	0.7	0.4
19	1.2	0.5
20	2.2	0.3
21	0.5	0.1
22	1.3	0.3
23	2.0	0.5
24	N/A	1.6
25	0.9	0.2
Average	**1.01**	**0.42**
Standard Deviation	**0.69**	**0.3**

Ca^{2+} uptake is expressed in μM/g protein/min, and Ca^{2+} leak is expressed in μM/g protein/min. A description of the Ca^{2+} uptake and leak assay is found in the Methods section.

Appendix G

Coupling Ratio Data

Participant Values for Coupling Ratio:

Participant	Coupling Ratio
1	0.07
2	0.26
3	0.02
4	0.05
5	0.08
6	0.07
7	0.07
8	0.25
9	0.14
10	0.18
11	0.18
12	0.10
13	0.07
14	0.03
15	0.05
16	0.13
17	0.10
18	0.33
19	0.12
20	0.11
21	0.02
22	0.29
23	0.13
24	N/A
25	0.36
Average	**0.13**
Standard Deviation	**0.1**

The coupling ratio is assessed as Ca^{2+} uptake/ Ca^{2+}-ATPase activity, at a matching pCa value which ranged between 5.96 and 6.74.

Appendix H

Western Blot Analysis Data

Participant Values for PLN (monomer), SERCA1a, SERCA2a and SERCA1a/SERCA2a Ratio:

Participant	PLN (monomer)	CSQ	SERCA1a	SERCA2a	SERCA1a/SERCA2a Ratio	SERCAtotal
1	0.469	3.72	4.33	2.74	1.58	7.07
2	0.075	3.12	6.05	2.40	2.52	8.45
3	0.058	2.57	4.72	3.29	1.43	8.01
4	0.687	4.05	5.04	6.73	0.75	11.77
5	0.093	4.08	5.70	2.45	2.33	8.15
6	0.046	2.53	3.36	3.15	1.07	6.51
7	0.076	3.83	3.75	2.70	1.39	6.45
8	0.050	3.10	4.78	1.92	2.49	6.70
9	0.041	2.63	5.11	1.56	3.27	6.67
10	1.151	3.23	4.52	6.41	0.71	10.93
11	1.563	4.67	10.46	6.48	1.61	16.95
12	0.091	3.46	6.08	3.20	1.90	9.28
13	0.153	2.27	3.15	4.15	0.76	7.30
14	0.468	1.94	2.46	5.34	0.46	7.80
15	0.260	1.62	2.67	6.09	0.44	8.76
16	0.289	3.52	5.44	4.62	1.18	10.07
17	0.387	4.41	7.27	4.81	1.51	12.08
18	0.283	2.61	4.30	6.46	0.67	10.76
19	0.109	3.32	6.03	4.56	1.32	10.59
20	0.370	3.16	4.31	6.63	0.65	10.94
21	0.211	3.52	5.11	5.93	0.86	11.04
22	0.447	3.24	4.67	5.19	0.90	9.86
23	0.359	5.19	4.16	4.30	0.97	8.46
24	0.932	7.97	3.42	8.53	0.40	11.95
25	0.118	3.19	3.16	1.78	1.77	4.95
Average	**0.35**	**3.50**	**4.80**	**4.46**	**1.32**	**9.26**
Standard Deviation	**0.4**	**1**	**2**	**1.89**	**0.74**	**2.6**

All proteins were analyzed using Western Blot techniques and are expressed in densitometry units and all proteins are normalized to αActin. PLN content is the PLN monomer, and SERCAtotal is SERCA1a + SERCA2a. A description of Western Blot procedures and analysis is found in the Methods section.